

# Estimation of Over-parameterized Models from an Auto-Modeling Perspective

Yiran Jiang and Chuanhai Liu  
Department of Statistics, Purdue University

## Abstract

From a model-building perspective, we propose a paradigm shift for fitting over-parameterized models. Philosophically, the mindset is to fit models to future observations rather than to the observed sample. Technically, given an imputation method to generate future observations, we fit over-parameterized models to these future observations by optimizing an approximation of the desired expected loss function based on its sample counterpart and an adaptive *duality function*. The required imputation method is also developed using the same estimation technique with an adaptive *m-out-of-n* bootstrap approach. We illustrate its applications with the many-normal-means problem,  $n < p$  linear regression, and neural network-based image classification of MNIST digits. The numerical results demonstrate its superior performance across these diverse applications. While primarily expository, the paper conducts an in-depth investigation into the theoretical aspects of the topic. It concludes with remarks on some open problems.

*Keywords:* Bootstrap, Cross-Validation, Future Observations, Image Classification, Resampling

## 1 Introduction

Over-parameterized models such as neural networks play a crucial role in statistical analysis. Their primary benefit lies in their ability to flexibly and efficiently approximate non-linear functions across diverse structures. However, the application of over-parameterized models can present challenges (*c.f.*, Nalisnick et al. (2019)). The primary challenge arises during model estimation, which typically involves minimizing a loss function based on observed data (Vapnik, 1991). In this case, seemingly optimistic performance on the observed data fails to generalize to the population data, leading to the well-recognized issue of *overfitting* due to the existence of *generalization gap*. This issue of overfitting also serves as the main characteristic for the definition of over-parameterization (see, *e.g.*, Oneto et al., 2023, and references therein).

Traditionally, to enhance the effectiveness of over-parameterized models while mitigating their associated challenges, prediction-oriented model selection is essential. Implementation of methods of prediction is typically based on the simple and effective idea

of *cross-validation* with the key references Stone (1974, 1977), Geisser (1975), and Efron and Tibshirani (1994, p. 255, and references therein). In the modern machine learning era, *regularization* techniques (Bühlmann and Van De Geer, 2011) are commonly used for calibration by making the over-parameterized models “simpler” in order to prevent overfitting. The regularization process typically involves selecting *hyper-parameters*, making the process of model selection fundamentally a task of hyper-parameter optimization.

Despite its simplicity and overall effectiveness, the current framework for fitting over-parameterized models has certain limitations. First, the processes of model estimation and model selection are separated. This separation often requires limiting the number of candidate models to ensure computational feasibility. For instance, in  $L_1$  penalized models, a grid-search method is typically employed to explore a limited range of hyper-parameter values (denoted by  $\lambda$  in what follows). This approach can result in inconsistencies in the estimated models, arising from variations in the choice of candidate sets. Second, the hyper-parameters tuning process may not adapt well to the observed data. For example, in methods like  $K$ -fold cross-validation, the same tuned hyper-parameters are used across  $K$  models, each fitted on different observations, as well as the final model using the full observation data (see Tibshirani and Tibshirani, 2009, and references therein). Additionally, recent studies, such as Bates et al. (2023), have highlighted issues with cross-validation, suggesting that it may not adequately estimate the prediction error.

To overcome limitations in current frameworks, we take a model-building perspective and propose a paradigm shift for estimating over-parameterized models. Philosophically, the mindset is to fit models to future observations rather than to the observed sample. Technically, given an imputation method to generate future observations, we fit over-parameterized models to these future observations by optimizing an approximation to the desired expected loss function. This optimization is based on the empirical counterpart and an adaptive *duality function* that extends the penalty function with estimable hyper-parameters. The required imputation method is also developed using the same estimation technique with an adaptive  $m$ -out-of- $n$  bootstrap approach. We call the proposed method *Auto-Modeling* (AM), as it follows both a philosophical recognition that modeling is meant to fit unobserved or future observations and a technical facilitation of simultaneous model estimation and selection procedures.

The proposed estimation framework itself appears to be applicable and attractive for creating imputation models using bootstrap methods. This is because we have the bootstrap population to serve as future observations and bootstrap samples to serve as observed data, respectively. However, due to the difficulty of the standard ( $n$ -out-of- $n$ ) bootstrap method for high-dimensional problems (*c.f.*, Supp-CB, 2024, and references therein), we use an adaptive  $m$ -out-of- $n$  bootstrap-based imputation approach, which is motivated by Supp-CB (2024). Notably, it follows that the proposed method for final estimation serves as a genuine approach to combining the resampling-based results in the context of over-parameterization; see Remark 2.

The proposed method is illustrated through various applications, including the many-normal-means problem,  $n < p$  linear regression, and neural network-based image classification of MNIST digits. The numerical results show that for the many-normal-means problem, our method consistently outperforms James-Stein and Efron’s  $g$ -modeling across all examples. In the application of  $n < p$  linear regression, our method yields model parameter estimates that result in greatly improved performance, demonstrated by both lower prediction errors and enhanced prediction interval coverage, compared with leading-edge techniques. In the MNIST image classification, it significantly surpasses several commonly

used regularization methods when applied to standard model structures.

In the rest of the paper, we comprehensively explore the proposed AM framework in Section 2. The required numerical algorithms are discussed in Section 3. Section 4 provides relevant theoretical results. Applications of the method are given in Section 5 for the three different examples. Section 6 concludes with a few remarks.

## 2 The General Framework

### 2.1 The Setting

Consider a sample  $(\mathbf{x}, \mathbf{y}) := \{(x_i, y_i) : i = 1, \dots, n\}$  of measurements  $(X, Y)$  from an unknown population  $\mathbb{P}$ , where  $(X, Y) \in \mathbb{X} \times \mathbb{Y}$  with  $\mathbb{X} \subseteq \mathbb{R}^k$  and  $\mathbb{Y} \subseteq \mathbb{R}^q$ . The problem of interest is to build a model for predicting  $y$  given  $x$  based on the observed sample

$$Y|\{X = x\} \sim \mathbb{P}_{x,\theta} \quad (Y \in \mathbb{Y}, x \in \mathbb{X}, \theta \in \Theta^{(n)} \subseteq \mathbb{R}^p). \quad (1)$$

That is,  $\mathbb{P}_{x,\theta}$  is used as an approximation to the true underlying conditional distribution of  $Y$  given  $X = x$ . For simplicity, we write  $(X, Y) \sim \mathbb{P}_\theta$  as the distribution of the data sampled from the model. In such a case, we assume that the distribution of  $X$  is independent of  $\theta$  and that the problem of interest remains on  $\mathbb{P}_{x,\theta}$  in (1). The notation  $\Theta^{(n)}$  is used to imply that the parameter space and hence its dimension  $p$  depend on the sample size  $n$ .

**Remark 1.** *Besides over-parameterized modeling strategies, the fact that the model of choice changes potentially with the sample size has been recognized in the statistical literature, e.g., in non-parametric statistics underlying the sieve method; see Grenander (1981), Geman and Hwang (1982), Shen et al. (1999), Wasserman (2006), and references therein.*

We consider estimating the model  $\{\mathbb{P}_\theta : \theta \in \Theta^{(n)}\}$  from the observed data  $(\mathbf{x}, \mathbf{y})$ . Let  $\ell(\theta|X, Y)$  be the log-likelihood function of  $\theta \in \Theta^{(n)}$ , given  $(X, Y) \in \mathbb{X} \times \mathbb{Y}$ . Take

$$L(\theta|X, Y) = -\ell(\theta|X, Y) \quad (2)$$

to be the loss function. From the modeling perspective elaborated in Section 1, we define the optimal estimate of  $\theta$  as a set of  $\theta$ -values that minimizes the expected loss with respect to the population. That is, such  $\theta$ -values form the set

$$\Theta_*^{(n)} = \left\{ \theta : \theta \in \Theta^{(n)}; E_{(X,Y) \sim \mathbb{P}} L(\theta|X, Y) = \min_{\tilde{\theta} \in \Theta^{(n)}} E_{(X,Y) \sim \mathbb{P}} L(\tilde{\theta}|X, Y) \right\}. \quad (3)$$

Thus, for optimal prediction, our primary objective of estimation is to find some  $\theta$  in  $\Theta_*^{(n)}$ .

Notably, the set  $\{\mathbb{P}_\theta : \theta \in \Theta_*^{(n)}\}$  consists of the models that provide the closest approximation to the true population  $\mathbb{P}$ , as measured by the Kullback-Leibler (KL) divergence (Lehmann, 1983; Pardo, 2006). A similar concept, viewed from the perspective of population risk minimization in learning theory, is discussed in Vapnik (1991).

### 2.2 A New Method of Model Estimation

Now, we focus on finding some model estimate  $\hat{\theta} \in \Theta^{(n)}$  belonging to the targeted set  $\Theta_*^{(n)}$ . Let  $\hat{\mathbb{P}}$  denote the empirical distribution defined by the sample  $\{(x_i, y_i) : i = 1, \dots, n\}$ . Empirical risk minimization (ERM) aims at finding  $\hat{\theta}_{ERM}$  that minimizes the empirical loss

$$R(\theta) = E_{(X,Y) \sim \hat{\mathbb{P}}} L(\theta|X, Y) = \frac{1}{n} \sum_{i=1}^n L(\theta|x_i, y_i).$$

For over-parameterized models, however, ERM is unsatisfactory due to its difficulty with *generalization gap*. The problem of generalization gap is commonly dealt with the technique of regularization. The main idea is to fit simpler or, more generally, restricted models. While still being estimated by fitting the observed sample, the resulting  $\theta$  that is deviated from the ERM estimate of  $\theta$  is obtained to reduce the generalization error. A good review and discussion of a large collection of regularization techniques can be found in Bühlmann and Van De Geer (2011). As has been elaborated in Section 1, existing frameworks can have certain limitations.

The above discussions motivate us to find an approximate solution to

$$\hat{\theta} = \arg \min_{\theta} E_{(X,Y) \sim \mathbb{P}} L(\theta|X, Y). \quad (4)$$

In pursuit of this, we make use of the sample counterpart of (4) and decompose the objective function into the sum of the empirical loss and the generalization gap

$$\hat{\theta} = \arg \min_{\theta} \left[ E_{(X,Y) \sim \hat{\mathbb{P}}} L(\theta|X, Y) + \left( E_{(X,Y) \sim \mathbb{P}} L(\theta|X, Y) - E_{(X,Y) \sim \hat{\mathbb{P}}} L(\theta|X, Y) \right) \right].$$

In order for the fitting to the empirical distribution to be meaningful, here we introduce the duality function  $\pi(\theta, \lambda)$  ( $\theta \in \Theta^{(n)}, \lambda \in \Lambda^{(n)}$ ) as an extension of the penalty function, where  $\Lambda^{(n)}$  is the duality parameter space, and write the target objective function as

$$E_{(X,Y) \sim \mathbb{P}} L(\theta|X, Y) = G_{\hat{\mathbb{P}}}(\theta, \lambda) + V_{\mathbb{P}, \hat{\mathbb{P}}}(\theta, \lambda), \quad (5)$$

where  $G_{\hat{\mathbb{P}}}(\theta, \lambda)$  is the penalized empirical loss

$$G_{\hat{\mathbb{P}}}(\theta, \lambda) = E_{(X,Y) \sim \hat{\mathbb{P}}} L(\theta|X, Y) + \pi(\theta, \lambda) \quad (6)$$

and  $V_{\mathbb{P}, \hat{\mathbb{P}}}(\theta, \lambda)$  is the modified generalization gap

$$V_{\mathbb{P}, \hat{\mathbb{P}}}(\theta, \lambda) = E_{(X,Y) \sim \mathbb{P}} L(\theta|X, Y) - E_{(X,Y) \sim \hat{\mathbb{P}}} L(\theta|X, Y) - \pi(\theta, \lambda). \quad (7)$$

Accordingly, the duality function serves a dual purpose in equations (6) and (7) for model estimation and model selection, respectively.

Ideally, we would like to have a  $\hat{\theta}$  such that (5) is minimized at  $\theta = \hat{\theta}$ . Here, we impose an additional constraint such that  $G_{\hat{\mathbb{P}}}(\theta, \lambda)$  defined in (6) is also minimized at  $\theta = \hat{\theta}$  for some  $\lambda = \hat{\lambda}$ . Such estimation process is equivalent to finding the solution  $(\hat{\theta}, \hat{\lambda})$  for the optimization problem

$$\min_{\theta, \lambda} G_{\hat{\mathbb{P}}}(\theta, \lambda) + V_{\mathbb{P}, \hat{\mathbb{P}}}(\theta, \lambda), \quad \text{subject to} \quad \theta = \arg \min_{\tilde{\theta}} G_{\hat{\mathbb{P}}}(\tilde{\theta}, \lambda). \quad (8)$$

An effective iterative algorithm for finding the solution  $(\hat{\theta}, \hat{\lambda})$  is proposed in Section 3. More discussion on the theoretical properties of  $(\hat{\theta}, \hat{\lambda})$  is given in Section 4.

Since  $\mathbb{P}$  is not available in practice, we approximate it with an imputed population  $\mathbb{Q}$ . This leads to the following algorithm for point estimation of the model parameter  $\theta$ .

**Algorithm 1** (Estimation). Let  $\mathbb{Q}$  denote the imputation distribution. The AM estimate of  $\theta$ , denoted by  $\hat{\theta}_{AM}$ , is determined by the AM objective (8) with the empirical distribution  $\hat{\mathbb{P}} := (\mathbf{x}, \mathbf{y})$  and the future population  $\mathbb{P} = \mathbb{Q}$ .

An imputation method to create such an imputed population  $\mathbb{Q}$  is proposed in Section 2.3 by applying this same estimation method with the required  $\mathbb{P}$  and  $\hat{\mathbb{P}}$ , obtained via  $K$ -fold data splitting and adaptive  $m$ -out-of- $n$  bootstrap resampling.

### 2.3 Imputation via Data Splitting and Adaptive Resampling

In this paper, we primarily concern the imputation of  $Y$  given the observed covariates  $X = x$ . More precisely, we generate future observations via multiple imputations

$$Y|\{X = x\} \sim \mathbb{Q} := \frac{1}{B} \sum_{b=1}^B \mathbb{Q}_{\hat{\theta}_b}, \quad (9)$$

where  $x$  is the observed covariate and  $\mathbb{Q}$  is the final imputation distribution formed as a mixture of  $B$  imputation models with model parameters  $\hat{\theta}_b \in \Theta^{(n)}$ ,  $b = 1, \dots, B$ , which are estimates of the model parameter  $\theta$  in (1).

The imputation model  $\mathbb{Q}_{\hat{\theta}_b}$  in (9) is constructed using a  $K$ -fold data partition along with adaptive  $m$ -out-of- $n$  bootstrap resampling, where  $m$  serves as the adaptive parameter. For each fold, we set it aside as holdout and use its covariate data  $x$  for imputation and the responses  $y$  for estimating the adaptive parameter  $m$ . The model is then fit to the remaining data, serving as the required future population  $\mathbb{P}$ , and a bootstrap resample from these remaining data, representing the needed observed data  $\hat{\mathbb{P}}$ . Denote the  $m$ -out-of- $n$  resampling scheme as  $r(\cdot)$ . This imputation procedure is detailed by Algorithm 2, followed by a discussion on estimating the adaptive parameter  $m$  for the specification of  $r(\cdot)$ .

---

#### Algorithm 2: The Imputation of Future Observations

---

- 1 Specify the resampling scheme  $r(\cdot)$ ,  $B$ , and  $K$ ;
  - 2 **for**  $b \leftarrow 1$  **to**  $B$  **do**
  - 3     Randomly split the observations  $(\mathbf{x}, \mathbf{y})$  into  $K$  equal subsets  $\{(\mathbf{x}_b^{(k)}, \mathbf{y}_b^{(k)})\}_{k=1}^K$ ;
  - 4     **for**  $k \leftarrow 1$  **to**  $K$  **do**
  - 5         Estimate the imputation model  $\mathbb{Q}_{\hat{\theta}_b}^{(k)}$  by solving the AM objective (8) with  
 $\mathbb{P} = \hat{\mathbb{P}}_b^{(-k)} := (\mathbf{x}_b^{(-k)}, \mathbf{y}_b^{(-k)})$  and  $\tilde{\mathbb{P}}_b^{(k)} := r((\mathbf{x}_b^{(-k)}, \mathbf{y}_b^{(-k)}))$ ;
  - 6         Generate future observations  $(\mathbf{x}_b^{(k)}, \mathbf{y}_{*b}^{(k)})$  with  $\mathbf{x}_b^{(k)}$  using  $\mathbb{Q}_{\hat{\theta}_b}^{(k)}$ ;
  - 7 Return the generated future observations  $\mathbb{Q} := \{(\mathbf{x}_b^{(k)}, \mathbf{y}_{*b}^{(k)}) : b = 1, \dots, B \text{ and } k = 1, \dots, K\}$ .
- 

From Algorithm 2, the estimated data generation distribution (9) can be rewritten as

$$Y|\{X = x\} \sim \mathbb{Q} := \frac{1}{B} \sum_{b=1}^B \sum_{k=1}^K \mathbb{Q}_{\hat{\theta}_b}^{(k)} \cdot \mathbb{1}(x \in \{\mathbf{x}_b^{(k)}\}), \quad (10)$$

where  $\mathbb{1}(\cdot)$  denotes the indicator function and  $\{\mathbf{x}_b^{(k)}\}$  denotes the holdout set of  $x$  in the  $k$ -th fold. This process requires fitting  $B \cdot K$  imputation models, and a practical choice is  $B = 5$  and  $K = 5$ . According to our experiments for the examples in Section 5, increasing  $B$  and  $K$  does not show significant changes in the results. Incidentally, it is interesting to note that the use of a small number of imputations is also reported to be effective in a different imputation context of Rubin (1987) and Hopke et al. (2001).

To find a resampling scheme  $r(\cdot)$  that can effectively estimate the data distribution for imputation, we recall that for the continuous true distribution function  $F(\cdot|x)$ ,

$$F(y_i|x_i) \sim \text{Uniform}(0, 1), \quad i = 1, \dots, n, \quad (11)$$

given *i.i.d.* samples  $(\mathbf{x}, \mathbf{y}) := \{(x_i, y_i) : i = 1, \dots, n\}$ . Based on (10) and (11), to better approximate the true data distribution, we check against the condition that for  $b = 1, \dots, B$ ,

$$\hat{F}_{\hat{\theta}_b}^{(k)}(y_{bi}^{(k)}|x_{bi}^{(k)}) \sim \text{Uniform}(0, 1), \quad i = 1, \dots, n - n_k \text{ and } k = 1, \dots, K, \quad (12)$$

where  $\hat{F}_{\hat{\theta}_b}^{(k)}(\cdot|x)$  denotes the distribution function of the imputation model  $\mathbb{Q}_{\hat{\theta}_b}^{(k)}$ . The term  $n_k$  denotes the sample size of the observations  $\hat{\mathbb{P}}_b^{(k)} := (\mathbf{x}^{(-k)}, \mathbf{y}^{(-k)})$  used to estimate  $\mathbb{Q}_{\hat{\theta}_b}^{(k)}$ , and  $\{(x_{bi}^{(k)}, y_{bi}^{(k)}) : i = 1, \dots, n - n_k\}$  denotes the holdout set in the  $k$ -th fold, as outlined in Algorithm 2. This implementation has the desired property of finite-sample valid predictive coverage. From a model checking perspective, this serves as an important indicator of the imputation model’s proficiency in efficiently approximating the true data distribution, and is further elaborated in Supplement S.8. When  $y$  follows a discrete distribution, a simple randomization approach of Dunn and Smyth (1996) can be used to provide a surrogate value of  $\hat{F}(y|x)$ . This approach is discussed in detail in Section 5.3.

Checking the condition (12) in a simple and efficient way guides us to use the Kolmogorov–Smirnov test (KS-test, Massey(1951); see also Liu (2023)) for evaluating the effectiveness of the imputation model. Specifically, the  $p$ -value from the KS-test, comparing the imputation distribution outlined in (12) against the standard uniform distribution, serves as a measurement of the effectiveness of imputations. Such a measurement, in turn, serves as a pivotal guide for selecting an appropriate resampling scheme to estimate imputation models.

As investigated in Bickel and Sakov (2008) and Supp-CB (2024), by adaptively choosing the resampling data size  $m$  (with replacement), the  $m$ -out-of- $n$  bootstrap can be a powerful tool in capturing the uncertainty of parameter estimation, especially in high-dimensional settings. In the context of AM, the value of  $m$  is pivotal in regulating “how much we know about the future population.” The smaller the value of  $m$ , the greater the anticipated uncertainty. More specifically, we consider setting  $m = \lceil \tilde{\alpha}n \rceil$ , where  $\tilde{\alpha}$  is the ratio used to control the resampled data size, thereby influencing the effectiveness of the imputation model for achieving (12). The effect of varying  $m$  on such effectiveness is demonstrated using an application example discussed in Section 5. Further illustrations of this are provided in Supplement S.12.1. Based on the goal (12), the following algorithm provides an efficient and straightforward way to choose  $\tilde{\alpha}$  using a small candidate set.

---

**Algorithm 3:** Resampling Scheme Selection

---

- 1 Choose a candidate set of  $\tilde{\alpha}$ , such as  $\{0.2, 0.5, 0.8, 1.0, 1.5\}$ , denoted as  $\tilde{\alpha}$ ;
  - 2 Randomly split the observations  $(\mathbf{x}, \mathbf{y})$  into  $K$  equal subsets  $\{(\mathbf{x}^{(k)}, \mathbf{y}^{(k)})\}_{k=1}^K$ ;
  - 3 **for**  $\tilde{\alpha}$  **in**  $\tilde{\alpha}$  **do**
  - 4     **for**  $k \leftarrow 1$  **to**  $K$  **do**
  - 5         Obtain the empirical distribution  $\tilde{\mathbb{P}}^{(k)}$  by resampling  $m_k = \lceil \tilde{\alpha}n_k \rceil$  observations with replacement from the samples  $(\mathbf{x}^{(-k)}, \mathbf{y}^{(-k)})$  whose sample size is  $n_k$ ;
  - 6         Estimate the imputation model  $\mathbb{Q}_{\hat{\theta}}^{(k)}$  by solving the AM objective (8) with the empirical distribution  $\hat{\mathbb{P}} = \tilde{\mathbb{P}}^{(k)}$  and the future population  $\mathbb{P} = \hat{\mathbb{P}}^{(k)} := (\mathbf{x}^{(-k)}, \mathbf{y}^{(-k)})$ ;
  - 7         Calculate the KS-test statistic of the imputation distribution described in (12) against the standard uniform distribution, denoted by  $P_{\tilde{\alpha}}$  the corresponding  $p$ -value;
  - 8 Return  $\tilde{\alpha} = \arg \max_{\tilde{\alpha}} P_{\tilde{\alpha}}$ .
- 

In our experiments, the optimal  $\tilde{\alpha}$  typically results in  $p$ -values ranging from 0.8 to 1 with small to moderate sample sizes ( $n = 10$  to  $n = 100$ , Sections 5.1 and 5.2). In the  $n = 60,000$  case in Section 5.3, our numerical experiments have shown that the best  $p$ -value typically ranges from 0.1 to 0.3 and is never lower than 0.05, which is satisfactory given the greatly increased large-sample sensitivity of KS-test. Moreover, the results are demonstrated to be robust with respect to the grid density of the candidate set, as long as the set covers a reasonable range, for example, from 0.2 to 1.5. Further evidence supporting

Algorithm 3 is presented by the quantile-quantile (Q-Q) plots in Supplement S.12.2, which indicate effective approximations to (12) and, thereby, satisfactory imputation.

Once a satisfactory  $\tilde{\alpha}$  is obtained, Algorithm 2 can be readily applied to estimate imputation models and generate future observations, by choosing the resampling scheme  $r(\cdot)$  as the  $m$ -out-of- $n$  bootstrap with  $m = \lceil \tilde{\alpha}n \rceil$ .

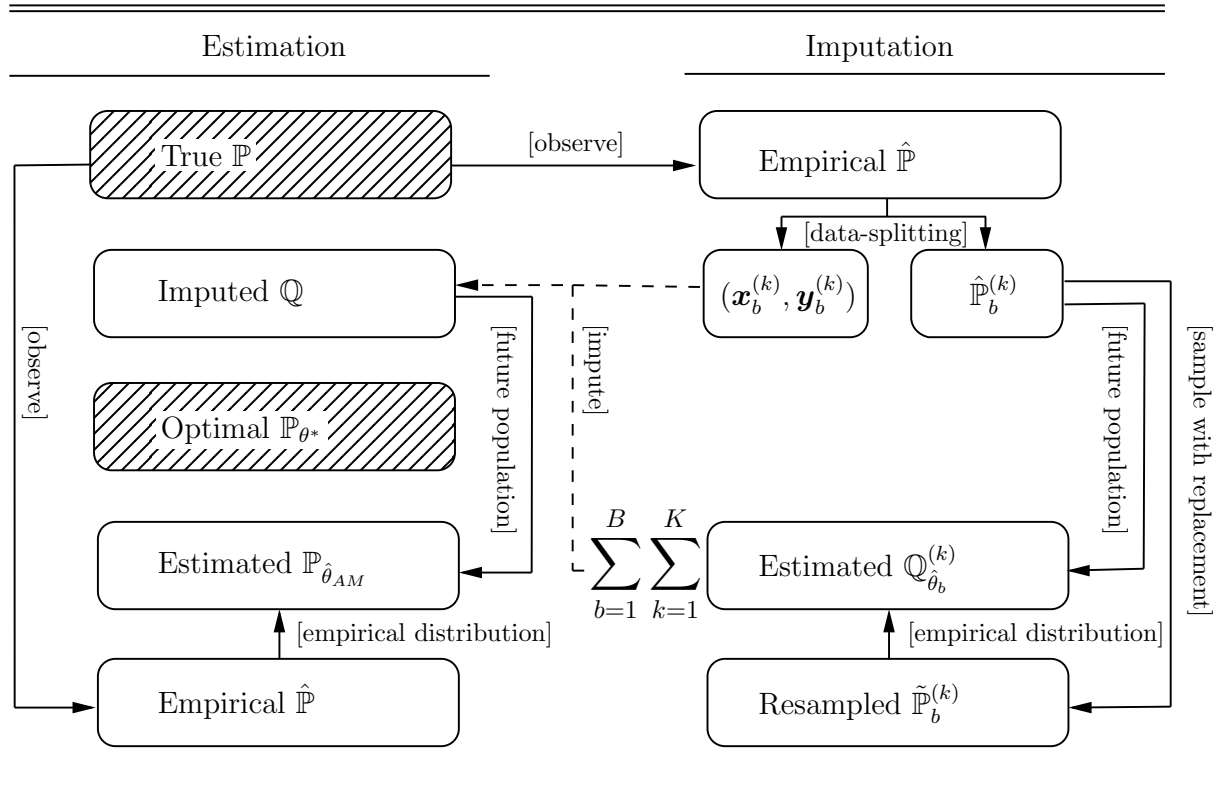


**Figure 1:** The graphical illustration of the proposed imputation-estimation scheme described in Algorithms 2 and 1. The symbol  $\sum_{b=1}^B \sum_{k=1}^K$  between the two columns stands for a mixture of  $B \cdot K$  imputation models. The notation  $\mathbb{P}_{\theta^*}$  denotes the distribution obtained with the optimal estimate by (3). The two distributions denoted by  $\hat{\mathbb{P}}$  in both columns are identical. The unknown distributions are shaded.

For clarity, a pictorial representation of the main components of the proposed framework is given in Figure 1. A simple illustrative example is provided in Supplement S.1. The clarity of AM is elaborated further by the following remarks. Furthermore, the computational efficiency of the AM method, along with its advantages over the cross-validation framework, is detailed in Supplement S.13.

**Remark 2.** *The estimation procedure (Algorithm 1) can also be viewed as combining individual imputation models to obtain a single model, analogous to bootstrap and Bayesian averaging. This approach is particularly relevant to over-parameterized models, where the effectiveness of bootstrap and Bayesian-like averaging is questionable.*

**Remark 3.** *The proposed imputation method shares the conceptual similarities with existing ensemble techniques, notably Bagging and Stacking, which are well-established in the fields of statistics and machine learning (Breiman, 1996; Wolpert, 1992). The essence of the ensemble approach is to develop multiple high-variance base models and integrate them to achieve a robust prediction system. Similarly, our method involves the generation of  $B \cdot K$  base imputation models, each based on a different subset of the resampled data. This approach aligns with the principles of the bagging technique (Breiman, 1996), where multiple models are generated from varied data subsets. The integration of these  $B \cdot K$  base*

models incorporates principles from the stacking technique (Wolpert, 1992), where the collective outputs of the base models are further leveraged. However, being different from the ensemble approach, our method is motivated by statistical modeling and only keeps a single model. Because of this key difference, our method contributes significantly to the ease of both interpreting and inferring the model.

### 3 Numerical Optimization Methods

In this section, we develop efficient numerical optimization algorithms for the AM estimator. For ease of analysis, we assume that the regularity conditions for both the loss function and the duality function, as detailed in Supplement S.2, are satisfied. Since the imputation step, implemented with Algorithm 2 and 3, and the estimation step with Algorithm 1 involve identical optimization problems, this section will focus on the estimation step. Specifically, we aim to solve

$$\min_{\theta, \lambda} G_{\hat{\mathbb{P}}}(\theta, \lambda) + V_{\mathbb{Q}, \hat{\mathbb{P}}}(\theta, \lambda), \quad \text{subject to} \quad \theta = \arg \min_{\tilde{\theta}} G_{\hat{\mathbb{P}}}(\tilde{\theta}, \lambda), \quad (13)$$

where the  $G$  function and the  $V$  function take the form (6) and (7) respectively. Ideally, the solution  $(\hat{\theta}, \hat{\lambda})$  can minimize both  $G_{\hat{\mathbb{P}}}(\theta, \lambda)$  and  $V_{\mathbb{Q}, \hat{\mathbb{P}}}(\theta, \lambda)$ . This amounts to requiring

$$\left. \frac{\partial G_{\hat{\mathbb{P}}}(\theta, \lambda)}{\partial \theta_j} \right|_{\theta=\hat{\theta}, \lambda=\hat{\lambda}} = \left( \frac{1}{n} \sum_{i=1}^n \frac{\partial L(\theta|x_i, y_i)}{\partial \theta_j} + \frac{\partial \pi(\theta, \lambda)}{\partial \theta_j} \right) \Big|_{\theta=\hat{\theta}, \lambda=\hat{\lambda}} = 0 \quad (14)$$

for  $j = 1, \dots, p$ , and  $V_{\mathbb{Q}, \hat{\mathbb{P}}}(\theta, \lambda)$  satisfying

$$\left. \frac{\partial V_{\mathbb{Q}, \hat{\mathbb{P}}}(\theta, \lambda)}{\partial \theta_j} \right|_{\theta=\hat{\theta}, \lambda=\hat{\lambda}} = 0 \quad (15)$$

for  $j = 1, \dots, p$ . Subgradient methods (Shor et al., 1985) can be used if the duality function  $\pi(\theta, \lambda)$  is non-differentiable.

However, the requirement (15) may not be achievable due to the constraints on the duality parameter space  $\Lambda^{(n)}$  such as  $\Lambda^{(n)} = \{\lambda : \lambda \in \mathbb{R}^p, \lambda_j \geq 0 \text{ for } j = 1, \dots, p\}$ . For a generalized method to overcome the difficulty, we consider the values of  $\lambda_j$ 's that minimize the magnitude of the quantity on the left-hand side of (15) for  $j = 1, \dots, p$ . This can be done by considering

$$\hat{\lambda} = \arg \min_{\lambda} \sum_{j=1}^p \left| \frac{\partial V_{\mathbb{Q}, \hat{\mathbb{P}}}(\theta, \lambda)}{\partial \theta_j} \right|_{\theta=\hat{\theta}}, \quad (16)$$

where

$$\left| \frac{\partial V_{\mathbb{Q}, \hat{\mathbb{P}}}(\theta, \lambda)}{\partial \theta_j} \right| = \left| E_{(X, Y) \sim \mathbb{Q}} \left[ \frac{\partial L(\theta|X, Y)}{\partial \theta_j} \right] - \frac{1}{n} \sum_{i=1}^n \frac{\partial L(\theta|x_i, y_i)}{\partial \theta_j} - \frac{\partial \pi(\theta, \lambda)}{\partial \theta_j} \right|$$

for  $j = 1, \dots, p$ . It is interesting to see that for many types of the duality function, including those used in the numerical examples in this paper such as  $\pi(\theta, \lambda) = \sum_{j=1}^p \lambda_j |\theta_j|$  with  $\Lambda = \{\lambda : \lambda \in \mathbb{R}^p, \lambda_j \geq 0 \text{ for } j = 1, \dots, p\}$ ,  $\hat{\lambda}$  in (16) is given by

$$\hat{\lambda}_j = \arg \min_{\lambda_j} \left| \frac{\partial V_{\mathbb{Q}, \hat{\mathbb{P}}}(\theta, \lambda)}{\partial \theta_j} \right|_{\theta=\hat{\theta}} \quad (17)$$



for  $j = 1, \dots, p$ .

To conclude, the solution  $(\hat{\theta}, \hat{\lambda})$  is an equilibrium point that simultaneously satisfies (14) and (16). Intuitively, for obtaining a feasible solution  $(\hat{\theta}, \hat{\lambda})$ , first note that the objective (14) provides a constraint on  $\theta$  given  $\lambda$ , from which  $\theta$  can be seen as a function of  $\lambda$ , denoted by  $\theta_\lambda$ . With such a constraint, the other objective (16) can be seen as a function solely depending on  $\lambda$ , given by  $\zeta(\lambda) = \sum_{j=1}^p \left| \frac{\partial V_{\mathbb{Q}, \hat{\mathbb{P}}}(\theta, \lambda)}{\partial \theta_j} \right|_{\theta=\theta_\lambda}$ . In this way, it remains to solve the single  $\theta$ -free objective function for  $\hat{\lambda} = \arg \min_{\lambda} \zeta(\lambda)$ . This naturally leads to Algorithm 4. For ease of implementation, the target (16) can also be implemented to minimize

$$\left\| \frac{\partial V_{\mathbb{Q}, \hat{\mathbb{P}}}(\theta, \lambda)}{\partial \theta} \right\|_2^2 = \left\| E_{(X,Y) \sim \mathbb{Q}} \left[ \frac{\partial L(\theta|X, Y)}{\partial \theta} \right] - \frac{1}{n} \sum_{i=1}^n \frac{\partial L(\theta|x_i, y_i)}{\partial \theta} - \frac{\partial \pi(\theta, \lambda)}{\partial \theta} \right\|_2^2$$

over  $\lambda$ , where  $\|\cdot\|_2^2$  denotes the squared Euclidean norm.

---

**Algorithm 4:** Coordinate Descent Algorithm for Iterative Updates of  $\theta$  and  $\lambda$

---

- 1 Choose starting values  $(\theta^{(0)}, \lambda^{(0)})$  and set  $t \leftarrow 0$ ;
  - 2 **while**  $\theta^{(t)}$  **has not converged** **do**
  - 3     Compute  $\frac{1}{n} \sum_{i=1}^n \frac{\partial L(\theta|x_i, y_i)}{\partial \theta}$  and  $E_{(X,Y) \sim \mathbb{Q}} \left[ \frac{\partial L(\theta|X, Y)}{\partial \theta} \right]$  at the current estimate  $\theta^{(t)}$ ;
  - 4     Fix  $\lambda = \lambda^{(t)}$ , update  $\theta^{(t)}$  to  $\theta^{(t+1)}$  toward the target (14) with one gradient descent step;
  - 5     Fix  $\theta = \theta^{(t+1)}$ , update  $\lambda^{(t)}$  to  $\lambda^{(t+1)}$  toward the target (16) with one gradient descent step;
  - 6     Set  $t = t + 1$ ;
  - 7 Return converged values  $\theta^{(t)}$ .
- 

Numerous variants of Algorithm 4 can be developed. For example, a stochastic coordinate descent algorithm can be easily obtained as a stochastic variant of Algorithm 4 by replacing the update steps for  $\theta$  and  $\lambda$  with, for example, the stochastic gradient descent (SGD) updates or the ADAM updates (Kingma and Ba, 2014). This variant is used in Section 5.3 for the neural network application. For all the numerical examples in this paper, Algorithm 4 and its variants produce satisfactory convergence results. Formal theoretical properties of these numerical methods will be reported elsewhere.

## 4 Theoretical Considerations

### 4.1 Model Validity and Estimation Validity

The success of using modern over-parameterized models for big data has led us to believe that it is important to both consider modeling processes for increasing sample sizes and introduce a new concept of validity or, perhaps more precisely, effectiveness regarding the underlying potential modeling strategies. It is within this context that our mathematical definition of validity is formulated below in this section.

Using the KL divergence denoted by  $D_{KL}(\cdot, \cdot)$ , we measure the optimal efficiency of the model  $\{\mathbb{P}_\theta : \theta \in \Theta^{(n)}\}$  by the *model error*

$$D_{KL}(\mathbb{P}, \mathbb{P}_{\theta^*}) = \min_{\theta \in \Theta^{(n)}} D_{KL}(\mathbb{P}, \mathbb{P}_\theta) \quad (18)$$

with  $\theta^* \in \Theta_*^{(n)}$ , where  $\Theta_*^{(n)}$  is the set of optimal estimate defined in (3). It is noteworthy that for each  $n$ , the model error  $D_{KL}(\mathbb{P}, \mathbb{P}_{\theta^*})$  remains the same for all  $\theta^* \in \Theta_*^{(n)}$ . Moreover,

this model error is irrelevant to estimation methods and depends purely on the model. This leads to the following definition of model validity, which concerns the asymptotic performance of the underlying model as a way of summarizing a relaxed requirement in practice that has something to do with the cognition that “all models are wrong” (Box, 1976, see also Tukey (1954) and von Neumann (1947)).

**Definition 1** (Model Validity). *A model  $\{\mathbb{P}_\theta : \theta \in \Theta^{(n)}\}$ , or a sequence of models indexed by the sample size  $n$ , is said to be valid iff  $\lim_{n \rightarrow \infty} D_{KL}(\mathbb{P}, \mathbb{P}_{\theta^*}) = 0$  for any  $\theta^* \in \Theta_*^{(n)}$ .*

Conceptually, Definition 1 relaxes the canonical assumption of exact correct specification of the model with any finite sample sizes, which is typically used to establish the asymptotic “correctness” the model. The following Proposition 1 and 2 illustrate how this definition of model validity relates to conventional statistical assumptions. To begin, we introduce the concept of model generality for future reference.

**Definition 2** (Model Generality). *A parametric model  $\mathbb{P}_\theta$  with parameter  $\theta \in \Theta$  is said to be a special case of another parametric model  $\mathbb{P}_\phi$  with parameter  $\phi \in \Phi$ , written as  $\mathbb{P}_\theta \preceq \mathbb{P}_\phi$  or  $\Theta \preceq \Phi$ , if there exists a continuous onto mapping  $\psi : \Phi \mapsto \Theta$  such that for all  $\theta \in \Theta$ , there exists a  $\phi \in \psi^{-1}(\theta) \subseteq \Phi$  satisfying  $\mathbb{P}_\theta = \mathbb{P}_\phi$ . If  $\mathbb{P}_\theta \preceq \mathbb{P}_\phi$ ,  $\mathbb{P}_\phi$  is said to be more general than or equal to  $\mathbb{P}_\theta$ , written as  $\mathbb{P}_\phi \succeq \mathbb{P}_\theta$  or  $\Phi \succeq \Theta$ .*

**Proposition 1.** *Suppose  $\mathbb{P} = \mathbb{P}_{\theta_0}$ ,  $\theta_0 \in \Theta_0$ , where  $\Theta_0$  is the parameter space for the true model parameter  $\theta_0$ . Then, the model  $\{\mathbb{P}_\theta : \theta \in \Theta_0\}$  is valid by Definition 1.*

**Proposition 2.** *Suppose  $\mathbb{P} = \mathbb{P}_{\theta_0}$ ,  $\theta_0 \in \Theta_0$ . If there exists a positive integer  $N$  such that  $\Theta_0 \preceq \Theta^{(n)}$  for all  $n \geq N$ , then the model  $\{\mathbb{P}_\theta : \theta \in \Theta^{(n)}\}$  is valid by Definition 1.*

The proof of the two propositions is given in Supplement S.3. As demonstrated in Proposition 2, Definition 1 validates the applicability of some over-parameterized models whose parameter space consistently covers the true parameter space. Accordingly, for a given data set  $\{(x_i, y_i)\}_{i=1}^n$ , estimation methods strive for reducing the non-negative estimation error

$$D_{KL}(\mathbb{P}, \mathbb{P}_{\hat{\theta}}) - D_{KL}(\mathbb{P}, \mathbb{P}_{\theta^*}) \tag{19}$$

with some parameter estimate  $\hat{\theta} \in \Theta^{(n)}$ , where  $\theta^* \in \Theta_*^{(n)}$ . This leads to the following definition of estimation validity, indicating an asymptotically vanishing estimation error.

**Definition 3** (Estimation Validity). *An estimator  $\hat{\theta} \in \Theta^{(n)}$  is said to be valid iff*

$$D_{KL}(\mathbb{P}, \mathbb{P}_{\hat{\theta}}) - D_{KL}(\mathbb{P}, \mathbb{P}_{\theta^*}) \xrightarrow{p} 0, \quad n \rightarrow \infty,$$

*for any  $\theta^* \in \Theta_*^{(n)}$ . Such an estimator is said to provide a method of valid estimation.*

**Proposition 3.** *Suppose that  $\mathbb{P} = \mathbb{P}_{\theta_0}$ ,  $\theta_0 \in \Theta_0$  and that the likelihood function is continuous on  $\Theta_0$ . Any consistent estimator  $\hat{\theta} \in \Theta_0$  such that  $\hat{\theta} \xrightarrow{p} \theta_0$ , is valid by Definition 3.*

The proof of Proposition 3 is given in Supplement S.3. Using the above definitions, it can be concluded that valid estimation (Definition 3) using a valid model (Definition 1) results in the asymptotic “correctness” in terms of  $D_{KL}(\mathbb{P}, \mathbb{P}_{\hat{\theta}}) \xrightarrow{p} 0$ .

## 4.2 Estimation Validity of AM

Here, we show that the proposed AM estimator is valid by Definition 3 under mild conditions. Note that the AM objective (8) involves two distributions: one for the future population and the other for the empirical distribution. The AM imputation-estimation scheme introduced in Sections 2.2 and 2.3 requires utilizing different data samples to represent these two distributions. For simplicity, with a modified notation, we define the AM operator  $\mathfrak{A}_\theta : \mathbb{P}_{fut} \times \mathbb{P}_{emp} \rightarrow \mathbb{R}^p$ , where  $\mathbb{P}_{fut}$  plays the role of the future population and  $\mathbb{P}_{emp}$  plays the role of the empirical distribution. The operator results in a vector representing the parameter estimated by solving (8). The AM imputation-estimation framework, utilizing these simplified notations, is illustrated in Figure 2. For ease of theoretical analysis, it is assumed that each optimization process, as denoted by the AM operator  $\mathfrak{A}_\theta$ , gives the global optimal solution with respect to its objective function. Similar to other methods of model estimation, the pursuit of the global optimal solution for the AM objective function depends on the numerical optimization algorithm, particularly the optimizer. However, this aspect is beyond the scope of our current discussion.

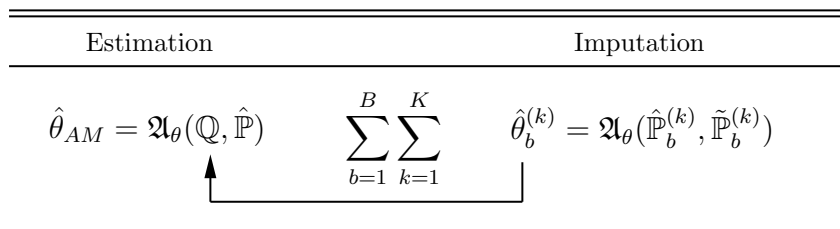


**Figure 2:** The simplified AM imputation-estimation framework using the AM operator  $\mathfrak{A}_\theta$ . The involved distributions are described in Algorithm 2 and 1.

With the above notation, the desired AM estimator is expressed as

$$\hat{\theta}_{AM}^* = \mathfrak{A}_\theta(\mathbb{P}, \hat{\mathbb{P}}) \quad (20)$$

with  $\hat{\theta}_{AM}^* \in \Theta^{(n)}$ . Since the true distribution  $\mathbb{P}$  is unknown in practice, (20) represents the optimal estimator achievable with AM under the assumption of “perfect” imputation. The following theorem and its corollary demonstrate the validity of the estimator (20) under mild conditions, with the proof given in Supplement S.4 and S.5, respectively.

**Theorem 1** (Validity of AM). *Suppose that there exists a model  $\{\mathbb{P}_\phi : \phi \in \Phi\}$  with compact parameter space  $\Phi$  such that  $\Phi \preceq \Theta^{(n)}$  for every  $n \geq N$ , where  $N$  is some positive integer, satisfying*

$$\min_{\phi \in \Phi} D_{KL}(\mathbb{P}, \mathbb{P}_\phi) = \lim_{n \rightarrow \infty} D_{KL}(\mathbb{P}, \mathbb{P}_{\theta^*}) \quad (21)$$

for any  $\theta^* \in \Theta_*^{(n)}$ . Assume that the loss function takes the form (2) and the regularity conditions in Supplement S.2 hold. Then, the optimal AM estimator  $\hat{\theta}_{AM}^* = \mathfrak{A}_\theta(\mathbb{P}, \hat{\mathbb{P}}) \in \Theta^{(n)}$  is valid by Definition 3.

**Corollary 1.** *Suppose  $\mathbb{P} = \mathbb{P}_{\theta_0}$ ,  $\theta_0 \in \Theta_0$ , where  $\Theta_0$  is the parameter space for the true model parameter  $\theta_0$ . Assume  $|\theta_{0j}| < \infty$ , for  $j = 1, \dots, p$ . If there exists a positive integer  $N$  such that  $\Theta_0 \preceq \Theta^{(n)}$  for every  $n \geq N$ , the condition (21) holds.*

In practice, Algorithm 2 provides an imputation population  $\mathbb{Q}$  as an approximation to the true population distribution  $\mathbb{P}$ , and the AM estimator takes the form  $\hat{\theta}_{AM} = \mathfrak{A}_\theta(\mathbb{Q}, \hat{\mathbb{P}})$ . Lemma 1 below demonstrates the validity of the AM estimator using the “asymptotically correct” imputation distribution, with the proof given in Supplement S.6.

**Lemma 1.** Assume that  $D_{KL}(\mathbb{P}, \mathbb{Q}) \xrightarrow{P} 0$ , and that the conditions in Theorem 1 hold. Then, the AM estimator  $\hat{\theta}_{AM} = \mathfrak{A}_\theta(\mathbb{Q}, \hat{\mathbb{P}}) \in \Theta^{(n)}$  is valid by Definition 3.

Next, we establish the asymptotic correctness of the imputation distribution. The result is summarized by the following theorem, with its proof provided in Supplement S.7.

**Theorem 2** (Imputation Consistency). *Let the parameters  $B$  and  $K$ , which determine the number of imputation models, be fixed. Suppose that there exists a constant  $\tilde{\alpha}_0 \in (0, 1)$  such that the resampling ratio  $\tilde{\alpha}$  used in the  $m$ -out-of- $n$  bootstrap has  $\tilde{\alpha} \geq \tilde{\alpha}_0$  for every  $n \geq N$ , where  $N$  is some positive integer. Assume that  $D_{KL}(\mathbb{P}, \hat{\mathbb{P}}) \xrightarrow{P} 0$  and that the model is valid by Definition 1. If the conditions in Theorem 1 hold, then  $D_{KL}(\mathbb{P}, \mathbb{Q}) \xrightarrow{P} 0$ .*

Finally, by synthesizing the results of Theorem 1 and Lemma 1, Theorem 2 establishes the validity of the AM estimator  $\hat{\theta}_{AM} = \mathfrak{A}_\theta(\mathbb{Q}, \hat{\mathbb{P}})$  according to Definition 3.

## 5 Applications

### 5.1 Simultaneous Estimation of Many Normal Means

The many-normal-means problem is about making inference on the unknown means  $\mu_1, \dots, \mu_n$  from the sample  $y_1, \dots, y_n$  with the model  $Y_i | \{\mu_1, \dots, \mu_n\} \sim N(\mu_i, 1)$ ,  $i = 1, \dots, n$ , where  $y_1, \dots, y_n$  are independent of each other (*c.f.* a recent discussion by Qiu and Wang (2021) and references therein). In the context of Section 2, where  $y_1, \dots, y_n$  are assumed to be sampled from a single unknown population, an intriguing way of formulating this problem is to consider  $\mu_1, \dots, \mu_n$  as missing values taken from a different unknown population. That is, at a high level, we consider the empirical Bayes approach similar to the  $g$ -modeling (Efron, 2016). More specifically, the model can be written as

$$\mu_i \sim \mathbb{P}_\theta \quad \text{and} \quad Y_i | \mu_i \sim N(\mu_i, 1) \quad (Y_i \in \mathbb{Y}, \theta \in \Theta^{(n)} \subseteq \mathbb{R}^p)$$

for  $i = 1, \dots, n$ . Although more general and alternative non-parametric models for  $\mathbb{P}_\theta$  can be considered, we opt for a simple approach by considering a discrete distribution at  $l$  ( $l \geq n$ ) unknown points  $\eta_1 \leq \eta_2 \leq \dots \leq \eta_l$  with the probability mass  $P(\mu = \eta_j) = \alpha_j$ ,  $j = 1, \dots, l$ .

It follows that the observed-data likelihood based on  $y_i$  is given by  $\frac{1}{\sqrt{2\pi}} \sum_{j=1}^l \alpha_j e^{-\frac{(y_i - \eta_j)^2}{2}}$ .

Unlike Efron (2016) where  $\eta_1, \dots, \eta_l$  are fixed, in our approach,  $\eta_1, \dots, \eta_l$  are parameters to be estimated, resulting in an over-parameterized empirical Bayes model. In the following simulation studies, the AM framework is used for estimating the discrete distribution model  $\mathbb{P}_\theta$ , which provides an approximation to the true distribution. By writing  $\theta_1 = \eta_1$ ,  $\theta_j = \eta_j - \eta_{j-1}$  for  $j = 2, \dots, l$  and  $\theta_{l+j} = \alpha_j$  for  $j = 1, \dots, l$ , we define the duality function as

$$\pi(\theta, \lambda) = \sum_{j=2}^l \lambda_j |\theta_j| \quad (\lambda_j \geq 0 \text{ for } j = 2, \dots, l).$$

It is important to note that imposing  $\lambda_2 = \dots = \lambda_l$  simplifies the duality function to  $\pi(\theta, \lambda) = \lambda(\eta_l - \eta_1)$  where  $\lambda \geq 0$ . However, this reduced form is less ideal since it provides much less flexibility for parameter estimation; See Section 6. The technical and implementation details of the AM framework for this problem are provided in Supplement S.9.

With the estimated parameter  $\hat{\theta}_1, \dots, \hat{\theta}_{2l}$ , the posterior mean of  $\mu_i$  given  $y_i$  is taken as the point estimate of  $\mu_i$ , namely  $\hat{\mu}_i = \hat{\mu}_i^{AM} = E_{\mu_i \sim \mathbb{P}_{\hat{\theta}}}(\mu_i | y_i)$ . The mean prediction error (MPE), equivalent to the average total squared error, is calculated as

$$\text{MPE} = \frac{1}{n} \sum_{i=1}^n (\mu_i - \hat{\mu}_i)^2. \quad (22)$$

For comparison with other methods in addition to the  $g$ -modeling, we consider the maximum likelihood estimator (MLE)  $\hat{\mu}_i^{MLE} = y_i$  and the James-Stein estimator

$$\hat{\mu}_i^{JS} = \bar{y} + \left[ 1 - \frac{n-3}{\sum_{i=1}^n (y_i - \bar{y})^2} \right] (y_i - \bar{y}), \quad i = 1, \dots, n,$$

where  $\bar{y}_i = (1/n) \sum_{i=1}^n y_i$ . The James-Stein estimator shrinks the MLE estimator of each  $\mu$  towards the overall sample mean of the observed data and has been shown to dominate the MLE estimator when  $n \geq 3$  (James and Stein, 1961; Stein, 1956).

For numerical comparison, three simulation studies are considered. The first simulation study is on the case in favor of the James-Stein estimator:  $\mu_i \sim N(0, A)$ , where  $A$  is the scale parameter. Efron and Hastie (2016) shows that the expected MPE of the James-Stein estimator has the closed-form expression  $E \left( \frac{1}{n} \sum_{i=1}^n (\mu_i - \hat{\mu}_i^{JS})^2 \right) = \frac{A}{A+1} + \frac{3}{n} \left( 1 - \frac{A}{A+1} \right)$ . Also note that for MLE, the expected MPE is  $E \left( \frac{1}{n} \sum_{i=1}^n (\mu_i - \hat{\mu}_i^{MLE})^2 \right) = 1$ . This suggests that when  $n \geq 3$  and  $A = 0$ , the James-Stein estimator performs the best such that it will provide the greatest reduction of MPE compared to MLE. To maintain the randomness of  $\mu$ , we set  $A = 0.01$ , a value that is close to 0.

The second simulation study concerns the multi-modal case: half of the  $n$  unknown means are from  $N(-2, 0.01)$  and the other half from  $N(2, 0.01)$ . This generates a bimodal distribution of the observed samples. Ideally, the sample means should shrink towards the two modes, depending on their locations. Since the James-Stein estimator can only shrink the sample means toward its overall mean, it will not provide satisfactory shrinkage in this case. More discussion along this line can also be found in Escobar (1994).

The third simulation study, considers a normal model example presented in Narasimhan and Efron (2020), which is used to introduce the developed statistical software for  $g$ -modeling, `deconvolveR`. Each  $\mu$  is set to be 0 with probability 0.9 and is generated from  $N(-3, 1)$  with probability 0.1. This simulates a scenario where the true model is zero-inflated and the true non-zeros  $\mu$ s are sparse.

For all simulation studies, three different sample sizes,  $n = 10, 20$ , and 50 are considered. For each case,  $M = 200$  data sets are generated. AM, the James-Stein estimator, and  $g$ -modeling are applied to each data set with MPE calculated as in (22). The mean of the MPE is taken over the corresponding estimate in  $M$  data sets. For the AM method, we set the number of unknown points to be  $l = n$  and performed the imputation with  $B = 5$  and  $K = 5$  using Algorithm 2, with the resampling parameter  $\tilde{\alpha}$  selected by Algorithm 3.

The results are summarized in Table 1. They suggest that the AM method performs better than the other three methods in all three simulation examples. Notably, the reduction in MPE by AM is most significant in the second simulation, which involves bimodal distribution samples, compared to the James-Stein estimator. Figure 3 visualizes the shrinkage patterns of the AM and James-Stein methods in a typical data set from the simulation. It shows that AM shrinks all of the sample mean towards the correct direction. In contrast, the James-Stein estimator uniformly pulls sample means towards the overall mean, regardless of their original location.

**Table 1:** MPE results under three simulation settings with different methods. Each entry is taken as the average value obtained with 200 repetitions and the standard deviation of each value (estimated with bootstrap) is given in parentheses. The best result in each setting is highlighted in boldface.

Method	$\mu \sim N(0, 0.01)$			$\mu^1 \sim N(-2, 0.01)$ $\mu^2 \sim N(2, 0.01)$			$\mu^1 = 0$ $\mu^2 \sim N(-3, 1)$		
	$n = 10$	$n = 20$	$n = 50$	$n = 10$	$n = 20$	$n = 50$	$n = 10$	$n = 20$	$n = 50$
MLE	0.996 (0.031)	0.977 (0.023)	1.012 (0.013)	0.936 (0.028)	1.016 (0.023)	1.020 (0.014)	1.015 (0.032)	0.999 (0.023)	0.998 (0.013)
James-Stein	0.302 (0.022)	0.161 (0.012)	0.064 (0.004)	0.836 (0.025)	0.857 (0.019)	0.829 (0.012)	0.548 (0.028)	0.497 (0.019)	0.499 (0.011)
$g$ -modeling	0.375 (0.019)	0.383 (0.015)	0.180 (0.006)	0.722 (0.026)	0.738 (0.019)	0.758 (0.014)	0.571 (0.025)	0.528 (0.018)	0.384 (0.010)
Auto-Modeling	<b>0.204</b> <b>(0.022)</b>	<b>0.120</b> <b>(0.012)</b>	<b>0.061</b> <b>(0.005)</b>	<b>0.544</b> <b>(0.039)</b>	<b>0.482</b> <b>(0.029)</b>	<b>0.384</b> <b>(0.018)</b>	<b>0.446</b> <b>(0.031)</b>	<b>0.383</b> <b>(0.022)</b>	<b>0.328</b> <b>(0.013)</b>

As a remark, the gain of AM over  $g$ -modeling may be explained by (i) AM provides a more flexible choice of the means  $\mu_1, \dots, \mu_n$ , and (ii) AM provides a better method in estimation by fitting models to future observations, while the hyper-parameters of  $g$ -modeling are still estimated by the method of maximum likelihood.

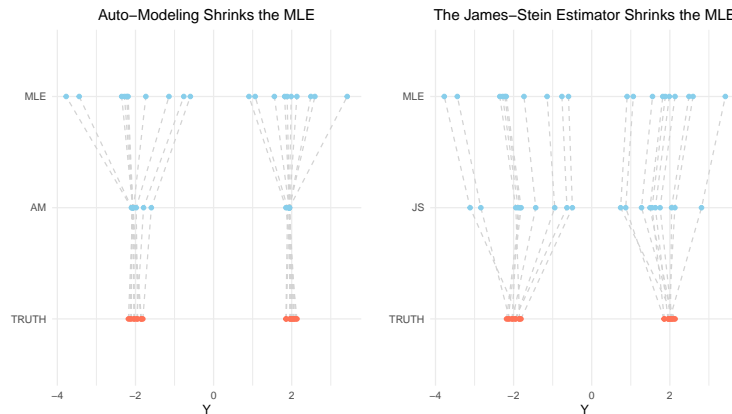


**Figure 3:** Shrinkage pattern of the James-Stein estimator and AM in the bimodal simulation example with a typical data set.

## 5.2 The $n < p$ Linear Regression

Consider the linear regression with  $p$  predictors and  $n$  observations  $\{(x_i, y_i) : i = 1, \dots, n\}$ :

$$y_i = x_i' \beta + \epsilon_i \quad (y_i \in \mathbb{R}, x_i \in \mathbb{R}^p \text{ for } i = 1, \dots, n; \beta \in \mathbb{R}^p),$$

where  $x_i = (x_{i1}, \dots, x_{ip})'$  is a  $p$ -dimensional vector,  $\epsilon_i \sim N(0, \sigma^2)$ , and  $\beta = (\beta_1, \dots, \beta_p)'$ . In the high-dimensional case of  $n < p$ , the estimation of the model parameters can be challenging due to the residuals approaching zero, and may rely on regularization techniques such as Lasso (Tibshirani, 1996) and ridge (Hoerl and Kennard, 1970). However, these methods can not directly provide a good estimate of the variance term  $\hat{\sigma}$ , and additional techniques (Reid et al., 2016; Yu and Bien, 2019) are required. Moreover, even with the estimated variance term, the finite-sample parametric prediction interval coverage can not be guaranteed. Here with a simulation study, we show that the proposed AM can not only produce an efficient point estimate of future observations but also provide a satisfactory parametric prediction interval coverage.

For AM, we write the loss function as

$$L(\beta, \sigma | X = x, Y = y) = \frac{1}{2} \log(\sigma^2) + \frac{1}{2\sigma^2 n} \sum_{i=1}^n (y_i - x_i' \beta)^2$$

and consider the weighted  $L_1$  duality function

$$\pi(\beta, \sigma, \lambda) = \lambda_0 \log\left(\frac{1}{\sigma^2}\right) + \sum_{j=1}^p \lambda_j |\beta_j| \quad (\lambda_j \geq 0, j = 0, 1, \dots, p),$$

the weighted  $L_2$  duality function

$$\pi(\beta, \sigma, \lambda) = \lambda_0 \log\left(\frac{1}{\sigma^2}\right) + \sum_{j=1}^p \lambda_j \beta_j^2 \quad (\lambda_j \geq 0, j = 0, 1, \dots, p),$$

as well as their unweighted versions obtained by imposing  $\lambda_1 = \dots = \lambda_p$ . The technical and implementation details of the AM framework are provided in Supplement S.10.

We consider the simulation setting in Reid et al. (2016) and Yu and Bien (2019). Let  $p = 500$  and  $n = 100$ . Each row of the design matrix  $\mathbf{x}$  is generated from a multivariate normal distribution  $N(0, \Sigma)$ . The covariance matrix  $\Sigma$  is structured such that  $\Sigma_{ii} = 1$  and  $\Sigma_{ij} = \rho$  for  $i \neq j$ . The regression coefficient vector  $\beta$  has  $\lceil n^\alpha \rceil$  non-zero elements, where  $\alpha$  is a parameter that controls the sparsity of  $\beta$ . These non-zero elements of  $\beta$  are randomly selected and follow a Laplace distribution with unit rate. The error variance in the model is determined by the parameter  $\tau$  and is calculated as  $\sigma^2 = \frac{1}{\tau} \beta^T \Sigma \beta$ . We set  $\rho = 0.5$  and vary  $\alpha \in \{0.3, 0.6, 0.9\}$  and  $\tau \in \{0.3, 1, 3\}$ . 100 data sets are generated under each specific setting. For other methods to be compared with, we consider Lasso (Tibshirani, 1996), ridge (Hoerl and Kennard, 1970), the elastic net (Zou and Hastie, 2005), and the adaptive Lasso (Zou, 2006). These methods are applied with the cross-validation framework implemented in the R package `glmnet` (Friedman et al., 2010). We evaluate the mean-squared error (ME) of different methods with

$$\text{ME} = (\hat{\beta} - \beta)^T \Sigma (\hat{\beta} - \beta),$$

a performance measure provided in Tibshirani (1996). We also evaluate the 95% prediction interval coverage with the additionally simulated data ( $n = 1,000$ ). The prediction interval for the new observed covariate value  $\hat{x}_{new}$  is given by  $\left(\hat{x}_{new} \hat{\beta} - Z_{1-\alpha/2} \hat{\sigma}, \hat{x}_{new} \hat{\beta} + Z_{1-\alpha/2} \hat{\sigma}\right)$ , where  $Z_{1-\alpha/2}$  denotes the CDF value of the standard normal distribution at  $1 - \alpha/2$ , with  $\alpha = 0.05$  in this case. The variance estimator of other methods is obtained with the effective canonical method described in Reid et al. (2016). For AM, the imputation process is performed with the unweighted duality functions, and the final estimation is performed with both weighted and unweighted duality functions for comparison.

The results are summarized in Table 2 and Table 3. We can see that AM greatly outperforms all other methods in terms of ME, regardless of the duality function it uses. Moreover, AM can provide a satisfactory prediction interval coverage under all settings at the 95% level, while all other methods show significant undercoverage.

### 5.3 Image classification with Neural Networks

For an application of the proposed method to the neural network model, we consider a numerical example of image classification with the famous MNIST data set (LeCun et al.,

**Table 2:** Summary of ME results for the linear regression examples with different methods with the simulation data ( $p = 500$ ,  $n = 100$ ). The parameters  $\alpha$  and  $\tau$  are those that control the sparsity of the true signals and the signal-to-noise ratio (SNR). Each entry is taken as the average value obtained with 100 repetitions and the standard deviation of each value (estimated with bootstrap) is given in parentheses. The best result in each setting is highlighted in boldface.

<i>Method</i>	$\alpha = 0.3$			$\alpha = 0.6$			$\alpha = 0.9$		
	$\tau = 0.3$	$\tau = 1$	$\tau = 3$	$\tau = 0.3$	$\tau = 1$	$\tau = 3$	$\tau = 0.3$	$\tau = 1$	$\tau = 3$
AM-weighted- $L_1$	4.24 (0.33)	4.42 (0.47)	4.49 (0.50)	19.08 (0.94)	16.34 (0.87)	16.70 (1.11)	70.79 (1.95)	66.48 (1.90)	67.39 (1.97)
AM-unweighted- $L_1$	<b>3.46</b> <b>(0.27)</b>	<b>2.79</b> <b>(0.31)</b>	<b>2.47</b> <b>(0.34)</b>	17.68 (0.87)	<b>13.51</b> <b>(0.72)</b>	<b>12.71</b> <b>(0.88)</b>	71.79 (2.12)	64.88 (2.05)	<b>61.19</b> <b>(1.84)</b>
AM-weighted- $L_2$	4.45 (0.34)	4.36 (0.46)	4.41 (0.48)	20.07 (0.99)	16.17 (0.86)	16.34 (1.09)	77.01 (2.35)	65.74 (1.85)	65.75 (1.84)
AM-unweighted- $L_2$	3.79 (0.30)	4.03 (0.43)	4.16 (0.46)	<b>17.26</b> <b>(0.85)</b>	15.04 (0.79)	15.55 (1.04)	<b>64.92</b> <b>(1.80)</b>	<b>61.45</b> <b>(1.68)</b>	62.82 (1.79)
Adaptive Lasso	6.19 (0.46)	7.53 (0.92)	6.45 (0.80)	26.22 (1.47)	25.40 (2.20)	25.76 (2.40)	122.94 (8.14)	114.80 (8.65)	128.07 (8.73)
Lasso	5.78 (0.44)	6.34 (0.82)	4.68 (0.67)	25.56 (1.42)	23.93 (2.14)	22.68 (2.34)	121.14 (8.04)	112.83 (8.43)	123.53 (8.39)
Elastic Net	5.72 (0.43)	6.36 (0.82)	4.69 (0.67)	25.33 (1.41)	23.91 (2.14)	22.65 (2.34)	120.37 (8.03)	112.03 (8.43)	123.24 (8.40)
Ridge	6.02 (0.45)	7.11 (0.85)	6.18 (0.74)	25.83 (1.41)	25.11 (2.14)	25.17 (2.36)	121.06 (8.03)	113.47 (8.41)	125.68 (8.36)

**Table 3:** Summary of 95% prediction interval coverage with different methods, under the same settings as Table 2. The result closest to 95% in each setting is highlighted in boldface.

<i>Method</i>	$\alpha = 0.3$			$\alpha = 0.6$			$\alpha = 0.9$		
	$\tau = 0.3$	$\tau = 1$	$\tau = 3$	$\tau = 0.3$	$\tau = 1$	$\tau = 3$	$\tau = 0.3$	$\tau = 1$	$\tau = 3$
AM-weighted- $L_1$	<b>0.947</b> <b>(0.002)</b>	<b>0.950</b> <b>(0.002)</b>	<b>0.948</b> <b>(0.002)</b>	0.947 (0.002)	0.943 (0.002)	0.942 (0.002)	0.947 (0.002)	0.946 (0.002)	<b>0.947</b> <b>(0.002)</b>
AM-unweighted- $L_1$	0.955 (0.002)	0.970 (0.002)	0.982 (0.002)	<b>0.952</b> <b>(0.002)</b>	0.955 (0.002)	0.966 (0.002)	<b>0.951</b> <b>(0.002)</b>	<b>0.952</b> <b>(0.002)</b>	0.960 (0.002)
AM-weighted- $L_2$	0.956 (0.002)	0.958 (0.002)	0.961 (0.002)	0.960 (0.002)	<b>0.954</b> <b>(0.003)</b>	<b>0.952</b> <b>(0.003)</b>	0.957 (0.002)	0.958 (0.002)	0.957 (0.002)
AM-unweighted- $L_2$	0.960 (0.002)	0.963 (0.002)	0.966 (0.002)	0.963 (0.002)	0.958 (0.002)	0.957 (0.002)	0.961 (0.002)	0.962 (0.002)	0.962 (0.002)
Adaptive Lasso	0.923 (0.004)	0.874 (0.007)	0.769 (0.012)	0.902 (0.009)	0.873 (0.007)	0.767 (0.010)	0.916 (0.005)	0.883 (0.010)	0.833 (0.011)
Lasso	0.923 (0.004)	0.908 (0.007)	0.898 (0.009)	0.898 (0.010)	0.885 (0.007)	0.854 (0.009)	0.918 (0.006)	0.885 (0.010)	0.859 (0.010)
Elastic Net	0.915 (0.005)	0.893 (0.008)	0.888 (0.009)	0.891 (0.010)	0.875 (0.007)	0.847 (0.009)	0.906 (0.006)	0.876 (0.010)	0.855 (0.011)
Ridge	0.925 (0.004)	0.871 (0.007)	0.754 (0.010)	0.907 (0.009)	0.868 (0.007)	0.764 (0.011)	0.925 (0.005)	0.891 (0.010)	0.845 (0.011)

1998). The MNIST database is a large database of handwritten digits that is commonly used for training various image processing systems. The training and test sample sizes are 60,000 and 10,000, respectively. For each handwritten digit (0-9), the image size is  $28 \times 28$  pixels, with pixel values measured at gray-scale levels from 0 to 255. Thus, for each observation,  $x_i$  stands for the image and  $y_i$  stands for the label or digit. The classification problem is to predict  $y_i$  given  $x_i$ .

The imputation-estimation scheme of AM proposed in Section 2.3 applied in this particular example is concisely summarized here for better clarity. The imputation process (Algorithm 2) involves estimating models that predict new labels for training digit images. These training images, along with their newly predicted labels, form the imputed future



observations used in the final estimation process with Algorithm 1. Conceptually, each individual image in the data set is associated with multiple, potentially varying labels. This variety in labels acts as a mechanism to effectively prevent the model from overfitting to a single label on the training image.

Two different neural network structures are used to investigate the efficiency of the proposed method. The first structure is a feed-forward neural network with two fully connected layers. The number of nodes in the two hidden layers is chosen to be 400, 800, and 1600. The final layer uses the multivariate logistic link and returns the probabilities for the 10 labels. This classic structure is commonly used in the literature for evaluating model training strategies. The second structure to be considered is described in Jarrett et al. (2009). It is obtained by using the output from a convolutional neural networks (CNN) feature extractor as the input to the first structure. The feature extractor is constructed with two convolutional layers with 32 and 64 channels respectively, each followed by a  $2 \times 2$  max-pooling layer. The size of the filters in each CNN layer is chosen to be  $5 \times 5$  and the number of hidden nodes in the fully connected layers is chosen to be 200. The rectified linear unit (ReLU) activation function is used in all structures.

For each model, denote all the trainable parameters in the model as  $\theta_1, \dots, \theta_p$ . The duality function of AM is defined as the counterpart of the  $L_1$  and  $L_2$  penalty functions,

$$\pi(\theta, \lambda) = \sum_{j=1}^p \lambda_j |\theta_j| \quad \text{or} \quad \pi(\theta, \lambda) = \sum_{j=1}^p \lambda_j \theta_j^2 \quad (\lambda_j \geq 0 \text{ for } j = 1, \dots, p). \quad (23)$$

When applying Algorithm 3 to choose  $m$  for the  $m$ -out-of- $n$  resampling scheme, a continuous CDF value of the data distribution within the range of 0 to 1 is necessary. Here, we adopt and extend the randomization approach proposed by Dunn and Smyth (1996). Denote by  $p_0, p_1, \dots, p_9$  the predicted probabilities for the 10 digits obtained from the final layer for an input image  $x$ , and let  $y$  denote the true label of the image. We randomly select  $F(y|x)$  from a uniform distribution over the interval  $[\sum_{k=0}^{y-1} p_k, \sum_{k=0}^y p_k]$ , where  $\sum_{k=0}^{-1} p_k$  is defined as 0. Comprehensive details and theoretical justifications for this approach are available in Supplement S.11.3. We use  $B = 5$  and  $K = 2$  in the imputation process with Algorithm 2. Further details are given in Supplement S.11 for a comprehensive overview.

For comparison with other methods, the same model structures are trained on the full data set accompanied with fixed scalar (or unweighted)  $L_1$  and  $L_2$  penalties, which are commonly used in neural network training. We record the best outcomes across a reasonable range of penalty values. Additionally, we incorporate the early-stopping technique and the widely-used dropout method (Srivastava et al., 2014). To isolate the effectiveness of our framework from the impact of using weighted duality functions, we perform an additional estimation procedure. In this procedure, we remove this confounding factor by setting  $\lambda_1 = \dots = \lambda_p$  in (23), thereby creating what we refer to as the unweighted duality functions.

The test error results for all the methods, using four different models, are presented in Table 4. A significant performance improvement can be seen when AM is used. Notably, the performance of AM exceeds that of the Dropconnect (Mobiny et al., 2021; Wan et al., 2013), a current state-of-the-art regularization technique, with identical model structures as reported in Wan et al. (2013) and Mobiny et al. (2021). Compared to their method, AM not only demonstrates faster convergence but also offers a more straightforward implementation. The details of the estimation process of AM and the resultant parameters are visually depicted in Supplement S.11.4.

An intriguing aspect of the AM estimator is its tendency to achieve nearly, but not quite, 100% prediction accuracy on training images. By aggregating the training images

**Table 4:** The test error (%) of different methods on the MNIST data set with different structures. FC X-X in the header of the table denotes the fully-connected network with two hidden layers where the number of hidden nodes is X, and the values in the parentheses denote the number of parameters in the corresponding structure. The reported value is the mean taken over 5 repetitions (with standard deviations given in parentheses). The best two results in each structure are highlighted in boldface.

<i>Method</i>	FC 400-400 (478,410)	FC 800-800 (127,6810)	FC 1600-1600 (383,3610)	CNN (299,306)
AM-weighted- $L_1$	1.222 (0.040)	1.244 (0.042)	1.202 (0.052)	<b>0.584 (0.043)</b>
AM-unweighted- $L_1$	<b>1.180 (0.040)</b>	<b>1.172 (0.064)</b>	<b>1.093 (0.059)</b>	0.586 (0.038)
AM-weighted- $L_2$	<b>1.178 (0.040)</b>	<b>1.184 (0.040)</b>	<b>1.129 (0.046)</b>	<b>0.569 (0.040)</b>
AM-unweighted- $L_2$	1.246 (0.046)	1.204 (0.025)	1.146 (0.020)	0.608 (0.016)
$L_1$ - regularization	1.476 (0.046)	1.442 (0.052)	1.386 (0.044)	0.668 (0.068)
$L_2$ - regularization	1.408 (0.018)	1.386 (0.066)	1.446 (0.065)	0.602 (0.039)
Early-stopping	1.770 (0.084)	1.608 (0.121)	1.602 (0.067)	0.870 (0.093)
Dropout	1.512 (0.141)	1.478 (0.087)	1.494 (0.068)	0.592 (0.050)

that were incorrectly predicted across all experiments (as detailed in Table 4), we identified 62 unique images. Closer examination of these images revealed that many seem to possess incorrect labels. A selection of these images is showcased in Figure 4, with the complete set of 62 images detailed in Supplement S.11.5. Notably, some of the labels we identified as questionable also align with findings from recent research by Northcutt et al. (2021), which focused on detecting label inaccuracies. Our method, however, uncovered a greater number of potential errors. Therefore, AM shows promise as a tool for effectively detecting incorrectly labeled data, serving as an ancillary benefit to its primary purpose.

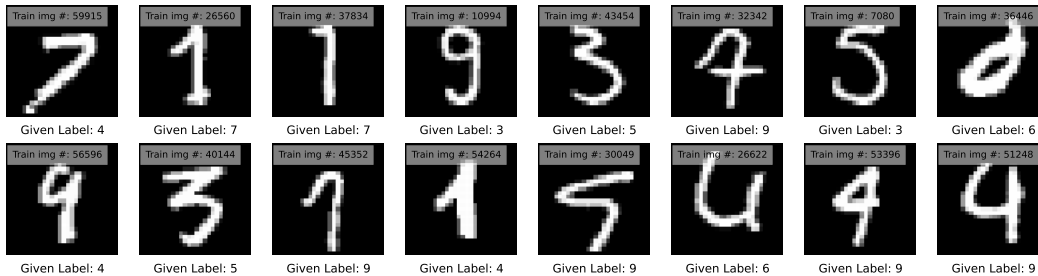


**Figure 4:** Selection of images detected by AM as having questionable labels, displayed in a left-to-right, top-to-bottom sequence, sorted by the decreasing frequency of their identification.

As a remark, the imputation algorithm introduced in this paper does not create new images ( $x$ ). The overall performance can be further improved by introducing a new imputation algorithm that can effectively impute new  $x$ . For example, data augmentation methods like random deformation (Simard et al., 2003) which is shown to be effective in practice, can be used to create more images. A popular technique in recent years called the generative adversarial network (GAN, Goodfellow et al., 2020) also provides a potential strategy towards this direction. For simplicity, such extended experiments have not been conducted here and will be reported elsewhere.

## 6 Concluding Remarks

In this paper, we proposed a new method for the estimation of over-parameterized models from a model-building perspective. Theoretical results and applications to the many-normal-means problem, linear regression with  $n < p$ , as well as the neural network model, have shown that the proposed method is promising.

The proposed method, while promising, warrants further investigation. Future developments should focus on enhancing both over-parameterized and non-overparameterized models in machine learning and statistics. For instance, the numerical results from the many-normal-means example demonstrate that over-parameterization, when combined with the proposed estimation method, effectively enhances model flexibility and applicability. This, in turn, improves the efficiency in predicting future observations. These insights align with the widespread consensus on the success of deep neural networks. We believe that further investigations of this phenomenon for the many-normal-means problem, as well as other well-known statistical models such as linear regression, factor analysis, mixed-effects models, mixture models, and Student-t models, could yield intriguing and valuable theoretical advancements. These advancements could enhance and extend beyond traditional likelihood-based inference methods. In addition, it should be noted that structured models play a fundamental role in statistical modeling and should always be considered for effectiveness when analyzing data with over-parameterized models.

Technically, the purpose of constructing the duality function  $\pi(\theta, \lambda)$  is to approximate the discrepancy between the population loss and the sample loss. Therefore, it remains as an integrating topic to formulate  $\pi(\theta, \lambda)$  as a preference to more structured models such as the many-normal-means example. While we employed an adaptive bootstrap imputation method, exploring alternative imputation methods such as resampling-based and Bayesian oriented approaches could yield improvements in computational efficiency, statistical validity, and robustness. Additionally, the development of more efficient computational techniques would enhance the success of our proposed method, particularly in enabling more effective and valid analysis of large datasets. Finally, methods of statistical inference, including conformal prediction (*c.f.* Cella and Martin (2022) and references therein), can be effectively applied and developed within our proposed framework.

## References

- Bates, S., Hastie, T., and Tibshirani, R. (2023). Cross-validation: What does it estimate and how well does it do it? *Journal of the American Statistical Association*, ahead-of-print(ahead-of-print):1–12.
- Bickel, P. J. and Sakov, A. (2008). On the choice of  $m$  in the  $m$  out of  $n$  bootstrap and confidence bounds for extrema. *Statistica Sinica*, pages 967–985.
- Box, G. E. (1976). Science and statistics. *Journal of the American Statistical Association*, 71(356):791–799.
- Breiman, L. (1996). Bagging predictors. *Machine learning*, 24(2):123–140.
- Bühlmann, P. and Van De Geer, S. (2011). *Statistics for high-dimensional data: methods, theory and applications*. Springer.
- Cella, L. and Martin, R. (2022). Validity, consonant plausibility measures, and conformal prediction. *Internat. J. Approx. Reason.*, 141:110–130.
- Dunn, P. K. and Smyth, G. K. (1996). Randomized quantile residuals. *Journal of Computational and graphical statistics*, 5(3):236–244.
- Efron, B. (2016). Empirical bayes deconvolution estimates. *Biometrika*, 103(1):1–20.

- Efron, B. and Hastie, T. (2016). *Computer Age Statistical Inference: Algorithms, Evidence, and Data Science*. Institute of Mathematical Statistics Monographs. Cambridge University Press.
- Efron, B. and Tibshirani, R. J. (1994). *An introduction to the bootstrap*. CRC press.
- Escobar, M. D. (1994). Estimating normal means with a dirichlet process prior. *Journal of the American Statistical Association*, 89(425):268–277.
- Friedman, J., Hastie, T., and Tibshirani, R. (2010). Regularization paths for generalized linear models via coordinate descent. *Journal of statistical software*, 33(1):1–22.
- Geisser, S. (1975). The predictive sample reuse method with applications. *Journal of the American statistical Association*, 70(350):320–328.
- Geman, S. and Hwang, C.-R. (1982). Nonparametric maximum likelihood estimation by the method of sieves. *The annals of Statistics*, pages 401–414.
- Goodfellow, I., Pouget-Abadie, J., Mirza, M., Xu, B., Warde-Farley, D., Ozair, S., Courville, A., and Bengio, Y. (2020). Generative adversarial networks. *Communications of the ACM*, 63(11):139–144.
- Grenander, U. (1981). *Abstract inference*. John Wiley. New York, NY.
- Hoerl, A. E. and Kennard, R. W. (1970). Ridge regression: Biased estimation for nonorthogonal problems. *Technometrics*, 12(1):55–67.
- Hopke, P. K., Liu, C., and Rubin, D. B. (2001). Multiple imputation for multivariate data with missing and below-threshold measurements: time-series concentrations of pollutants in the arctic. *Biometrics*, 57(1):22–33.
- James, W. and Stein, C. (1961). Estimation with quadratic loss. Proc. 4th Berkeley Symp. Math. Stat. Probab. 1, 361–379 (1961).
- Jarrett, K., Kavukcuoglu, K., Ranzato, M., and LeCun, Y. (2009). What is the best multi-stage architecture for object recognition? *International Conference on Computer Vision*, pages 2146–2153.
- Kingma, D. P. and Ba, J. (2014). Adam: A method for stochastic optimization. *arXiv preprint arXiv:1412.6980*.
- LeCun, Y., Bottou, L., Bengio, Y., and Haffner, P. (1998). Gradient-based learning applied to document recognition. *Proceedings of the IEEE*, 86(11):2278–2324.
- Lehmann, E. (1983). *Theory of Point Estimation*. Wadsworth & Brooks/Cole Advanced Books & Software, Pacific Grove, California.
- Liu, C. (2023). Reweighted and circularised anderson-darling tests of goodness-of-fit. *Journal of Nonparametric Statistics*, 35(4):869–904.
- Massey, F. J. (1951). The kolmogorov-smirnov test for goodness of fit. *Journal of the American Statistical Association*, 46(253):68–78.

- Mobiny, A., Yuan, P., Moulik, S. K., Garg, N., Wu, C. C., and Nguyen, H. V. (2021). DropConnect is effective in modeling uncertainty of bayesian deep networks. *Scientific Reports*, 11(1).
- Nalisnick, E., Matsukawa, A., Teh, Y. W., Gorur, D., and Lakshminarayanan, B. (2019). Do deep generative models know what they don't know? *ICLR*.
- Narasimhan, B. and Efron, B. (2020). deconvolveR : A  $g$ -modeling program for deconvolution and empirical bayes estimation. *Journal of Statistical Software*, 94(11).
- Northcutt, C., Jiang, L., and Chuang, I. (2021). Confident learning: Estimating uncertainty in dataset labels. *The Journal of artificial intelligence research*, 70:1373–1411.
- Oneto, L., Ridella, S., and Anguita, D. (2023). Do we really need a new theory to understand over-parameterization? *Neurocomputing*, 543:126227.
- Pardo, L. (2006). Statistical inference based on divergence measures.
- Qiu, Y. and Wang, X. (2021). Almond: Adaptive latent modeling and optimization via neural networks and langevin diffusion. *Journal of the American Statistical Association*, 116(535):1224–1236.
- Reid, S., Tibshirani, R., and Friedman, J. (2016). A study of error variance estimation in lasso regression. *Statistica Sinica*, 26(1):35–67.
- Rubin, D. B. (1987). *Multiple imputation for nonresponse in surveys*. John Wiley & Sons, New York.
- Shen, X., Shi, J., and Wong, W. H. (1999). Random sieve likelihood and general regression models. *Journal of the American Statistical Association*, 94(447):835–846.
- Shor, N. Z., Kiwiel, K. C., and Ruszcayński, A. (1985). *Minimization methods for non-differentiable functions*. Springer-Verlag New York, Inc., New York, NY, USA.
- Simard, P. Y., Steinkraus, D., and Platt, J. C. (2003). Best practices for convolutional neural networks applied to visual document analysis. *Seventh International Conference on Document Analysis and Recognition, 2003. Proceedings.*, pages 958–963.
- Srivastava, N., Hinton, G., Krizhevsky, A., Sutskever, I., and Salakhutdinov, R. (2014). Dropout: A simple way to prevent neural networks from overfitting. *Journal of machine learning research*, 15:1929–1958.
- Stein, C. (1956). Inadmissibility of the usual estimator for the mean of a multivariate normal distribution. Proc. 3rd Berkeley Sympos. Math. Statist. Probability 1, 197-206 (1956).
- Stone, M. (1974). Cross-validatory choice and assessment of statistical predictions. *Journal of the royal statistical society: Series B (Methodological)*, 36(2):111–133.
- Stone, M. (1977). An asymptotic equivalence of choice of model by cross-validation and akaike's criterion. *Journal of the Royal Statistical Society: Series B (Methodological)*, 39(1):44–47.

- Supp-CB, C. B. (2024). Finite sample valid inference via calibrated bootstrap. *Technical Report, to be available at arXiv*.
- Tibshirani, R. (1996). Regression shrinkage and selection via the lasso. *Journal of the Royal Statistical Society. Series B (Methodological)*, pages 267–288.
- Tibshirani, R. J. and Tibshirani, R. (2009). A bias correction for the minimum error rate in cross-validation. *The annals of applied statistics*, 3(2):822–829.
- Tukey, J. W. (1954). Unsolved problems of experimental statistics. *Journal of the American Statistical Association*, 49(268):706.
- Vapnik, V. (1991). Principles of risk minimization for learning theory. In Moody, J., Hanson, S., and Lippmann, R., editors, *Advances in Neural Information Processing Systems*, volume 4. Morgan-Kaufmann.
- von Neumann, J. (1947). The mathematician. In *Works of the Mind*, (Ed., R. B. Haywood), University of Chicago Press, pages 180–196.
- Wan, L., Zeiler, M. D., Zhang, S., LeCun, Y., and Fergus, R. (2013). Regularization of neural networks using dropconnect. *International Conference on Machine Learning*, 28:1058–1066.
- Wasserman, L. (2006). *All of nonparametric statistics*. Springer Science & Business Media.
- Wolpert, D. H. (1992). Stacked generalization. *Neural Networks*, 5(2):241–259.
- Yu, G. and Bien, J. (2019). Estimating the error variance in a high-dimensional linear model. *Biometrika*, 106(3):533–546.
- Zou, H. (2006). The adaptive lasso and its oracle properties. *Journal of the American Statistical Association*, 101(476):1418–1429.
- Zou, H. and Hastie, T. (2005). Regularization and variable selection via the elastic net. *Journal of the Royal Statistical Society: Series B*, 67(2):301–320.

# Estimation of Over-parameterized Models from an Auto-Modeling Perspective:

*Derivations, Proofs, and Implementation Details*

Yiran Jiang and Chuanhai Liu

Department of Statistics, Purdue University

## Contents

S.1	A Simple Example for Continuous Data with $p = 1$	3
S.1.1	Settings	3
S.1.2	Imputation with Resampling	3
S.1.3	Estimation of $\theta$	4
S.1.4	The Shrinkage Effect and Sampling Distribution of $\hat{\theta}$	4
S.2	Regularity Conditions	6
S.3	Proof of Propositions 1 to 3	6
S.4	Proof of Theorem 1	7
S.5	Proof of Corollary 1	9
S.6	Proof of Lemma 1	10
S.7	Proof of Theorem 2	13
S.8	Imputation with Finite-sample Valid Predictive Coverage	15
S.8.1	Theoretical Support	15
S.8.2	Empirical Evidence	15
S.9	Implementation Details in the Many-Normal-Means Example	17
S.9.1	Technical Details	17
S.9.2	Implementation Details of AM	19
S.9.3	Implementation Details of Other Methods	20
S.10	Implementation Details in the Linear Regression Example	20
S.10.1	Technical Details	20
S.10.2	Implementation Details of AM	23
S.10.3	Implementation Details of Other Methods	23
S.11	Implementation Details in the Neural Network Example	24
S.11.1	Technical Details	24
S.11.2	Implementation Details of AM	26
S.11.3	Implementation Details of Other Methods	27
S.11.4	Surrogate CDF Values	28
S.11.5	Estimation Process of AM	28
S.11.6	Questionable Labels Found by AM	28
S.12	Imputation Efficiency Evaluation with Q-Q Plots	31
S.12.1	The Effect of $m$ on Imputation Efficiency	31
S.12.2	Imputation Efficiency with the Optimal $m$	32

S.13	Computational Efficiency of AM . . . . .	37
S.13.1	Computational Time Analysis . . . . .	37
S.13.2	Computational Time of the Application Examples . . . . .	37



## S.1 A Simple Example for Continuous Data with $p = 1$

### S.1.1 Settings

Suppose that  $y_1, \dots, y_n$  is a sample of size of  $n$  from the model:  $y = \theta + z$  where  $z \sim N(0, 1)$ . Take the AM duality function as  $\pi(\theta, \lambda) = \lambda|\theta|$  with  $\lambda \in \mathbb{R}_+$ , *i.e.*,  $\lambda$  is a positive scalar.

### S.1.2 Imputation with Resampling

We demonstrate Algorithm 2 with an arbitrary  $k = 1, \dots, K$  and  $b = 1, \dots, B$ . Let  $\tilde{y}_1, \dots, \tilde{y}_m$ , denoted by  $\tilde{\mathbb{P}}_b^{(k)}$ , be a re-sampled data drawn from the sample data  $y_1, \dots, y_{n_k}$  denoted by  $\hat{\mathbb{P}}_b^{(k)}$  when leaving out the  $k$ -th fold, where  $m$  denotes the sample size of  $\tilde{\mathbb{P}}_b^{(k)}$  and  $n_k$  denotes the sample size of  $\hat{\mathbb{P}}_b^{(k)}$ . In this case, we have

$$G_{\tilde{\mathbb{P}}_b^{(k)}}(\theta, \lambda) = \frac{1}{2m} \sum_{i=1}^m (\theta - \tilde{y}_i)^2 + \lambda|\theta|$$

and

$$V_{\hat{\mathbb{P}}_b^{(k)}, \tilde{\mathbb{P}}_b^{(k)}}(\theta, \lambda) = \frac{1}{2n_k} \sum_{i=1}^{n_k} (\theta - y_i)^2 - \frac{1}{2m} \sum_{i=1}^m (\theta - \tilde{y}_i)^2 - \lambda|\theta|.$$

The derivative of  $V_{\hat{\mathbb{P}}_b^{(k)}, \tilde{\mathbb{P}}_b^{(k)}}(\theta, \lambda)$  is given by

$$\begin{aligned} \frac{\partial V_{\hat{\mathbb{P}}_b^{(k)}, \tilde{\mathbb{P}}_b^{(k)}}(\theta, \lambda)}{\partial \theta} &= \theta - \bar{y}^{(k)} - \theta + \bar{\tilde{y}}^{(k)} - \lambda \cdot \text{sign}(\theta) \\ &= \bar{\tilde{y}}^{(k)} - \bar{y}^{(k)} - \lambda \cdot \text{sign}(\theta), \end{aligned}$$

where  $\bar{\tilde{y}}^{(k)} = \frac{1}{m} \sum_{i=1}^m \tilde{y}_i$ ,  $\bar{y}^{(k)} = \frac{1}{n_k} \sum_{i=1}^{n_k} y_i$ . It is required to find

$$\arg \min_{\lambda} \left| \frac{\partial V_{\hat{\mathbb{P}}_b^{(k)}, \tilde{\mathbb{P}}_b^{(k)}}(\theta, \lambda)}{\partial \theta} \right| = \arg \min_{\lambda} |\bar{\tilde{y}}^{(k)} - \bar{y}^{(k)} - \lambda \cdot \text{sign}(\theta)|.$$

With the constraint on  $\lambda \in \mathbb{R}_+$ , it follows that

$$\hat{\lambda}_b^{(k)} = \begin{cases} (\bar{\tilde{y}}^{(k)} - \bar{y}^{(k)}) \cdot \text{sign}(\theta) & \text{if } (\bar{\tilde{y}}^{(k)} - \bar{y}^{(k)}) \cdot \text{sign}(\theta) > 0, \\ 0 & \text{otherwise.} \end{cases}$$

Hence, in order to minimize  $G_{\tilde{\mathbb{P}}_b^{(k)}}(\theta, \lambda)$  over  $\theta$ , we have

$$\hat{\theta}_b^{(k)} = \begin{cases} \arg \min_{\theta} \frac{1}{2m} \sum_{i=1}^m (\theta - \tilde{y}_i)^2 & \text{if } (\bar{\tilde{y}}^{(k)} - \bar{y}^{(k)}) \cdot \text{sign}(\hat{\theta}_b^{(k)}) \leq 0, \\ \arg \min_{\theta} \left( \frac{1}{2m} \sum_{i=1}^m (\theta - \tilde{y}_i)^2 + |\bar{\tilde{y}}^{(k)} - \bar{y}^{(k)}| \cdot |\theta| \right) & \text{otherwise.} \end{cases}$$

One can further write the problem as

$$\min_{\theta} \frac{1}{2m} \sum_{i=1}^m (\theta - \tilde{y}_i)^2 \quad \text{s.t.} \quad |\theta| \cdot \mathbb{1}((\bar{\tilde{y}}^{(k)} - \bar{y}^{(k)}) \cdot \text{sign}(\theta) > 0) \leq |\bar{\tilde{y}}^{(k)} - \bar{y}^{(k)}|,$$

where  $\mathbb{1}(\cdot)$  denotes the indicator function. This can be seen as the canonical convex optimization problem with the inequality constraint known as the halved Lasso constraint.

Consider the following strategy to solve for  $\theta$ . Firstly, one can solve for the non-constrained optimization problem to get  $\theta_{mle}^*$ . Then in the case of  $(\bar{y}^{(k)} - \bar{y}^{(k)}) \cdot \text{sign}(\theta_{mle}^*) \leq 0$ , we have  $\hat{\theta}_b^{(k)} = \theta_{mle}^*$ . Otherwise, we solve the constrained optimization problem (lasso) to get  $\hat{\theta}_b^{(k)} = \theta_{lasso}^*$ . In this simple example, one can show that the closed form solution of  $\hat{\theta}_b^{(k)}$  is given by

$$\hat{\theta}_b^{(k)} = \begin{cases} \bar{y}^{(k)} & \text{if } |\bar{y}^{(k)}| \leq |\bar{y}^{(k)}| \text{ and } \text{sign}(\bar{y}^{(k)}) = \text{sign}(\bar{y}^{(k)}), \\ \bar{y}^{(k)} & \text{if } |\bar{y}^{(k)}| > |\bar{y}^{(k)}| \text{ and } \text{sign}(\bar{y}^{(k)}) = \text{sign}(\bar{y}^{(k)}), \\ 0 & \text{if } \text{sign}(\bar{y}^{(k)}) \neq \text{sign}(\bar{y}^{(k)}). \end{cases}$$

It should be noted that  $|\hat{\theta}_b^{(k)}| \leq |\bar{y}^{(k)}|$  in all cases, indicating shrinkage of the estimate toward zero.

### S.1.3 Estimation of $\theta$

In the estimation step, we have

$$G_{\hat{\mathbb{P}}}(\theta, \lambda) = \frac{1}{2n} \sum_{i=1}^n (\theta - y_i)^2 + \lambda|\theta|$$

and

$$V_{\mathbb{Q}, \hat{\mathbb{P}}}(\theta, \lambda) = \frac{1}{2n} E \left[ \sum_{i=1}^n (\theta - \mathbf{y}_i)^2 \right] - \frac{1}{2n} \sum_{i=1}^n (\theta - y_i)^2 - \lambda|\theta|.$$

Let  $\bar{\mathbf{y}} = E[\mathbf{y}]$ . Notice that the imputation data generator is  $\mathbf{y} \sim \hat{\theta}_b^{(k)} + \mathbf{z}$ , where  $\mathbf{z} \sim N(0, 1)$ . Thus, we have  $\bar{\mathbf{y}} = E[\mathbf{y}] = E[\hat{\theta}_b^{(k)}]$ , which concludes the derivation.

To obtain an approximate analytical solution, we assume that the sampling distribution can be approximated by  $\bar{y}^{(k)} \sim N(\bar{y}, 1/n)$ . In such a case,  $E[\hat{\theta}_b^{(k)}]$  takes an explicit form as

$$E[\hat{\theta}_b^{(k)}] = (1 - \Phi(-\sqrt{n}|\bar{y}|)) \bar{y} - \frac{1}{\sqrt{n}} |\phi(-\sqrt{n}|\bar{y}|) - \phi(0)| \cdot \text{sign}(\bar{y}),$$

where  $\Phi(\cdot)$  and  $\phi(\cdot)$  denote the cumulative distribution function (CDF) and the probability distribution function (PDF) of the standard normal distribution, respectively. With arguments similar to those in Section S.1.2, one has the closed-form expression of the final estimate of  $\theta$  as  $\hat{\theta}_{AM} = E[\hat{\theta}_b^{(k)}]$ .

### S.1.4 The Shrinkage Effect and Sampling Distribution of $\hat{\theta}$

The shrinkage effect of AM in this simple example is shown in Figure S.1 for different sample size  $n$ . It can be seen that the AM estimator effectively shrinks the MLE of  $\theta$  towards zero. We simulated  $B = 10,000$  data sets for different choices of  $\theta$  and  $n$  to study the sampling distribution of  $\hat{\theta}_{AM}$ . The pattern of  $\hat{\theta}_{AM}$ 's sampling distribution is shown in the Quantile-Quantile plots (Q-Q plots) in Figure S.2, where it can be seen that the AM estimate are close to the MLEs but slightly shrunk towards zero.

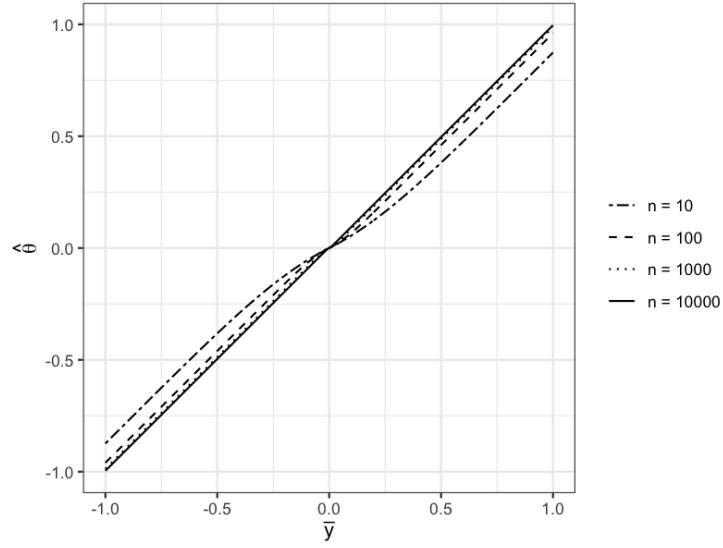


**Figure S.1:** The shrinkage effect of the AM estimator in the simple example in Section S.1.

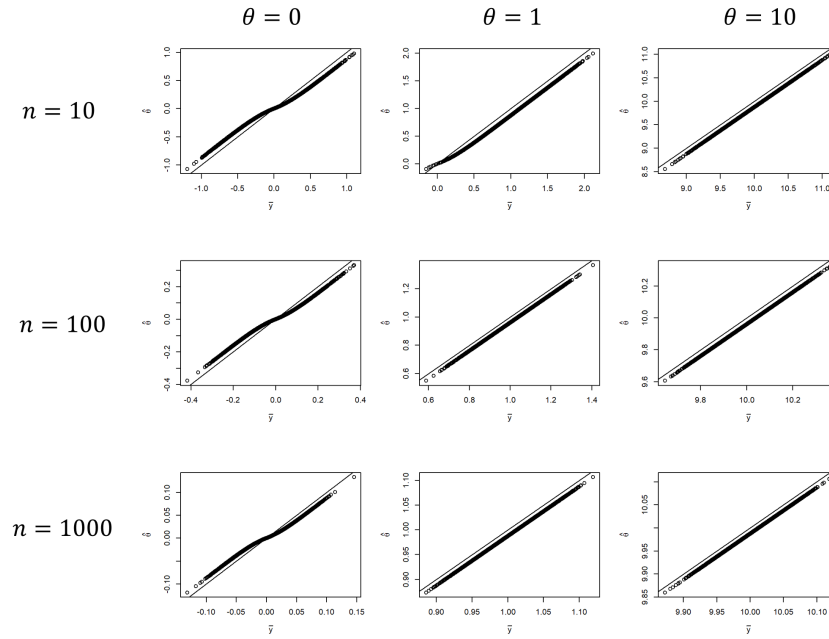


**Figure S.2:** Q-Q plots of the AM estimate versus MLEs under different settings in the simple example in S.1. The plots show that the AM estimates are close to the MLEs but slightly shrunk towards zero.

## S.2 Regularity Conditions

Let  $(X, Y)$  take values in  $\mathbf{W} \subseteq \mathbb{R}^{k+q}$  and  $\theta \in \Theta^{(n)} \subseteq \mathbb{R}^p$ ,  $\lambda \in \Lambda^{(n)} \subseteq \mathbb{R}^p$  with  $p$  dependent on  $n$ . Assume that the loss function  $L(\theta|X, Y)$  and the duality function  $\pi(\theta, \lambda)$  satisfies the regularity conditions:

- C1. for each  $n$  and  $\theta \in \Theta^{(n)}$ ,  $L(\theta|\cdot)$  is Borel Measurable on  $\mathbf{W}$ ,
- C2. for each  $n$  and  $(X, Y) \in \mathbf{W}$ ,  $L(\cdot|X, Y)$  is continuous on  $\Theta^{(n)}$ ,
- C3. for every  $n$  and for all  $\theta \in \Theta^{(n)}$ , the inequality  $|L(\theta|X, Y)| < b(X, Y)$  is satisfied uniformly, where  $b$  is a non-negative function on  $\mathbf{W}$  such that  $E|b(X, Y)| < \infty$ ,
- C4. for each  $n$ , there exists  $\theta_0 = \arg \min_{\theta \in \Theta^{(n)}} E_{(X, Y) \sim \mathbb{P}} L(\theta|X, Y)$ ,
- C5. for each  $n$ , there exists  $\delta \in (0, 1)$  such that  $\mathbb{E} \left( \sup_{\theta \in \Theta^{(n)}} |L(\theta|X, Y)|^{1-\delta} \right) < \infty$  (required for Theorem 2),
- C6. for each  $n$  and  $\theta \in \Theta^{(n)}$ ,  $\pi(\theta, \lambda)$  is continuous on  $\lambda \in \Lambda^{(n)}$ ,
- C7. for each  $n$  and  $\lambda \in \Lambda^{(n)}$ ,  $\pi(\theta, \lambda)$  is continuous on  $\theta \in \Theta^{(n)}$ , and
- C8. for each  $n$ ,  $\lambda_0 = \mathbf{0} \in \Lambda^{(n)}$  and  $\pi(\theta, \lambda_0) = C$  for any  $\theta \in \Theta^{(n)}$ , where  $C \in \mathbb{R}$  is some constant.

## S.3 Proof of Propositions 1 to 3

To prove Proposition 1, by the definition of KL divergence, we have

$$D_{KL}(\mathbb{P}, \mathbb{P}_\theta) = E_{(X, Y) \sim \mathbb{P}} (\log p(X, Y) - \log p'(\theta|X, Y)),$$

where  $p(X, Y)$  denotes the true unknown population distribution and  $p'(\theta|X, Y)$  denotes the likelihood function of the model with parameter  $\theta \in \Theta_0$ . By assumption,  $\mathbb{P} = \mathbb{P}_{\theta_0}$ ,  $\theta_0 \in \Theta_0$ , resulting in  $D_{KL}(\mathbb{P}, \mathbb{P}_\theta) = D_{KL}(\mathbb{P}_{\theta_0}, \mathbb{P}_\theta)$  and, thereby,  $D_{KL}(\mathbb{P}_{\theta_0}, \mathbb{P}_\theta) = 0$  holds by taking  $\theta = \theta_0$ . Note that

$$E_{(X, Y) \sim \mathbb{P}} \log p'(\theta_0|X, Y) \geq E_{(X, Y) \sim \mathbb{P}} \log p'(\tilde{\theta}|X, Y) \tag{S.1}$$

for any  $\tilde{\theta} \in \Theta_0$ , as the KL divergence is non-negative. By the definition of the optimal estimate in (3), it follows that  $D_{KL}(\mathbb{P}, \mathbb{P}_{\theta^*}) = 0$  for  $\theta^* \in \Theta_0^*$ , where  $\Theta_0^*$  denotes the set of  $\theta$  that maximizes the expected log-likelihood function. This concludes the model validity since the parameter space is not dependent on  $n$ .

For Proposition 2, it is assumed that there exists a positive integer  $N$  such that  $\Theta_0 \preceq \Theta^{(n)}$  for all  $n \geq N$ . By the definition of model generality, for each  $n \geq N$ , there exists  $\Theta_{\mathcal{A}}^{(n)} \subseteq \Theta^{(n)}$  such that

$$\{\mathbb{P}_\theta : \theta \in \Theta_0\} = \{\mathbb{P}_\theta : \theta \in \Theta_{\mathcal{A}}^{(n)}\}.$$

As a result, we have

$$\begin{aligned} \min_{\tilde{\theta} \in \Theta^{(n)}} E_{(X, Y) \sim \mathbb{P}} L(\tilde{\theta}|X, Y) &= \min \left( \min_{\tilde{\theta} \in \Theta_{\mathcal{A}}^{(n)}} E_{(X, Y) \sim \mathbb{P}} L(\tilde{\theta}|X, Y), \min_{\tilde{\theta} \in \Theta^{(n)} \setminus \Theta_{\mathcal{A}}^{(n)}} E_{(X, Y) \sim \mathbb{P}} L(\tilde{\theta}|X, Y) \right) \\ &\leq \min_{\tilde{\theta} \in \Theta_{\mathcal{A}}^{(n)}} E_{(X, Y) \sim \mathbb{P}} L(\tilde{\theta}|X, Y) \\ &= \min_{\tilde{\theta} \in \Theta_0} E_{(X, Y) \sim \mathbb{P}} L(\tilde{\theta}|X, Y) \end{aligned}$$

holds for all  $n \geq N$ . Let  $L(\theta|X, Y)$  denote the negative log-likelihood function. We obtain from the proof of Proposition 1 that

$$\min_{\tilde{\theta} \in \Theta_0} E_{(X, Y) \sim \mathbb{P}} L(\tilde{\theta}|X, Y) = -E_{(X, Y) \sim \mathbb{P}} \log p'(\theta_0|X, Y)$$

with the true parameter  $\theta_0 \in \Theta_0$  and (S.1) holds for any  $\tilde{\theta} \in \Theta^{(n)}$ . As a result, we can conclude that  $\lim_{n \rightarrow \infty} D_{KL}(\mathbb{P}, \mathbb{P}_{\theta^*}) = 0$ , where  $\theta^* \in \Theta_*^{(n)}$ .

For Proposition 3, given that the likelihood function is continuous and  $\hat{\theta}_0 \xrightarrow{p} \theta_0$  for  $\hat{\theta} \in \Theta_0$ , by the continuous mapping theorem (CMT), we have

$$E_{(X, Y) \sim \mathbb{P}} \log p'(\hat{\theta}|X, Y) \xrightarrow{p} E_{(X, Y) \sim \mathbb{P}} \log p'(\theta_0|X, Y).$$

Since  $\theta_0$  is the true parameter, this is equivalent to  $D_{KL}(\mathbb{P}, \mathbb{P}_{\hat{\theta}}) \xrightarrow{p} 0$ , completing the proof.  $\square$

## S.4 Proof of Theorem 1

By assumption, for some  $N > 0$ , there exists a model  $\{\mathbb{P}_\phi : \phi \in \Phi\}$  with compact parameter space  $\Phi$  such that  $\Phi \preceq \Theta^{(n)}$ , satisfying  $\min_{\phi \in \Phi} D_{KL}(\mathbb{P}, \mathbb{P}_\phi) = \lim_{n \rightarrow \infty} D_{KL}(\mathbb{P}, \mathbb{P}_{\theta^*})$ . By the definition of model generality, for every  $n \geq N$ , there exists  $\Theta_{\mathcal{A}}^{(n)} \subseteq \Theta^{(n)}$  such that

$$\{\mathbb{P}_\phi : \phi \in \Phi\} = \{\mathbb{P}_\theta : \theta \in \Theta_{\mathcal{A}}^{(n)}\}. \quad (\text{S.2})$$

Since the mapping  $\psi$  is continuous by definition, the set  $\Theta_{\mathcal{A}}^{(n)}$  is also compact for every  $n \geq N$ . Furthermore, we have

$$\min_{\theta \in \Theta_{\mathcal{A}}^{(n)}} D_{KL}(\mathbb{P}, \mathbb{P}_\theta) = \lim_{n \rightarrow \infty} D_{KL}(\mathbb{P}, \mathbb{P}_{\theta^*})$$

for any  $\theta^* \in \Theta_*^{(n)}$ , as defined in (3), and  $n \geq N$ . This further implies

$$\begin{aligned} \min_{\theta \in \Theta_{\mathcal{A}}^{(n)}} E_{(X, Y) \sim \mathbb{P}} L(\theta|X, Y) &= \lim_{n \rightarrow \infty} \min_{\theta \in \Theta^{(n)}} E_{(X, Y) \sim \mathbb{P}} L(\theta|X, Y). \\ &= \lim_{n \rightarrow \infty} E_{(X, Y) \sim \mathbb{P}} L(\theta^*|X, Y) \end{aligned} \quad (\text{S.3})$$

for some optimal estimate  $\theta^* \in \Theta_*^{(n)}$  and  $n \geq N$ .

For simplicity in the asymptotic analysis, all subsequent expressions involving  $n$  implicitly assume  $n \geq N$ . With the regularity conditions C1—C4 for the loss function in Section S.2, the uniform law of large numbers (ULLN) can be applied (see, *e.g.*, Newey and McFadden, 1994) to the restricted parameter space  $\Theta_{\mathcal{A}}^{(n)}$  due to its compactness. Thus,

$$\sup_{\theta \in \Theta_{\mathcal{A}}^{(n)}} \left| E_{(X, Y) \sim \mathbb{P}} L(\theta|X, Y) - \frac{1}{n} \sum_{i=1}^n L(\theta|x_i, y_i) \right| \xrightarrow{p} 0. \quad (\text{S.4})$$

The result in (S.4) further implies

$$\sup_{\theta \in \Theta_{\mathcal{A}}^{(n)}} \left| E_{(X, Y) \sim \mathbb{P}} L(\theta|X, Y) + \pi(\theta, \lambda) - \left( \frac{1}{n} \sum_{i=1}^n L(\theta|x_i, y_i) + \pi(\theta, \lambda) \right) \right| \xrightarrow{p} 0$$

for any  $\lambda \in \Lambda^{(n)}$  and

$$\frac{1}{n} \sum_{i=1}^n L(\theta|x_i, y_i) + \pi(\theta, \lambda) \xrightarrow{p} E_{(X,Y) \sim \mathbb{P}} L(\theta|X, Y) + \pi(\theta, \lambda)$$

for all  $\theta \in \Theta_{\mathcal{A}}^{(n)}$  and  $\lambda \in \Lambda^{(n)}$ . We define the  $\lambda$ -dependent AM estimator in the restricted parameter space as

$$(\hat{\theta}_{\mathcal{A}}^*)_{\lambda} = \arg \min_{\theta \in \Theta_{\mathcal{A}}^{(n)}} \left( \frac{1}{n} \sum_{i=1}^n L(\theta|x_i, y_i) + \pi(\theta, \lambda) \right) \quad (\text{S.5})$$

for any given  $\lambda \in \Lambda^{(n)}$ . By the global optimal assumption of the AM estimator elaborated in Section 4.2, the duality parameter  $\lambda$  is chosen at  $\lambda = \hat{\lambda}$  such that

$$\hat{\lambda} = \arg \min_{\lambda \in \Lambda^{(n)}} E_{(X,Y) \sim \mathbb{P}} L \left( (\hat{\theta}_{\mathcal{A}}^*)_{\lambda} | X, Y \right). \quad (\text{S.6})$$

Note that  $\pi(\theta, \lambda) \geq 0$  for any  $\theta \in \Theta_{\mathcal{A}}^{(n)}$ ,  $\lambda \in \Lambda^{(n)}$ . We then consider  $\lambda_0 = \mathbf{0}$ , which is assumed that  $\lambda_0 \in \Lambda^{(n)}$  by the regularity condition C8 for the duality function in Section S.2. Furthermore, by the same regularity condition, we have

$$\frac{1}{n} \sum_{i=1}^n L \left( (\hat{\theta}_{\mathcal{A}}^*)_{\lambda_0} | x_i, y_i \right) + \pi \left( (\hat{\theta}_{\mathcal{A}}^*)_{\lambda_0}, \lambda_0 \right) \xrightarrow{p} E_{(X,Y) \sim \mathbb{P}} L \left( (\hat{\theta}_{\mathcal{A}}^*)_{\lambda_0} | X, Y \right) + C,$$

where  $C \in \mathbb{R}$  is a constant. By (S.5),  $(\hat{\theta}_{\mathcal{A}}^*)_{\lambda_0}$  is the empirical loss minimizer in the parameter space  $\Theta_{\mathcal{A}}^{(n)}$ . The uniform convergence of the empirical loss in (S.4) indicates the convergence of its minimizer to the true population risk minimizer (Shalev-Shwartz et al., 2010). By (S.3) and the definition of the optimal estimate in (3), the asymptotic optimality

$$E_{(X,Y) \sim \mathbb{P}} L \left( (\hat{\theta}_{\mathcal{A}}^*)_{\lambda_0} | X, Y \right) \xrightarrow{p} E_{(X,Y) \sim \mathbb{P}} L(\theta^* | X, Y) \quad (\text{S.7})$$

is achievable for some optimal estimate  $\theta^* \in \Theta_{\mathcal{A}}^{(n)}$ . By the AM objective function (S.6), we know that for any  $\hat{\lambda} \in \Lambda^{(n)}$ ,

$$E_{(X,Y) \sim \mathbb{P}} L(\theta^* | X, Y) \leq E_{(X,Y) \sim \mathbb{P}} L \left( (\hat{\theta}_{\mathcal{A}}^*)_{\hat{\lambda}} | X, Y \right) \leq E_{(X,Y) \sim \mathbb{P}} L \left( (\hat{\theta}_{\mathcal{A}}^*)_{\lambda_0} | X, Y \right)$$

for each  $(X, Y) \in \mathbf{W}$ . Now, we consider the unrestricted model with the full parameter space  $\Theta^{(n)}$  and  $\Lambda^{(n)}$ . By the AM objective functions (S.5) and (S.6) again, the optimal AM estimator  $\hat{\theta}_{AM}^* \in \Theta^{(n)}$  satisfies

$$E_{(X,Y) \sim \mathbb{P}} L(\theta^* | X, Y) \leq E_{(X,Y) \sim \mathbb{P}} L \left( \hat{\theta}_{AM}^* | X, Y \right) \leq E_{(X,Y) \sim \mathbb{P}} L \left( (\hat{\theta}_{\mathcal{A}}^*)_{\hat{\lambda}} | X, Y \right) \quad (\text{S.8})$$

for each  $(X, Y) \in \mathbf{W}$ . As a result, for any  $\epsilon > 0$ , the two events

$$\begin{aligned} A &= \{ E_{(X,Y) \sim \mathbb{P}} L \left( \hat{\theta}_{AM}^* | X, Y \right) - E_{(X,Y) \sim \mathbb{P}} L(\theta^* | X, Y) \geq \epsilon \} \\ B &= \{ E_{(X,Y) \sim \mathbb{P}} L \left( (\hat{\theta}_{\mathcal{A}}^*)_{\lambda_0} | X, Y \right) - E_{(X,Y) \sim \mathbb{P}} L(\theta^* | X, Y) \geq \epsilon \}, \end{aligned}$$

defined using  $\hat{\theta}_{AM}^*$  and  $(\hat{\theta}_{\mathcal{A}}^*)_{\lambda_0}$ , satisfy  $A \subseteq B$ . With (S.7) and (S.8), this implies for any  $\epsilon > 0$ ,

$$\lim_{n \rightarrow \infty} P \left( \left| E_{(X,Y) \sim \mathbb{P}} L \left( \hat{\theta}_{AM}^* | X, Y \right) - E_{(X,Y) \sim \mathbb{P}} L(\theta^* | X, Y) \right| \geq \epsilon \right) = 0$$

and, thereby, we have

$$E_{(X,Y) \sim \mathbb{P}} L \left( \hat{\theta}_{AM}^* | X, Y \right) \xrightarrow{p} E_{(X,Y) \sim \mathbb{P}} L(\theta^* | X, Y)$$

for  $\hat{\theta}_{AM}^* \in \Theta^{(n)}$  and some optimal estimate  $\theta^* \in \Theta_*^{(n)}$ . For the KL divergence distance measure denoted as  $D_{KL}(\cdot, \cdot)$ , by definition,

$$\begin{aligned} D_{KL}(\mathbb{P}, \mathbb{P}_{\hat{\theta}_{AM}^*}) &= E_{(X,Y) \sim \mathbb{P}} \left( \log p(X, Y) - \log p' \left( \hat{\theta}_{AM}^* | X, Y \right) \right) \\ D_{KL}(\mathbb{P}, \mathbb{P}_{\theta^*}) &= E_{(X,Y) \sim \mathbb{P}} \left( \log p(X, Y) - \log p'(\theta^* | X, Y) \right), \end{aligned} \quad (\text{S.9})$$

where  $p(X, Y)$  is the true unknown population distribution and  $p'(\cdot | X, Y)$  is the likelihood function of the model with given parameters. When the negative log-likelihood function is used as the loss function, by (S.7), we conclude that

$$D_{KL}(\mathbb{P}, \mathbb{P}_{\hat{\theta}_{AM}^*}) \xrightarrow{p} D_{KL}(\mathbb{P}, \mathbb{P}_{\theta^*}),$$

completing the proof.  $\square$

## S.5 Proof of Corollary 1

By assumption,  $\mathbb{P} = \mathbb{P}_{\theta_0}$ ,  $\theta_0 \in \Theta_0$ , where  $\Theta_0$  is the parameter space for the true model parameter  $\theta_0$ . Moreover,  $|\theta_{0j}| < \infty$ , for  $j = 1, \dots, p$ . We construct a compact parameter space

$$\Theta_{0,A} := \{ \theta : \theta \in \Theta_0 \text{ and } \theta_j = 0 \text{ if } |\theta_j| > |\theta_{0j}| + \epsilon, \text{ for } j = 1, \dots, p \},$$

where  $\epsilon > 0$  is a small constant. Since  $|\theta_{0j}| < \infty$ , for  $j = 1, \dots, p$ , the set  $\Theta_{0,A}$  is compact. Furthermore, we have  $\theta_0 \in \Theta_{0,A}$ . By assumption, there exists a positive integer  $N$  such that  $\Theta_0 \preceq \Theta^{(n)}$  for every  $n \geq N$ . This implies that  $\Theta_{0,A} \preceq \Theta^{(n)}$  for all  $n \geq N$ . By the definition of model generality, there exists  $\Theta_{\mathcal{A}}^{(n)} \in \Theta^{(n)}$  for all  $n \geq N$  such that

$$\{ \mathbb{P}_{\theta} : \theta \in \Theta_{0,A} \} = \{ \mathbb{P}_{\theta} : \theta \in \Theta_{\mathcal{A}}^{(n)} \}.$$

With similar arguments used in Section S.3, the expected negative log-likelihood function denoted by  $E_{(X,Y) \sim \mathbb{P}} L(\tilde{\theta} | X, Y)$  is minimized at  $\tilde{\theta} = \theta_0$ . Since  $\theta_0 \in \Theta_{0,A}$ , we have

$$\begin{aligned} & \lim_{n \rightarrow \infty} \min_{\theta \in \Theta^{(n)}} E_{(X,Y) \sim \mathbb{P}} L(\theta | X, Y) \\ &= \min \left( \min_{\theta \in \Theta_{\mathcal{A}}^{(n)}} E_{(X,Y) \sim \mathbb{P}} L(\theta | X, Y), \lim_{n \rightarrow \infty} \min_{\theta \in \Theta^{(n)} \setminus \Theta_{\mathcal{A}}^{(n)}} E_{(X,Y) \sim \mathbb{P}} L(\theta | X, Y) \right) \\ &\leq \min_{\theta \in \Theta_{\mathcal{A}}^{(n)}} E_{(X,Y) \sim \mathbb{P}} L(\theta | X, Y) \\ &= \min_{\theta \in \Theta_{0,A}} E_{(X,Y) \sim \mathbb{P}} L(\theta | X, Y) \\ &= E_{(X,Y) \sim \mathbb{P}} L(\theta_0 | X, Y). \end{aligned} \quad (\text{S.10})$$

The first equality in (S.10) follows since  $\Theta_{\mathcal{A}}^{(n)} \subseteq \Theta^{(n)}$  for all  $n \geq N$ . Given that

$$D_{KL}(\mathbb{P}, \mathbb{P}_\theta) = E_{(X,Y) \sim \mathbb{P}} L(\theta|X, Y) - E_{(X,Y) \sim \mathbb{P}} L(\theta_0|X, Y) \geq 0$$

for any  $\theta \in \Theta^{(n)}$ , it follows that

$$\lim_{n \rightarrow \infty} \min_{\theta \in \Theta^{(n)}} E_{(X,Y) \sim \mathbb{P}} L(\theta|X, Y) \geq E_{(X,Y) \sim \mathbb{P}} L(\theta_0|X, Y),$$

resulting in

$$\lim_{n \rightarrow \infty} \min_{\theta \in \Theta^{(n)}} E_{(X,Y) \sim \mathbb{P}} L(\theta|X, Y) = \min_{\theta \in \Theta_{\mathcal{A}}^{(n)}} E_{(X,Y) \sim \mathbb{P}} L(\theta|X, Y) = E_{(X,Y) \sim \mathbb{P}} L(\theta_0|X, Y)$$

from (S.10). This further implies

$$\min_{\theta \in \Theta_{\mathcal{A}}^{(n)}} D_{KL}(\mathbb{P}, \mathbb{P}_\theta) = \lim_{n \rightarrow \infty} D_{KL}(\mathbb{P}, \mathbb{P}_{\theta^*})$$

for any  $\theta^* \in \Theta_*^{(n)}$ , by the definition of the optimal estimate in (3), completing the proof.  $\square$

## S.6 Proof of Lemma 1

By assumption,  $D_{KL}(\mathbb{P}, \mathbb{Q})$  converges to zero in probability as  $n \rightarrow \infty$ . By Pinsker's inequality (Tsybakov, 2009, Lemma 2.5), it implies the convergence in total variation distance denoted by  $d_{TV}(\cdot, \cdot)$  between  $\mathbb{P}$  and  $\mathbb{Q}$ . That is, for any  $\epsilon > 0$ ,

$$\lim_{n \rightarrow \infty} P(d_{TV}(\mathbb{P}, \mathbb{Q}) \geq \epsilon) = 0. \quad (\text{S.11})$$

The total variation distance is defined as

$$d_{TV}(\mathbb{P}, \mathbb{Q}) = \sup_A |\mathbb{P}(A) - \mathbb{Q}(A)|,$$

where the supremum is taken over all measurable sets  $A$ .

By regularity condition C3 in Section S.2, the loss function is bounded by a non-negative function  $b$  such that  $|L(\theta|X, Y)| < b(X, Y)$  for all  $\theta \in \Theta^{(n)}$  and  $E|b(X, Y)| < \infty$ . Thus, we have

$$\begin{aligned} \left| E_{(X,Y) \sim \mathbb{P}} L(\theta|X, Y) - E_{(X,Y) \sim \mathbb{Q}} L(\theta|X, Y) \right| &= \left| \int L(\theta|X, Y) d\mathbb{P} - \int L(\theta|X, Y) d\mathbb{Q} \right| \\ &\leq \int b(X, Y) d|\mathbb{P} - \mathbb{Q}| \end{aligned} \quad (\text{S.12})$$

for any  $\theta \in \Theta^{(n)}$ . The condition  $E|b(X, Y)| < \infty$  implies that the function  $b(X, Y)$  is almost surely bounded. Thus, it can be approximated by simple functions. As a result, by the property of total variation distance, for any  $\epsilon > 0$ , there exists a  $\delta > 0$  such that if  $d_{TV}(\mathbb{P}, \mathbb{Q}) < \delta$ , then  $\int b(X, Y) d|\mathbb{P} - \mathbb{Q}| < \epsilon$ . Thus, by (S.11), we have for any  $\epsilon > 0$ ,

$$\lim_{n \rightarrow \infty} P\left(\int b(X, Y) d|\mathbb{P} - \mathbb{Q}| \geq \epsilon\right) = 0.$$

With (S.12), this further implies

$$\sup_{\theta \in \Theta^{(n)}} \left| E_{(X,Y) \sim \mathbb{P}} L(\theta|X, Y) - E_{(X,Y) \sim \mathbb{Q}} L(\theta|X, Y) \right| \xrightarrow{P} 0. \quad (\text{S.13})$$



The uniform convergence in (S.13) indicates the convergence of the empirical risk minimizer to the true population risk minimizer (Shalev-Shwartz et al., 2010), that is,

$$\min_{\theta \in \Theta^{(n)}} E_{(X,Y) \sim \mathbb{Q}} L(\theta|X, Y) \xrightarrow{p} \lim_{n \rightarrow \infty} \min_{\theta \in \Theta^{(n)}} E_{(X,Y) \sim \mathbb{P}} L(\theta|X, Y)$$

or, by definition,

$$E_{(X,Y) \sim \mathbb{Q}} L(\hat{\theta}^*|X, Y) \xrightarrow{p} E_{(X,Y) \sim \mathbb{P}} L(\theta^*|X, Y) \quad (\text{S.14})$$

for some optimal estimate  $\theta^* \in \Theta^*$ , and  $\hat{\theta}^* \in \Theta^{(n)}$  is some minimizer of the expected loss function with regard to  $(X, Y) \sim \mathbb{Q}$ .

Following the same arguments in Section S.4, we construct the restricted parameter space  $\Theta_{\mathcal{A}}^{(n)} \subseteq \Theta^{(n)}$  specified in (S.2). We further define the  $\lambda$ -dependent AM estimator in the restricted parameter space  $\Theta_{\mathcal{A}}^{(n)} \subseteq \Theta^{(n)}$  such that

$$(\hat{\theta}_{\mathcal{A}}^*)_{\lambda} = \arg \min_{\theta \in \Theta_{\mathcal{A}}^{(n)}} \left( \frac{1}{n} \sum_{i=1}^n L(\theta|x_i, y_i) + \pi(\theta, \lambda) \right) \quad (\text{S.15})$$

for any given  $\lambda \in \Lambda^{(n)}$  and the duality parameter  $\lambda$  is chosen at  $\lambda = \hat{\lambda}$  with

$$\hat{\lambda} = \arg \min_{\lambda \in \Lambda^{(n)}} E_{(X,Y) \sim \mathbb{Q}} L\left((\hat{\theta}_{\mathcal{A}}^*)_{\lambda}|X, Y\right). \quad (\text{S.16})$$

We then consider  $\lambda_0 = \mathbf{0}$ , which is assumed that  $\lambda_0 \in \Lambda^{(n)}$  by the regularity condition C8 for the duality function in Section S.2. Such  $\lambda_0$  results in  $\pi(\theta, \lambda_0) = C$  for any  $\theta \in \Theta_{\mathcal{A}}^{(n)}$ , where  $C \in \mathbb{R}$  is a constant, by the same regularity condition. By (S.13), we have

$$E_{(X,Y) \sim \mathbb{Q}} L\left((\hat{\theta}_{\mathcal{A}}^*)_{\lambda_0}|X, Y\right) \xrightarrow{p} E_{(X,Y) \sim \mathbb{P}} L\left((\hat{\theta}_{\mathcal{A}}^*)_{\lambda_0}|X, Y\right). \quad (\text{S.17})$$

By (S.15),  $(\hat{\theta}_{\mathcal{A}}^*)_{\lambda_0}$  is the empirical risk minimizer in the parameter space  $\Theta_{\mathcal{A}}^{(n)}$ . Since  $\Theta_{\mathcal{A}}^{(n)} \subseteq \Theta^{(n)}$  for  $n \geq N$ , the uniform convergence of the empirical risk in (S.13) indicates the convergence of its minimizer to the true population risk minimizer (Shalev-Shwartz et al., 2010). As a result, it follows from (S.17) and (S.3) that

$$E_{(X,Y) \sim \mathbb{Q}} L\left((\hat{\theta}_{\mathcal{A}}^*)_{\lambda_0}|X, Y\right) \xrightarrow{p} E_{(X,Y) \sim \mathbb{P}} L(\theta^*|X, Y)$$

for some  $\theta^* \in \Theta^*$ . Thus, with the duality parameter estimated in the parameter space  $\hat{\lambda} \in \Lambda^{(n)}$ , it follows from (S.16) that

$$E_{(X,Y) \sim \mathbb{Q}} L\left((\hat{\theta}_{\mathcal{A}}^*)_{\lambda_0}|X, Y\right) \geq E_{(X,Y) \sim \mathbb{Q}} L\left((\hat{\theta}_{\mathcal{A}}^*)_{\hat{\lambda}}|X, Y\right)$$

for each  $(X, Y) \in \mathbf{W}$ . It follows from (S.13) that

$$E_{(X,Y) \sim \mathbb{Q}} L\left((\hat{\theta}_{\mathcal{A}}^*)_{\hat{\lambda}}|X, Y\right) \xrightarrow{p} E_{(X,Y) \sim \mathbb{P}} L\left((\hat{\theta}_{\mathcal{A}}^*)_{\hat{\lambda}}|X, Y\right)$$

with

$$E_{(X,Y) \sim \mathbb{P}} L\left((\hat{\theta}_{\mathcal{A}}^*)_{\hat{\lambda}}|X, Y\right) \geq E_{(X,Y) \sim \mathbb{P}} L(\theta^*|X, Y)$$

for each  $(X, Y) \in \mathbf{W}$  and some optimal estimate  $\theta^* \in \Theta_*^{(n)}$ . For simplifying the notations, we define the random variables  $A, C, D$  and the value  $B$  dependent on  $n$  as follows:

$$\begin{aligned} A &:= E_{(X,Y) \sim \mathbb{Q}} L\left(\left(\hat{\theta}_{\mathcal{A}}^*\right)_{\lambda_0} | X, Y\right) & B &:= E_{(X,Y) \sim \mathbb{P}} L(\theta^* | X, Y) \\ C &:= E_{(X,Y) \sim \mathbb{Q}} L\left(\left(\hat{\theta}_{\mathcal{A}}^*\right)_{\hat{\lambda}} | X, Y\right) & D &:= E_{(X,Y) \sim \mathbb{P}} L\left(\left(\hat{\theta}_{\mathcal{A}}^*\right)_{\hat{\lambda}} | X, Y\right). \end{aligned}$$

It has been shown that  $A \xrightarrow{p} B$ ,  $C \xrightarrow{p} D$ , and  $\forall \omega \in \Omega$ ,  $A(\omega) \geq C(\omega)$  and  $D(\omega) \geq B(\omega)$ , where  $\Omega$  is the sample space. Here we prove that  $C \xrightarrow{p} B$ . For any  $\epsilon > 0$ , we have

$$\begin{aligned} P(|C - B| \geq \epsilon) &\leq P(|C - A| + |A - B| \geq \epsilon) \\ &\leq P(A - C \geq \epsilon/2) + P(|A - B| \geq \epsilon/2) \end{aligned}$$

by the union bound and the fact that  $\forall \omega \in \Omega$ ,  $A(\omega) \geq C(\omega)$ . From  $A \xrightarrow{p} B$  we know that  $\lim_{n \rightarrow \infty} P(|A - B| \geq \epsilon/2) = 0$  for any  $\epsilon > 0$ . It remains to show that  $\lim_{n \rightarrow \infty} P(A - C \geq \epsilon/2) = 0$  for any  $\epsilon > 0$ . We notice that

$$\begin{aligned} P(A - C \geq \epsilon/2) &= P((A - B) + (B - D) + (D - C) \geq \epsilon/2) \\ &\leq P((A - B) + (D - C) \geq \epsilon/2) \\ &\leq P(|A - B| \geq \epsilon/4) + P(|D - C| \geq \epsilon/4) \end{aligned}$$

by the union bound, which concludes  $\lim_{n \rightarrow \infty} P(A - C \geq \epsilon/2) = 0$  given  $A \xrightarrow{p} B$ ,  $C \xrightarrow{p} D$ . The first inequality above follows by the given condition  $\forall \omega \in \Omega$ ,  $D(\omega) \geq B(\omega)$ . Thus, we have proved that

$$E_{(X,Y) \sim \mathbb{Q}} L\left(\left(\hat{\theta}_{\mathcal{A}}^*\right)_{\hat{\lambda}} | X, Y\right) \xrightarrow{p} E_{(X,Y) \sim \mathbb{P}} L(\theta^* | X, Y). \quad (\text{S.18})$$

The estimation performed in the full parameter space  $\Theta^{(n)}$  and  $\Lambda^{(n)}$  with the unrestricted model results in the AM estimator  $\hat{\theta}_{AM} \in \Theta^{(n)}$ . We have

$$E_{(X,Y) \sim \mathbb{Q}} L\left(\hat{\theta}^* | X, Y\right) \leq E_{(X,Y) \sim \mathbb{Q}} L\left(\hat{\theta}_{AM} | X, Y\right) \leq E_{(X,Y) \sim \mathbb{Q}} L\left(\left(\hat{\theta}_{\mathcal{A}}^*\right)_{\hat{\lambda}} | X, Y\right)$$

for each  $(X, Y) \in \mathbf{W}$ , where  $\hat{\theta}^* \in \Theta^{(n)}$  is some optimal estimate with regard to  $(X, Y) \sim \mathbb{Q}$  defined in (S.14). Given the convergence results in (S.14) and (S.18) for the lower bound random variable and upper bound random variable, by the sandwich theorem, it follows that

$$E_{(X,Y) \sim \mathbb{Q}} L\left(\hat{\theta}_{AM} | X, Y\right) \xrightarrow{p} E_{(X,Y) \sim \mathbb{P}} L(\theta^* | X, Y), \quad (\text{S.19})$$

which further implies

$$E_{(X,Y) \sim \mathbb{P}} L\left(\hat{\theta}_{AM} | X, Y\right) \xrightarrow{p} E_{(X,Y) \sim \mathbb{P}} L(\theta^* | X, Y) \quad (\text{S.20})$$

by (S.13). Following the definition of the KL divergence elaborated in Section S.4, it can be concluded from (S.19) and (S.20) that

$$D_{KL}(\mathbb{P}, \mathbb{P}_{\hat{\theta}_{AM}}) \xrightarrow{p} D_{KL}(\mathbb{P}, \mathbb{P}_{\theta^*})$$

for any  $\theta^* \in \Theta^{(n)}$ , completing the proof.  $\square$

## S.7 Proof of Theorem 2

By Algorithm 2, in each imputation step at iteration  $(b, k)$  for arbitrary  $b = 1, \dots, B$  and  $k = 1, \dots, K$ , the samples  $\tilde{\mathbb{P}}_b^{(k)} := \{(\tilde{x}_i, \tilde{y}_i) : i = 1, \dots, m\}$  are treated as the current observations and the samples  $\hat{\mathbb{P}}_b^{(k)} := \{(x_i, y_i) : i = 1, \dots, n_k\}$  are treated as the future observations, where the sample sizes in  $\hat{\mathbb{P}}_b^{(k)}$  and  $\tilde{\mathbb{P}}_b^{(k)}$  are denoted as  $n_k$  and  $m$ , respectively. The index  $(b, -k)$  on each indexed observation  $(x, y)$  are omitted for simplicity. Recall that estimating the imputation model  $\mathbb{Q}_{\hat{\theta}_b}^{(k)}$  aims to minimize the objective function

$$E_{(X,Y) \sim \hat{\mathbb{P}}_b^{(k)}} L(\theta|X, Y) = G_{\tilde{\mathbb{P}}_b^{(k)}}(\theta, \lambda) + V_{\tilde{\mathbb{P}}_b^{(k)}, \hat{\mathbb{P}}_b^{(k)}}(\theta, \lambda).$$

By regularity conditions C1—C4 for the loss function in Section S.2, with the same ULLN argument in Section S.4, we have

$$\sup_{\theta \in \Theta_{\mathcal{A}}^{(n)}} \left| E_{(X,Y) \sim \hat{\mathbb{P}}_b^{(k)}} L(\theta|X, Y) - E_{(X,Y) \sim \mathbb{P}} L(\theta|X, Y) \right| \xrightarrow{p} 0 \quad (\text{S.21})$$

where  $\Theta_{\mathcal{A}}^{(n)}$  is the restricted parameter space specified in (S.2). The (strong) ULLN for the  $m$ -out-of- $n$  bootstrap sample mean is proved in (Spencer and Miller, 2023, Theorem 1), requiring the additional conditions: there exists  $\delta \in [0, 1)$  such that

$$\lim_{n_k \rightarrow \infty} \frac{n_k^{1-\delta} \log(n_k)}{m_{n_k}} = 0 \quad \text{and} \quad \mathbb{E} \left( \sup_{\theta \in \Theta_{\mathcal{A}}^{(n)}} |L(\theta|X, Y)|^{\frac{1}{1-\delta}} \right) < \infty, \quad (\text{S.22})$$

where  $n_k$  is the sample size of the future observations used to obtain the estimated model  $\mathbb{Q}_{\hat{\theta}_b}^{(k)}$ . The resampling sample size used to formulate current observations is denoted by  $m_{n_k} = \lceil \tilde{\alpha} n_k \rceil$ , where  $\tilde{\alpha}$  denotes the resampling ratio used in the  $m$ -out-of- $n$  bootstrap. By assumption, there exists a constant  $\tilde{\alpha}_0 \in (0, 1)$  such that the resampling ratio  $\tilde{\alpha}$  has  $\tilde{\alpha} \geq \tilde{\alpha}_0$  for every  $n \geq N$ , where  $N$  is some positive integer. Thereby, for any  $\delta \in (0, 1)$ , we have

$$\begin{aligned} \lim_{n_k \rightarrow \infty} \frac{n_k^{1-\delta} \log(n_k)}{m_{n_k}} &\leq \lim_{n_k \rightarrow \infty} \frac{n_k^{1-\delta} \log(n_k)}{\tilde{\alpha}_0 n_k} \\ &= \lim_{n_k \rightarrow \infty} \frac{C \cdot \log(n_k)}{n_k^\delta} \\ &= 0, \end{aligned} \quad (\text{S.23})$$

where  $C = 1/\tilde{\alpha}_0$  is a constant. Thus, the condition specified in (S.22) is satisfied given the regularity condition C5 in Section S.2. By assumption, the parameter  $K$  used for data-splitting is fixed, implying  $n_k \rightarrow \infty$  as  $n \rightarrow \infty$ . Together with (Spencer and Miller, 2023, Theorem 1) and (S.23), this validates the ULLN for the bootstrap samples obtained by AM:

$$\sup_{\theta \in \Theta_{\mathcal{A}}} \left| E_{(X,Y) \sim \tilde{\mathbb{P}}_b^{(k)}} L(\theta|X, Y) - E_{(X,Y) \sim \mathbb{P}} L(\theta|X, Y) \right| \xrightarrow{p} 0. \quad (\text{S.24})$$

The assumption  $D_{KL}(\mathbb{P}, \hat{\mathbb{P}}) \xrightarrow{p} 0$  implies  $D_{KL}(\mathbb{P}, \hat{\mathbb{P}}_b^{(k)}) \xrightarrow{p} 0$ . By taking  $\mathbb{Q} = \hat{\mathbb{P}}_b^{(k)}$ , the arguments in Section S.6 can then be used to show

$$E_{(X,Y) \sim \hat{\mathbb{P}}_b^{(k)}} L(\hat{\theta}^*|X, Y) \xrightarrow{p} E_{(X,Y) \sim \mathbb{P}} L(\theta^*|X, Y) \quad (\text{S.25})$$

for some optimal estimate  $\theta^* \in \Theta_*^{(n)}$ , and  $\hat{\theta}^* \in \Theta^{(n)}$  is some minimizer of the expected loss function with regard to  $(X, Y) \sim \hat{\mathbb{P}}_b^{(k)}$ .

Following the same arguments in Section S.4, we construct the restricted parameter space  $\Theta_{\mathcal{A}}^{(n)} \subseteq \Theta^{(n)}$  specified in (S.2). We further define the  $\lambda$ -dependent AM estimator in the restricted parameter space  $\Theta_{\mathcal{A}}^{(n)} \subseteq \Theta^{(n)}$  as

$$(\hat{\theta}_{\mathcal{A}}^*)_{\lambda} = \arg \min_{\theta \in \Theta_{\mathcal{A}}} \left( \frac{1}{m} \sum_{i=1}^m L(\theta | \tilde{x}_i, \tilde{y}_i) + \pi(\theta, \lambda) \right) \quad (\text{S.26})$$

for any given  $\lambda \in \Lambda^{(n)}$ , and the duality parameter  $\lambda$  is chosen at  $\lambda = \hat{\lambda}$  with

$$\hat{\lambda} = \arg \min_{\lambda \in \Lambda^{(n)}} E_{(X, Y) \sim \hat{\mathbb{P}}_b^{(k)}} L \left( (\hat{\theta}_{\mathcal{A}}^*)_{\lambda} | X, Y \right). \quad (\text{S.27})$$

We then consider  $\lambda_0 = \mathbf{0}$ , which is assumed that  $\lambda_0 \in \Lambda^{(n)}$  by the regularity condition C8 for the duality function in Section S.2. Such  $\lambda_0$  results in  $\pi(\theta, \lambda_0) = C$  for any  $\theta \in \Theta_{\mathcal{A}}^{(n)}$ , where  $C \in \mathbb{R}$  is a constant, by the same regularity condition. By (S.21), we have

$$E_{(X, Y) \sim \hat{\mathbb{P}}_b^{(k)}} L \left( (\hat{\theta}_{\mathcal{A}}^*)_{\lambda_0} | X, Y \right) \xrightarrow{p} E_{(X, Y) \sim \mathbb{P}} L \left( (\hat{\theta}_{\mathcal{A}}^*)_{\lambda_0} | X, Y \right). \quad (\text{S.28})$$

By (S.26),  $(\hat{\theta}_{\mathcal{A}}^*)_{\lambda_0}$  is the empirical risk minimizer in the parameter space  $\Theta_{\mathcal{A}}^{(n)}$ . The uniform convergence of the sample loss in (S.24) indicates the convergence of its minimizer to the true population risk minimizer (Shalev-Shwartz et al., 2010). As a result, it follows from (S.28) and (S.3) that

$$E_{(X, Y) \sim \hat{\mathbb{P}}_b^{(k)}} L \left( (\hat{\theta}_{\mathcal{A}}^*)_{\lambda_0} | X, Y \right) \xrightarrow{p} E_{(X, Y) \sim \mathbb{P}} L(\theta^* | X, Y). \quad (\text{S.29})$$

With (S.25) and (S.29), the exact same argument in the relevant part of Section S.7 can be used by simply replacing  $\mathbb{Q}$  with  $\hat{\mathbb{P}}_b^{(k)}$ , which concludes that

$$D_{KL}(\mathbb{P}, \mathbb{Q}_{\hat{\theta}_b}^{(k)}) \xrightarrow{p} D_{KL}(\mathbb{P}, \mathbb{P}_{\theta^*})$$

for the arbitrary pair  $(b, k)$ . Thus, when the model is valid,

$$D_{KL}(\mathbb{P}, \mathbb{Q}_{\hat{\theta}_b}^{(k)}) \xrightarrow{p} \lim_{n \rightarrow \infty} D_{KL}(\mathbb{P}, \mathbb{P}_{\theta^*}) = 0.$$

for the arbitrary pair  $(b, k)$ . Denote the final imputation distribution as the mixture distribution

$$\mathbb{Q} := \frac{1}{B \cdot K} \sum_{b=1}^B \sum_{k=1}^K \mathbb{Q}_{\hat{\theta}_b}^{(k)}$$

for fixed  $K > 0$  and  $B > 0$ . The convexity of the KL divergence implies

$$D_{KL}(\mathbb{P}, \mathbb{Q}) \leq \frac{1}{B \cdot K} \sum_{b=1}^B \sum_{k=1}^K D_{KL}(\mathbb{P}, \mathbb{Q}_{\hat{\theta}_b}^{(k)}).$$

Since the KL divergence is non-negative, for any  $\epsilon > 0$ , we have

$$\lim_{n \rightarrow \infty} P(D_{KL}(\mathbb{P}, \mathbb{Q}) \geq \epsilon) \leq \lim_{n \rightarrow \infty} \sum_{b=1}^B \sum_{k=1}^K P \left( D_{KL}(\mathbb{P}, \mathbb{Q}_{\hat{\theta}_b}^{(k)}) \geq \frac{\epsilon}{B \cdot K} \right) = 0,$$

by the union bound, which concludes that

$$D_{KL}(\mathbb{P}, \mathbb{Q}) \xrightarrow{p} 0.$$

□

## S.8 Imputation with Finite-sample Valid Predictive Coverage

### S.8.1 Theoretical Support

Here, we study the theoretical properties of the resampling-based imputation scheme in the finite-sample scenario. As proposed in Section 2.3, we utilize an adaptive  $m$ -out-of- $n$  bootstrap resampling scheme. Here,  $m$  is selected to ensure uniformly distributed cumulative distribution function (CDF) values of the data, as detailed in (11) and (12). Controlling the effectiveness of the data distribution in this manner can lead to desirable theoretical properties, which is summarized into the following theorem.

**Theorem 3** (Valid Predictive Coverage). *Consider an imputation model with the distribution function  $\hat{F}(\cdot|x)$ . Suppose that for an unseen data point  $(x_*, y_*) \sim \mathbb{P}$ , it holds that  $\hat{F}(y_*|x_*) \sim \text{Uniform}(0, 1)$ . Then, for any  $\alpha \in (0, 1)$  and an interval  $[a_0, b_0]$  such that  $\hat{F}(b_0|x_*) - \hat{F}(a_0|x_*) = 1 - \alpha$ , we have*

$$\text{Prob}(a_0 \leq y_* \leq b_0) = 1 - \alpha.$$

*Proof.* Without loss of generality, assume  $x$  is a random variable with a continuous distribution function  $G(\cdot)$ . We have

$$\begin{aligned} \text{Prob}(a_0 \leq y_* \leq b_0) &= \int \int_{a_0}^{b_0} d\hat{F}(y_*|x_*) dG(x_*) \\ &= (1 - \alpha) \int dG(x_*) \\ &= 1 - \alpha \end{aligned}$$

given that  $\hat{F}(y_*|x_*) \sim \text{Uniform}(0, 1)$ . □

Thus, imposing (12) ensures a  $(1 - \alpha)$  coverage rate of the observed data (unseen by the imputation model) using the  $(1 - \alpha)$  predictive interval of the imputation model for any  $\alpha \in (0, 1)$ . That is, suppose  $(x, y) \sim \hat{\mathbb{P}}$ , consider an interval  $[a_0, b_0]$  such that

$$\sum_{k=1}^K \left( \hat{F}_{\hat{\theta}_b}^{(k)}(b_0|x) - \hat{F}_{\hat{\theta}_b}^{(k)}(a_0|x) \right) \cdot \mathbb{1} \left( x \in \{\mathbf{x}_b^{(k)}\} \right) = 1 - \alpha$$

where  $\mathbb{1}(\cdot)$  denotes the indicator function and  $\{\mathbf{x}_b^{(k)}\}$  denotes the holdout set of  $x$  in the  $k$ -th fold. Then, we have

$$\text{Prob}(a_0 \leq y \leq b_0) = 1 - \alpha.$$

The coverage rate is an unbiased estimate of the true predictive coverage rate due to the use of the holdout data unseen by the imputation model, and the variance decreases with both the observed sample size  $n$  and the number of imputation models  $B \cdot K$ . This property provides a strong theoretical foundation for its similarity to the true but unknown data distribution.

### S.8.2 Empirical Evidence

In this section, we present empirical evidence to support the finite-sample predictive coverage theory discussed above in Section S.8.1. We consider the  $n < p$  linear regression scenario from Section 5.2, with different true model sparsity and signal-to-noise ratios

(SNR) controlled by  $\alpha$  and  $\tau$ . For the first repetition in each setting, we generate 1,000 new data points from the underlying true model and assess the coverage rate of the mixture of  $B \cdot K$  imputation models.

Algorithm 3 is used to impose (12). We first check the condition in Theorem 3 with the 1,000 new data points. That is, for each new data point  $(x_*, y_*) \sim \mathbb{P}$ , it is required that  $\hat{F}(y_*|x_*) \sim \text{Uniform}(0, 1)$ , where  $\hat{F}(\cdot|x)$  is the distribution function of the mixture of  $B \cdot K$  imputation models. The results are demonstrated in the Q-Q plots in Figure S.3. It can be seen that Algorithm 3 is effective in approximating this target.

To construct the  $(1 - \alpha_0)$  predictive interval where  $\alpha_0 \in (0, 1)$ , for each  $x_*$ , we sample  $N = 10,000$  values of  $\hat{y}_*$  from the mixture of  $B \cdot K$  imputation models. Then, we take the  $\alpha_0/2$ -th and  $(1 - \alpha_0/2)$ -th quantiles of the  $\hat{y}_*$  values as the lower bound and upper bound of the predictive interval respectively. Table S.1 displays the coverage rates of the 1,000 new data points with these constructed  $(1 - \alpha_0)$  predictive intervals across different values of  $\alpha_0$ . It can be seen that the coverage is satisfactory across various settings.

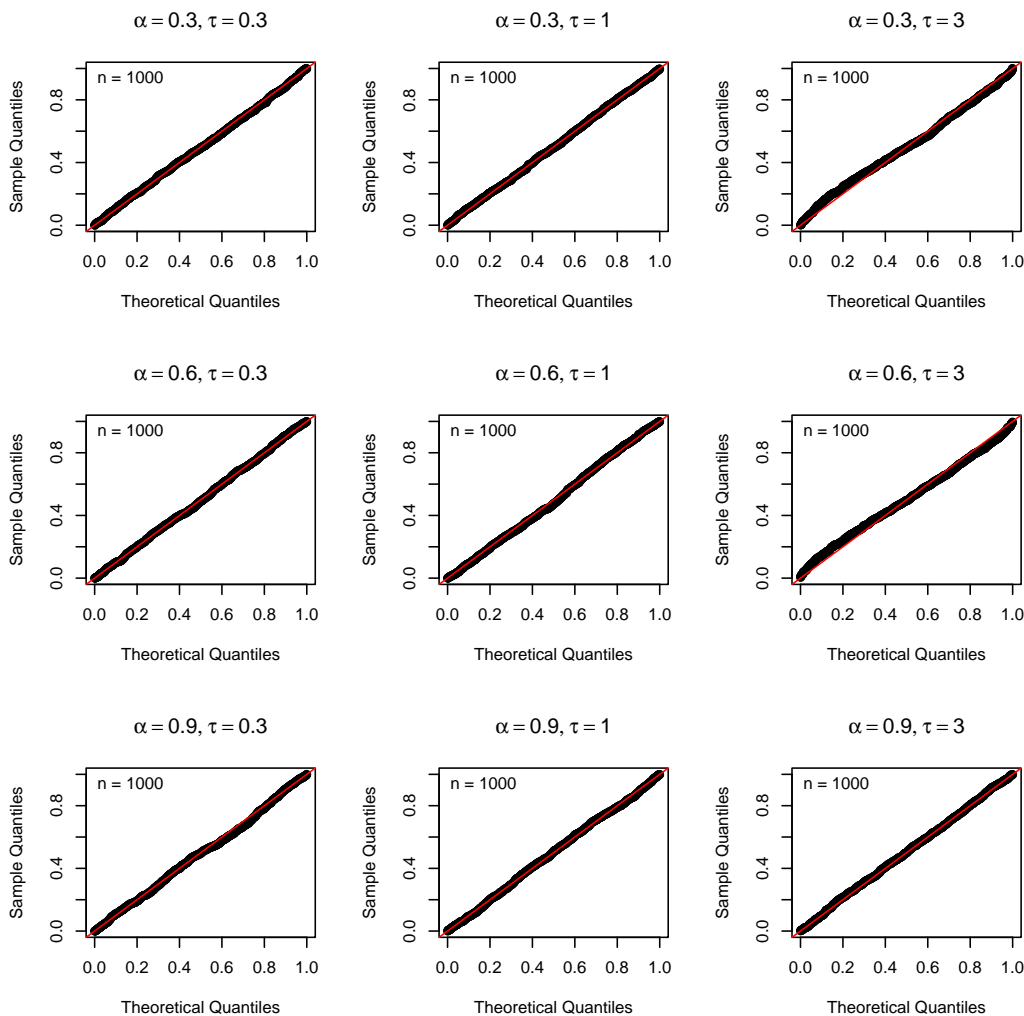


**Figure S.3:** Q-Q plots of the estimated CDF values of the 1,000 new data points with the mixture of  $B \cdot K$  imputation models obtained using Algorithm 2, against the standard uniform distribution, in the linear regression example (Section 5.2). Presented here are the results from the first repetition across various settings, using the (unweighted)  $L_1$  duality function.

**Table S.1:** Coverage rate of the 1,000 new data points with the  $(1 - \alpha_0)$  predictive interval (estimated by Monte-Carlo sampling) of the mixture of  $B \cdot K$  imputation models, with different values of  $\alpha_0$ , in the linear regression example (Section 5.2). Presented here are the results from the first repetition across various settings, using the (unweighted)  $L_1$  duality function.

Setting	0.90	0.80	0.70	0.60	0.50	0.40	0.30	0.20	0.10
$\alpha = 0.3, \tau = 0.3$	0.909	0.816	0.722	0.621	0.518	0.423	0.313	0.219	0.106
$\alpha = 0.3, \tau = 1$	0.919	0.812	0.705	0.607	0.497	0.39	0.295	0.198	0.105
$\alpha = 0.3, \tau = 3$	0.936	0.857	0.766	0.669	0.561	0.45	0.338	0.238	0.129
$\alpha = 0.6, \tau = 0.3$	0.889	0.789	0.697	0.604	0.508	0.404	0.298	0.195	0.085
$\alpha = 0.6, \tau = 1$	0.883	0.786	0.681	0.587	0.485	0.379	0.285	0.181	0.084
$\alpha = 0.6, \tau = 3$	0.946	0.876	0.78	0.68	0.566	0.461	0.351	0.24	0.115
$\alpha = 0.9, \tau = 0.3$	0.894	0.804	0.708	0.602	0.502	0.424	0.327	0.226	0.13
$\alpha = 0.9, \tau = 1$	0.905	0.796	0.703	0.61	0.492	0.384	0.299	0.201	0.098
$\alpha = 0.9, \tau = 3$	0.901	0.791	0.707	0.618	0.51	0.409	0.301	0.208	0.097

## S.9 Implementation Details in the Many-Normal-Means Example

### S.9.1 Technical Details

The problem of many normal means in this paper uses the model

$$Y_i | \mu_i \sim N(\mu_i, 1), \quad i = 1, \dots, n,$$

with  $\Pr(\mu_i = \eta_j) = \alpha_j$ ,  $k = 1, \dots, l$ , where  $\eta_1 \leq \eta_2 \leq \dots \leq \eta_l$ . The duality function takes the form

$$\pi(\eta, \lambda) = \sum_{j=2}^l \lambda_k (\eta_j - \eta_{j-1}) \quad (\lambda_j \geq 0 \text{ for } j = 2, \dots, l).$$

For convenience, let  $\lambda_1 = \lambda_{l+1} = 0$ . The loss function takes the form

$$L(\alpha, \eta | Y = y) = -\frac{1}{n} \ln \left( \sum_{i=1}^n \sum_{j=1}^l \alpha_j e^{-\frac{(y_i - \eta_j)^2}{2}} \right).$$

In this section, we elaborate on the derivation of estimation of imputation models. First, we obtain the data represented by  $\hat{\mathbb{P}}_b^{(k)}$  and  $\tilde{\mathbb{P}}_b^{(k)}$  following the data-splitting and resampling scheme in Algorithm 2 at iteration  $(b, k)$ , for any arbitrary  $b = 1, \dots, B$  and  $k = 1, \dots, K$ . For simplicity, we omit the index  $(b, -k)$  on each indexed observation  $(x, y)$ . The samples  $\tilde{\mathbb{P}}_b^{(k)} := \{(\tilde{x}_i, \tilde{y}_i) : i = 1, \dots, m\}$  are treated as the current observations and the samples  $\hat{\mathbb{P}}_b^{(k)} := \{(x_i, y_i) : i = 1, \dots, n_k\}$  are treated as the future observations, where the sample sizes in  $\hat{\mathbb{P}}_b^{(k)}$  and  $\tilde{\mathbb{P}}_b^{(k)}$  are denoted as  $n_k$  and  $m$  respectively. Using the matrix notation, the two samples are denoted by  $(\mathbf{x}, \mathbf{y})$  and  $(\tilde{\mathbf{x}}, \tilde{\mathbf{y}})$ , omitting the  $(b, -k)$  indexing used in Algorithm 2.

The estimation of  $(\alpha, \eta, \lambda)$  should satisfy

$$0 = \frac{\partial G_{\tilde{\mathbb{P}}_b^{(k)}}(\alpha, \eta, \lambda)}{\partial \alpha_j} = \frac{\partial L(\alpha, \eta | \tilde{\mathbf{y}})}{\partial \alpha_j} = -\frac{1}{m} \sum_{i=1}^m \frac{\exp(-\frac{1}{2}(\tilde{y}_i - \eta_j)^2)}{\sum_{j=1}^l \alpha_j \exp(-\frac{1}{2}(\tilde{y}_i - \eta_j)^2)}$$

and

$$\begin{aligned} 0 &= \frac{\partial G_{\tilde{\mathbb{P}}_b^{(k)}}(\alpha, \eta, \lambda)}{\partial \eta_j} = \frac{\partial L(\alpha, \eta | \tilde{\mathbf{y}})}{\partial \eta_j} + \frac{\partial \pi(\eta, \lambda)}{\partial \eta_j} \\ &= -\frac{1}{m} \sum_{i=1}^m \frac{\alpha_j \exp(-\frac{1}{2}(\tilde{y}_i - \eta_j)^2) (\tilde{y}_i - \eta_j)}{\sum_{j=1}^l \alpha_j \exp(-\frac{1}{2}(\tilde{y}_i - \eta_j)^2)} + (\lambda_j - \lambda_{j+1}) \end{aligned}$$

for  $j = 1, \dots, l$  and

$$\lambda = \min_{\tilde{\lambda}} \left\| \frac{\partial V_{\hat{\mathbb{P}}_b^{(k)}, \tilde{\mathbb{P}}_b^{(k)}}(\alpha, \eta, \lambda)}{\partial \eta} \right\|_2^2 = \min_{\tilde{\lambda}} \left\| d_\eta - \tilde{d}_\eta - M\tilde{\lambda} \right\|_2^2,$$

where

$$\begin{aligned} d_\eta &= \left( \frac{\partial L(\alpha, \eta | \mathbf{y})}{\partial \eta_1}, \dots, \frac{\partial L(\alpha, \eta | \mathbf{y})}{\partial \eta_l} \right)^T \\ \tilde{d}_\eta &= \left( \frac{\partial L(\alpha, \eta | \tilde{\mathbf{y}})}{\partial \eta_1}, \dots, \frac{\partial L(\alpha, \eta | \tilde{\mathbf{y}})}{\partial \eta_l} \right)^T \\ M &= \begin{bmatrix} 1 & 0 & 0 & \cdots & 0 & 0 \\ -1 & 1 & 0 & \cdots & 0 & 0 \\ 0 & -1 & 1 & \cdots & 0 & 0 \\ \vdots & \vdots & \vdots & \ddots & \vdots & \vdots \\ 0 & 0 & 0 & \cdots & 1 & 0 \\ 0 & 0 & 0 & \cdots & -1 & 1 \\ 0 & 0 & 0 & \cdots & 0 & -1 \end{bmatrix}_{l \times (l-1)} \\ \tilde{\lambda} &= (\lambda_2, \dots, \lambda_l). \end{aligned} \tag{S.30}$$

Following Section 3, the estimation can be done with the projected gradient descent approach (Boyd et al., 2003) to deal with the constraint on  $\alpha$ ,  $\eta$  and  $\lambda$ . Specifically, for  $\alpha$ , we have

$$\alpha_j^{(t+1/2)} = \alpha_j^{(t)} - \gamma_1 \cdot \left( -\frac{1}{m} \sum_{i=1}^m \frac{\exp\left(-\frac{1}{2}(\tilde{y}_i - \eta_j^{(t)})^2\right)}{\sum_{j=1}^l \alpha_j^{(t)} \exp\left(-\frac{1}{2}(\tilde{y}_i - \eta_j^{(t)})^2\right)} \right)$$

for  $i = 1, \dots, l$ , where  $\gamma_1$  is the step size, followed with solving

$$\begin{aligned} &\underset{\alpha^{(t+1)}}{\text{minimize}} && \frac{1}{2} \left\| \alpha^{(t+1)} - \alpha^{(t+1/2)} \right\|_2^2 \\ &\text{subject to} && 0 \leq \alpha^{(t+1)} \leq 1, \\ &&& \mathbf{1}^T \alpha^{(t+1)} = 1. \end{aligned} \tag{S.31}$$

Note that (S.31) is essentially the problem of projecting a vector onto the standard or probability simplex, where many existing solutions are available and we use the method in Blondel et al. (2014). For  $\eta$ , we have

$$\eta_j^{(t+1/2)} = \eta_j^{(t)} - \gamma_2 \cdot \left( -\frac{1}{m} \sum_{i=1}^m \frac{\alpha_j^{(t)} \exp\left(-\frac{1}{2}(\tilde{y}_i - \eta_j^{(t)})^2\right) (\tilde{y}_i - \eta_j^{(t)})}{\sum_{j=1}^l \alpha_j^{(t)} \exp\left(-\frac{1}{2}(\tilde{y}_i - \eta_j^{(t)})^2\right)} + (\lambda_j^{(t)} - \lambda_{j+1}^{(t)}) \right)$$

for  $j = 1, \dots, l$ , where  $\gamma_2$  is the step size, followed with finding

$$\begin{aligned} &\underset{\eta^{(t+1)}}{\text{minimize}} && \frac{1}{2} \left\| \eta^{(t+1)} - \eta^{(t+1/2)} \right\|_2^2 \\ &\text{subject to} && \eta_1^{(t+1)} \leq \eta_2^{(t+1)} \leq \dots \leq \eta_l^{(t+1)}, \end{aligned}$$



or equivalently,

$$\begin{aligned} & \underset{\eta^{(t+1)}}{\text{minimize}} && \frac{1}{2} \eta^{(t+1)T} \eta^{(t+1)} - \eta^{(t+\frac{1}{2})T} \eta^{(t+1)} \\ & \text{subject to} && M^T \eta^{(t+1)} \leq \mathbf{0}, \end{aligned} \tag{S.32}$$

where  $M$  is defined in (S.30). Note that (S.32) is a canonical quadratic programming problem with inequality constraint. For  $\lambda$ , we have

$$\lambda^{(t+1)} = \lambda^{(t)} - \gamma_3 \cdot \left( 2M^T M \lambda^{(t)} - 2M^T \left( d_{\eta^{(t+1)}} - \tilde{d}_{\eta^{(t+1)}} \right) \right),$$

where  $\gamma_3$  is the step size.

The estimation procedure for an imputation model is considered complete once both  $\eta^{(t)}$  and  $\alpha^{(t)}$  have converged. The resulting model, characterized by the parameters  $(\hat{\eta}_b^{(k)}, \hat{\alpha}_b^{(k)})$  is then applied on the hold-out set  $\mathbf{y}_b^{(k)}$ . Depending on the objective, this can be used for the purpose of imputing future observations using Algorithm 2, or for assessing the efficiency of the imputation model to select the resampling parameter with Algorithm 3.

Performing Algorithm 3 for selecting resampling parameter  $\tilde{\alpha}$  requires the calculation of CDF values with a single imputation model estimation iteration ( $B = 1$ ). The CDF value can be calculated with

$$F(y_{bi}^{(k)}) = \sum_{j=1}^l \hat{\alpha}_{bj}^{(k)} \Phi \left( y_{bi}^{(k)} - \hat{\eta}_{bj}^{(k)} \right),$$

for  $i = 1, \dots, n - n_k$ , where  $b = 1$  and  $\Phi(\cdot)$  represents the standard normal CDF. The hold-out set is denoted as  $(\mathbf{x}_b^{(k)}, \mathbf{y}_b^{(k)}) := \{(x_{bi}^{(k)}, y_{bi}^{(k)}) : i = 1, \dots, n - n_k\}$ . After iterating through  $k = 1, \dots, K$ , we can obtain  $n$  such CDF values. This collection of CDF values is then tested against the standard uniform distribution with the KS-test for the selection of the best  $\tilde{\alpha}$ .

Note that performing Algorithm 3 already yields an imputation model obtained with the selected  $\tilde{\alpha}$ . Thus, Algorithm 2 only requires  $B - 1$  iterations. In Algorithm 2, future observations are created with the mixture of normal distributions

$$y_{*bi}^{(k)} \sim \sum_{j=1}^l \hat{\alpha}_{bj}^{(k)} N(\hat{\eta}_{bj}^{(k)}, 1)$$

for  $i = 1, \dots, n_k$ . By iteratively performing the estimation of the imputation model and the imputation process for  $b = 1, \dots, B$  and  $k = 1, \dots, K$ , we construct the imputation distribution  $\mathbb{Q}$ , which consists of  $n \cdot B$  samples.

The estimation process with Algorithm 1 follows the same implementation of estimation of imputation models as described above, with a straightforward modification:  $\hat{\mathbb{P}}_b^{(k)}$  is replaced with  $\mathbb{Q}$  and  $\tilde{\mathbb{P}}_b^{(k)}$  with  $\hat{\mathbb{P}}$ , where the latter represents the full observations.

## S.9.2 Implementation Details of AM

We implemented AM for the many-normal-means example in R. The optimization problem for quadratic programming (S.9.1) is solved with the R package `quadprog`. Algorithm 2 was implemented with  $B = 5$  and  $K = 5$ . Algorithm 3 is used to select the resampling parameter  $\tilde{\alpha}$ , with the candidate set  $\{0.5, 0.8, 1.0, 1.2\}$ . The optimization-related parameters that apply to all experiments are selected as:  $\gamma_1 = 0.05$ ,  $\gamma_2 = 0.5$ , and  $\gamma_3 = 0.1$ .

### S.9.3 Implementation Details of Other Methods

We implemented the James-Stein estimator in its original form. For  $g$ -modeling, we use the relevant function in the R package `deconvolveR` (Narasimhan and Efron, 2020), with the default settings. The discrete support points were selected to range from the minimum to the maximum observed values of  $y$ , with a grid density of 0.1. Additionally, we included the point at 0 among the support points.

## S.10 Implementation Details in the Linear Regression Example

### S.10.1 Technical Details

For the observed data  $(\mathbf{x}, \mathbf{y})$ , we assume that  $\mathbf{x}$  is standardized to have mean 0 and variance 1 for each column. The response vector  $\mathbf{y}$  is also standardized to have mean 0 and variance 1. The loss function can be written as

$$L(\beta, \sigma | X = x, Y = y) = \frac{1}{2} \log(\sigma^2) + \frac{1}{2\sigma^2 n} \sum_{i=1}^n (y_i - x'_i \beta)^2.$$

The duality function takes the form  $\pi(\beta, \sigma, \lambda) = \lambda_0 \log\left(\frac{1}{\sigma^2}\right) + \sum_{i=1}^p \lambda_i |\beta_i|$  ( $\lambda_i \geq 0, i = 0, 1, \dots, p$ ) or  $\pi(\beta, \sigma, \lambda) = \lambda_0 \log\left(\frac{1}{\sigma^2}\right) + \sum_{i=1}^p \lambda_i \beta_i^2$  ( $\lambda_i \geq 0, i = 0, 1, \dots, p$ ). Note that the estimation of  $\beta$  is independent of the estimation of  $\sigma$ . For this reason, the estimation of  $\sigma$  can be done after the estimate of  $\beta$  converges to the solution. We denote the reparameterization  $\phi = \log\left(\frac{1}{\sigma^2}\right)$ .

In this section, we elaborate on the derivation for estimating an imputation model. First, we obtain the data represented by  $\hat{\mathbb{P}}_b^{(k)}$  and  $\tilde{\mathbb{P}}_b^{(k)}$  following the data-splitting and resampling scheme in Algorithm 2 at iteration  $(b, k)$ , for any arbitrary  $b = 1, \dots, B$  and  $k = 1, \dots, K$ . For simplicity, we omit the index  $(b, -k)$  on each indexed observation  $(x, y)$ . The samples  $\tilde{\mathbb{P}}_b^{(k)} := \{(\tilde{x}_i, \tilde{y}_i) : i = 1, \dots, m\}$  are treated as the current observations and the samples  $\hat{\mathbb{P}}_b^{(k)} := \{(x_i, y_i) : i = 1, \dots, n_k\}$  are treated as the future observations, where the sample sizes in  $\hat{\mathbb{P}}_b^{(k)}$  and  $\tilde{\mathbb{P}}_b^{(k)}$  are denoted as  $n_k$  and  $m$  respectively. Using the matrix notation, the two samples are denoted by  $(\mathbf{x}, \mathbf{y})$  and  $(\tilde{\mathbf{x}}, \tilde{\mathbf{y}})$ , omitting the  $(b, -k)$  indexing used in Algorithm 2.

Denotes the AM estimate of the parameters by  $(\hat{\beta}_b^{(k)}, \hat{\sigma}_b^{(k)}, \hat{\lambda}_b^{(k)})$ . Denote the reparameterized estimate of the standard deviation parameter by  $\hat{\phi}_b^{(k)}$ . When  $\beta = \hat{\beta}_b^{(k)}$ ,  $\sigma = \hat{\sigma}_b^{(k)}$ , and

$$\frac{\partial G_{\tilde{\mathbb{P}}_b^{(k)}}(\beta, \sigma, \lambda)}{\partial \phi} = 0.$$

Thus, we have

$$\begin{aligned} \hat{\lambda}_{b0}^{(k)} &= \min_{\lambda_0} \left\| \frac{\partial V_{\hat{\mathbb{P}}_b^{(k)}, \tilde{\mathbb{P}}_b^{(k)}}(\hat{\beta}_b^{(k)}, \hat{\sigma}_b^{(k)}, \lambda)}{\partial \hat{\phi}_b^{(k)}} \right\|_2^2 \\ &= \min_{\lambda_0} \left\| \frac{\partial L(\hat{\beta}_b^{(k)}, \hat{\sigma}_b^{(k)} | \tilde{\mathbf{x}}, \tilde{\mathbf{y}})}{\partial \hat{\phi}_b^{(k)}} \right\|_2^2, \end{aligned}$$

resulting in

$$\left(\hat{\sigma}_b^{(k)}\right)^2 = \frac{1}{\left(1 - 2\hat{\lambda}_{b0}^{(k)}\right) m} \sum_{i=1}^m (\tilde{y}_i - \tilde{x}'_i \hat{\beta}_b^{(k)})^2$$

and

$$\hat{\lambda}_{b0}^{(k)} = \begin{cases} \frac{1}{2} \left( 1 - \frac{\sum_{i=1}^m (\tilde{y}_i - \tilde{x}'_i \hat{\beta}_b^{(k)})^2 / m}{\sum_{i=1}^{n_k} (y_i - x'_i \hat{\beta}_b^{(k)})^2 / n_k} \right) & \text{if } \sum_{i=1}^m (\tilde{y}_i - \tilde{x}'_i \hat{\beta}_b^{(k)})^2 / m \leq \sum_{i=1}^{n_k} (y_i - x'_i \hat{\beta}_b^{(k)})^2 / n_k \\ 0 & \text{if } \sum_{i=1}^m (\tilde{y}_i - \tilde{x}'_i \hat{\beta}_b^{(k)})^2 / m > \sum_{i=1}^{n_k} (y_i - x'_i \hat{\beta}_b^{(k)})^2 / n_k. \end{cases}$$

This further implies that

$$\left( \hat{\sigma}_b^{(k)} \right)^2 = \max \left( \frac{1}{m} \sum_{i=1}^m (\tilde{y}_i - \tilde{x}'_i \hat{\beta}_b^{(k)})^2, \frac{1}{n_k} \sum_{i=1}^{n_k} (y_i - x'_i \hat{\beta}_b^{(k)})^2 \right). \quad (\text{S.33})$$

Next, we focus on the estimation of  $\beta$  with the modified loss function obtained by including only the terms related to  $\beta$ . This leads to the canonical mean squared error (MSE) loss function taking the form

$$L(\beta | X = x, Y = y) = \frac{1}{2n} (y - x\beta)^T (y - x\beta).$$

The duality function in its general form can be rewritten as:  $\pi(\beta, \lambda) = \lambda \sum_{i=1}^p |\beta_i|$  and  $\pi(\beta, \lambda) = \lambda \sum_{i=1}^p \beta_i^2$ , where  $\lambda$  can be considered as either a vector or a scalar, depending on whether the duality function is weighted. We first consider the  $L_1$  duality function. In this case, the estimate of  $(\beta, \lambda)$  should satisfy

$$\begin{aligned} 0 &= \frac{\partial G_{\hat{\mathbb{P}}_b^{(k)}}(\beta, \lambda)}{\partial \beta} = \frac{\partial L(\beta | \tilde{\mathbf{x}}, \tilde{\mathbf{y}})}{\partial \beta} + \frac{\partial \pi(\beta, \lambda)}{\partial \beta} \\ &= -\frac{1}{m} \tilde{\mathbf{x}}^T (\tilde{\mathbf{y}} - \tilde{\mathbf{x}}\beta) + \lambda \cdot \text{sign}(\beta) \end{aligned}$$

and

$$\begin{aligned} \lambda &= \min_{\lambda} \left\| \frac{\partial V_{\hat{\mathbb{P}}_b^{(k)}, \hat{\mathbb{P}}_b^{(k)}}(\beta, \lambda)}{\partial \beta} \right\|_2^2 \\ &= \min_{\lambda} \left\| \left( \frac{1}{n_k} \mathbf{x}^T \mathbf{x} - \frac{1}{m} \tilde{\mathbf{x}}^T \tilde{\mathbf{x}} \right) \beta - \left( \frac{1}{n_k} \mathbf{x}^T \mathbf{y} - \frac{1}{m} \tilde{\mathbf{x}}^T \tilde{\mathbf{y}} \right) - \lambda \cdot \text{sign}(\beta) \right\|_2^2 \end{aligned}$$

with the subgradient method (Shor et al., 1985). Thus, the stochastic update is given by

$$\beta^{(t+1)} = \beta^{(t)} - \gamma_1 \cdot \left( -\frac{1}{m} \tilde{\mathbf{x}}^T (\tilde{\mathbf{y}} - \tilde{\mathbf{x}}\beta^{(t)}) + \lambda^{(t)} \cdot \text{sign}(\beta^{(t)}) \right)$$

and

$$\lambda^{(t+1)} = (\lambda^{(t)} - \gamma_2 \cdot (2v_1^T v_1 \lambda^{(t)} - 2v_1^T v_2))_+$$

if  $\lambda$  is a scalar and

$$\lambda^{(t+1)} = (\lambda^{(t)} - \gamma_2 \cdot 2(v_1 - \lambda^{(t)} \odot v_1) \odot (-v_1))_+$$

otherwise, where  $v_1 = \text{sign}(\beta^{(t+1)})$ ,  $v_2 = \left( \frac{1}{n_k} \mathbf{x}^T \mathbf{x} - \frac{1}{m} \tilde{\mathbf{x}}^T \tilde{\mathbf{x}} \right) \beta^{(t+1)} - \left( \frac{1}{n_k} \mathbf{x}^T \mathbf{y} - \frac{1}{m} \tilde{\mathbf{x}}^T \tilde{\mathbf{y}} \right)$ , and  $\gamma_1$  and  $\gamma_2$  are the chosen step sizes. For faster convergence, the update of  $\beta$  can be replaced with the update scheme of the proximal gradient method (Parikh and Boyd, 2014), that is,

$$\beta^{(t+1/2)} = \beta^{(t)} - \gamma_1 \cdot \left( -\frac{1}{m} \tilde{\mathbf{x}}^T (\tilde{\mathbf{y}} - \tilde{\mathbf{x}}\beta^{(t)}) \right)$$

$$\beta^{(t+1)} = \text{sign}(\beta^{(t+1/2)}) (|\beta^{(t+1/2)}| - \gamma_1 \lambda^{(t)})_+,$$

where

$$\text{sign}(z) (|z| - \gamma)_+ = \begin{cases} z - \gamma & \text{if } z > 0 \text{ and } \gamma < |z| \\ z + \gamma & \text{if } z < 0 \text{ and } \gamma < |z| \\ 0 & \text{if } \gamma \geq |z|. \end{cases}$$

For the  $L_2$  duality function, we should have

$$\begin{aligned} 0 &= \frac{\partial G_{\hat{\mathbb{P}}_b^{(k)}}(\beta, \lambda)}{\partial \beta} = \frac{\partial L(\beta | \tilde{\mathbf{x}}, \tilde{\mathbf{y}})}{\partial \beta} + \frac{\partial \pi(\beta, \lambda)}{\partial \beta} \\ &= -\frac{1}{m} \tilde{\mathbf{x}}^T (\tilde{\mathbf{y}} - \tilde{\mathbf{x}} \beta) + 2\lambda \beta \end{aligned}$$

and

$$\begin{aligned} \lambda &= \min_{\lambda} \left\| \frac{\partial V_{\hat{\mathbb{P}}_b^{(k)}, \tilde{\mathbb{P}}_b^{(k)}}(\beta, \lambda)}{\partial \beta} \right\|_2^2 \\ &= \min_{\lambda} \left\| \left( \frac{1}{n_k} \mathbf{x}^T \mathbf{x} - \frac{1}{m} \tilde{\mathbf{x}}^T \tilde{\mathbf{x}} \right) \beta - \left( \frac{1}{n_k} \mathbf{x}^T \mathbf{y} - \frac{1}{m} \tilde{\mathbf{x}}^T \tilde{\mathbf{y}} \right) - 2\lambda \beta \right\|_2^2. \end{aligned}$$

Thus, the stochastic update is given by

$$\beta^{(t+1)} = \beta^{(t)} - \gamma_1 \cdot \left( -\frac{1}{m} \tilde{\mathbf{x}}^T (\tilde{\mathbf{y}} - \tilde{\mathbf{x}} \beta^{(t)}) + 2\lambda^{(t)} \beta^{(t)} \right)$$

and

$$\lambda^{(t+1)} = (\lambda^{(t)} - \gamma_2 \cdot (2v_1^T v_1 \lambda^{(t)} - 2v_1^T v_2))_+$$

if  $\lambda$  is a scalar and

$$\lambda^{(t+1)} = (\lambda^{(t)} - \gamma_2 \cdot 2(v_1 - \lambda^{(t)} \odot v_1) \odot (-v_1))_+$$

otherwise, where  $v_1 = 2\beta^{(t+1)}$ ,  $v_2 = \left( \frac{1}{n_k} \mathbf{x}^T \mathbf{x} - \frac{1}{m} \tilde{\mathbf{x}}^T \tilde{\mathbf{x}} \right) \beta^{(t+1)} - \left( \frac{1}{n_k} \mathbf{x}^T \mathbf{y} - \frac{1}{m} \tilde{\mathbf{x}}^T \tilde{\mathbf{y}} \right)$ , and  $\gamma_1$  and  $\gamma_2$  are chosen step sizes.

To accelerate convergence, the update process for  $\lambda$  with both duality functions can be replaced by the ADAM-type update (Kingma and Ba, 2014) which incorporates momentum. That is,

$$\begin{aligned} \mu^{(t+1)} &= \tilde{\beta}_1 \mu^{(t)} + (1 - \tilde{\beta}_1) \cdot \nabla_{\lambda} \left\| \frac{\partial V_{\hat{\mathbb{P}}_b^{(k)}, \tilde{\mathbb{P}}_b^{(k)}}(\beta^{(t+1)}, \lambda^{(t)})}{\partial \beta^{(t+1)}} \right\|_2^2 \\ \nu^{(t+1)} &= \tilde{\beta}_2 \nu^{(t)} + (1 - \tilde{\beta}_2) \left( \nabla_{\lambda} \left\| \frac{\partial V_{\hat{\mathbb{P}}_b^{(k)}, \tilde{\mathbb{P}}_b^{(k)}}(\beta^{(t+1)}, \lambda^{(t)})}{\partial \beta^{(t+1)}} \right\|_2^2 \right)^2 \\ \lambda^{(t+1)} &= \left( \lambda^{(t)} - \gamma_2 \frac{\mu_t^{(t+1)} / (1 + \tilde{\beta}_1)}{\sqrt{\nu_t^{(t+1)} / (1 - \tilde{\beta}_2) + \epsilon}} \right)_+, \end{aligned}$$

where  $\mu$  and  $\nu$  represent the first and second momentum vectors or scalars initialized as zero, the two scalars  $\tilde{\beta}_1$  and  $\tilde{\beta}_2$  are momentum parameters with  $\tilde{\beta}_1 \in [0, 1)$  and  $\tilde{\beta}_2 \in [0, 1)$ ,

the hyper-parameter  $\gamma_2$  represents the learning rate, and  $\epsilon$  is a small constant added for numerical stability.

An estimation procedure for an imputation model is considered complete once  $\beta^{(t)}$  has converged. The estimate of  $\sigma$  can then be obtained by (S.33) with the converged  $\beta^{(t)}$  using the argument above in this section. The resulting model, characterized by the parameters  $(\hat{\beta}_b^{(k)}, \hat{\sigma}_b^{(k)})$  is then applied to the hold-out set  $(\mathbf{x}_b^{(k)}, \mathbf{y}_b^{(k)})$ . Depending on the objective, this can be used for the purpose of imputing future observations using Algorithm 2, or for assessing the efficiency of the imputation model to select the resampling parameter with Algorithm 3.

Performing Algorithm 3 for selecting resampling parameter  $\tilde{\alpha}$  requires the calculation of CDF values with a single imputation model estimation iteration ( $B = 1$ ). The CDF value can be calculated with

$$F(y_{bi}^{(k)} | x_{bi}^{(k)}) = \Phi \left( \frac{y_{bi}^{(k)} - x_{bi}^{(k)} \hat{\beta}_b^{(k)}}{\hat{\sigma}_b^{(k)}} \right)$$

for  $i = 1, \dots, n - n_k$ , where  $b = 1$  and  $\Phi(\cdot)$  represents the standard normal CDF. The hold-out set is denoted as  $(\mathbf{x}_b^{(k)}, \mathbf{y}_b^{(k)}) := \{(x_{bi}^{(k)}, y_{bi}^{(k)}) : i = 1, \dots, n - n_k\}$ . After iterating through  $k = 1, \dots, K$ , we can obtain  $n$  such CDF values. This collection of CDF values is then tested against the standard uniform distribution with KS-test for the selection of best  $\tilde{\alpha}$ .

Note that performing Algorithm 3 already yields an imputation model obtained with the selected  $\tilde{\alpha}$ . Thus, Algorithm 2 only requires  $B - 1$  iterations. In Algorithm 2, future observations are created by the normal distribution

$$y_{*bi}^{(k)} \sim N \left( x_{bi}^{(k)} \hat{\beta}_b^{(k)}, \left( \hat{\sigma}_b^{(k)} \right)^2 \right)$$

for  $i = 1, \dots, n_k$ . By iteratively performing the estimation of the imputation model and the imputation process for  $b = 1, \dots, B$  and  $k = 1, \dots, K$ , we construct the imputation distribution  $\mathbb{Q}$ , which consists of  $n \cdot B$  samples.

The estimation process with Algorithm 1 follows the same implementation of estimation of imputation models as described above, with a straightforward modification:  $\hat{\mathbb{P}}_b^{(k)}$  is replaced with  $\mathbb{Q}$  and  $\tilde{\mathbb{P}}_b^{(k)}$  with  $\hat{\mathbb{P}}$ , where the latter represents the full empirical observations.

### S.10.2 Implementation Details of AM

We implemented AM for the linear regression example from scratch in R, with no contributed R packages utilized for the implementation. Algorithm 2 was implemented with  $B = 5$  and  $K = 5$ . Algorithm 3 was used to select the resampling parameter  $\tilde{\alpha}$ , with the candidate set  $\{0.1, 0.2, 0.3, 0.5\}$ . The optimization related parameters that apply to all experiments are listed as follows:

- Imputation process:  $\gamma_1 = 1e - 5$ ,  $\gamma_2 = 1.0$ ,  $\tilde{\beta}_1 = 0.9$ ,  $\tilde{\beta}_2 = 0.999$ , and  $\epsilon = 1e - 7$ ;
- Estimation process:  $\gamma_1 = 1e - 6$ ,  $\gamma_2 = 1.0$ ,  $\tilde{\beta}_1 = 0.9$ ,  $\tilde{\beta}_2 = 0.999$ , and  $\epsilon = 1e - 7$ .

### S.10.3 Implementation Details of Other Methods

We utilized the `cv.glmnet` and `glmnet` function from the R package `glmnet` (Friedman et al., 2010) for other methods, applying the default settings. For the elastic net, we chose

candidate  $\alpha$  values, which balance the  $L_1$  and  $L_2$  penalties, ranging from 0 to 1 in increments of 0.01. The residuals for the adaptive lasso were obtained with the ridge estimate generated by `cv.glmnet` and `glmnet`. The method of Reid et al. (2016), implemented in the R package `natural` (Yu and Bien, 2019), is used for estimating the standard deviation.

## S.11 Implementation Details in the Neural Network Example

### S.11.1 Technical Details

In the context of classification using neural networks, consider the observed data  $(x, y)$  and the model parameters  $\theta \in \mathbb{R}^p$ . A general loss function for this setting is defined as follows:

$$L(\theta|X = x, Y = y) = \frac{1}{n} \sum_{i=1}^n H(y_i, \hat{y}(x_i; \theta)),$$

where  $y_i$  is the observed response or category and  $\hat{y}(x_i; \theta)$  represents the vector of predicted output probabilities for input  $x_i$ . The function  $H(\cdot, \cdot)$  denotes the cross-entropy loss function, commonly used in machine learning. It takes the same form as the negative log-likelihood function used in (multinomial) logistic regression. For a multi-class classification problem with  $C$  classes (for instance,  $C = 10$  in the MNIST dataset), the loss function is expressed as:

$$H(y_i, \hat{y}(x_i; \theta)) = - \sum_{c=0}^{C-1} y_{ic} \log \hat{y}_c(x_i; \theta),$$

where  $\hat{y}_c(x_i; \theta)$  denotes the estimated probability of observing the class  $c$  given the input  $x_i$ ,  $y_{ic} = 1$  if  $y_i = c$ , and  $y_{ic} = 0$  otherwise.

In this section, we elaborate on the derivation for estimating an imputation model. First, we obtain the data represented by  $\hat{\mathbb{P}}_b^{(k)}$  and  $\tilde{\mathbb{P}}_b^{(k)}$  following the data-splitting and resampling scheme in Algorithm 2 at iteration  $(b, k)$ , for any arbitrary  $b = 1, \dots, B$  and  $k = 1, \dots, K$ . For simplicity, we omit the index  $(b, -k)$  on each indexed observation  $(x, y)$ . The samples  $\tilde{\mathbb{P}}_b^{(k)} := \{(\tilde{x}_i, \tilde{y}_i) : i = 1, \dots, m\}$  are treated as the current observations and the samples  $\hat{\mathbb{P}}_b^{(k)} := \{(x_i, y_i) : i = 1, \dots, n_k\}$  are treated as the future observations, where the sample sizes in  $\hat{\mathbb{P}}_b^{(k)}$  and  $\tilde{\mathbb{P}}_b^{(k)}$  are denoted as  $n_k$  and  $m$  respectively. Using the matrix notation, the two samples are denoted by  $(\mathbf{x}, \mathbf{y})$  and  $(\tilde{\mathbf{x}}, \tilde{\mathbf{y}})$ , omitting the  $(b, -k)$  indexing used in Algorithm 2.

The duality function in its general form can be rewritten as:  $\pi(\theta, \lambda) = \lambda \sum_{i=1}^p |\theta_i|$  and  $\pi(\theta, \lambda) = \lambda \sum_{i=1}^p \theta_i^2$ , where  $\lambda$  can be considered as a vector or scalar, depending on whether the duality function is weighted. We first consider the  $L_1$  duality function. In this case, the estimation of  $(\theta, \lambda)$  should satisfy

$$0 = \frac{\partial G_{\tilde{\mathbb{P}}_b^{(k)}}(\theta, \lambda)}{\partial \theta} = \frac{\partial L(\theta|\tilde{\mathbf{x}}, \tilde{\mathbf{y}})}{\partial \theta} + \frac{\partial \pi(\theta, \lambda)}{\partial \theta} = \tilde{g}(\theta; \tilde{\mathbf{x}}, \tilde{\mathbf{y}}) + \lambda \cdot \text{sign}(\theta)$$

and

$$\lambda = \min_{\lambda} \left\| \frac{\partial V_{\hat{\mathbb{P}}_b^{(k)}, \tilde{\mathbb{P}}_b^{(k)}}(\theta, \lambda)}{\partial \theta} \right\|_2^2 = \min_{\lambda} \left\| \hat{g}(\theta; \mathbf{x}, \mathbf{y}) - \tilde{g}(\theta; \tilde{\mathbf{x}}, \tilde{\mathbf{y}}) - \lambda \cdot \text{sign}(\theta) \right\|_2^2$$

with the subgradient method (Shor et al., 1985), where

$$\hat{g}(\theta; \mathbf{x}, \mathbf{y}) = \frac{\partial L(\theta|\mathbf{x}, \mathbf{y})}{\partial \theta} \quad \text{and} \quad \tilde{g}(\theta; \tilde{\mathbf{x}}, \tilde{\mathbf{y}}) = \frac{\partial L(\theta|\tilde{\mathbf{x}}, \tilde{\mathbf{y}})}{\partial \theta}$$

are the gradients of the loss function with respect to  $\theta$  on  $\hat{\mathbb{P}}_b^{(k)}$  and  $\tilde{\mathbb{P}}_b^{(k)}$ , respectively. These gradients are calculated using the chain rule, known as backpropagation, based on the specific structure of the neural network. Both  $\hat{g}(\theta; \mathbf{x}, \mathbf{y})$  and  $\tilde{g}(\theta; \tilde{\mathbf{x}}, \tilde{\mathbf{y}})$  can be computed over a small batch of data using the batch-specific loss function

$$L_{\text{batch}}^{(b')}(\theta) = \frac{1}{n_{\text{batch}}} \sum_{i=1}^{n_{\text{batch}}} H\left(y_i^{(b')}, \hat{y}\left(x_i^{(b')}; \theta\right)\right),$$

where  $n_{\text{batch}}$  denotes the batch size, typically chosen as 64, 128, or 256. There are  $B_{\text{batch}} = \text{floor}(m/n_{\text{batch}})$  batches, and the data in the  $b'$ -th batch ( $b' = 1, \dots, B_{\text{batch}}$ ) is denoted as  $\{(x_i^{(b')}, y_i^{(b')}) : i = 1, \dots, n_{\text{batch}}\}$ .

The required gradient for the optimizers to optimize  $\theta$  and  $\lambda$  can be expressed as

$$\nabla_{\theta} G_{\tilde{\mathbb{P}}_b^{(k)}}(\theta, \lambda) = \tilde{g}(\theta; \tilde{\mathbf{x}}, \tilde{\mathbf{y}}) + \lambda \cdot \text{sign}(\theta)$$

and

$$\nabla_{\lambda} \left\| \frac{\partial V_{\hat{\mathbb{P}}_b^{(k)}, \tilde{\mathbb{P}}_b^{(k)}}(\theta, \lambda)}{\partial \theta} \right\|_2^2 = -2 \cdot (\hat{g}(\theta; \mathbf{x}, \mathbf{y}) - \tilde{g}(\theta; \tilde{\mathbf{x}}, \tilde{\mathbf{y}}) - \lambda \odot \text{sign}(\theta)) \cdot \text{sign}(\theta),$$

when  $\lambda$  is weighted, and

$$\nabla_{\lambda} \left\| \frac{\partial V_{\hat{\mathbb{P}}_b^{(k)}, \tilde{\mathbb{P}}_b^{(k)}}(\theta, \lambda)}{\partial \theta} \right\|_2^2 = 2\lambda \cdot [\text{sign}(\theta)]^T [\text{sign}(\theta)] - 2 \cdot [\text{sign}(\theta)]^T (\hat{g}(\theta; \mathbf{x}, \mathbf{y}) - \tilde{g}(\theta; \tilde{\mathbf{x}}, \tilde{\mathbf{y}}))$$

otherwise, with the subgradient method (Shor et al., 1985). When the  $L_2$  duality function is used, we have

$$\nabla_{\theta} G_{\tilde{\mathbb{P}}_b^{(k)}}(\theta, \lambda) = \tilde{g}(\theta; \tilde{\mathbf{x}}, \tilde{\mathbf{y}}) + 2\lambda\theta$$

and

$$\nabla_{\lambda} \left\| \frac{\partial V_{\hat{\mathbb{P}}_b^{(k)}, \tilde{\mathbb{P}}_b^{(k)}}(\theta, \lambda)}{\partial \theta} \right\|_2^2 = -2 \cdot (\hat{g}(\theta; \mathbf{x}, \mathbf{y}) - \tilde{g}(\theta; \tilde{\mathbf{x}}, \tilde{\mathbf{y}}) - 2\lambda\theta) \cdot \text{sign}(\theta)$$

when  $\lambda$  is weighted, and

$$\nabla_{\lambda} \left\| \frac{\partial V_{\hat{\mathbb{P}}_b^{(k)}, \tilde{\mathbb{P}}_b^{(k)}}(\theta, \lambda)}{\partial \theta} \right\|_2^2 = 2\lambda \cdot (2\theta)^T (2\theta) - 2 \cdot (2\theta)^T (\hat{g}(\theta; \mathbf{x}, \mathbf{y}) - \tilde{g}(\theta; \tilde{\mathbf{x}}, \tilde{\mathbf{y}}))$$

otherwise. The parameter  $\theta$  is updated using the stochastic gradient descent with momentum (SGDM) optimizer with the updates:

$$\begin{aligned} v^{(t+1)} &= \rho v^{(t)} + \nabla_{\theta} G_{\hat{\mathbb{P}}_b^{(k)}}(\theta^{(t)}, \lambda^{(t)}) \\ \theta^{(t+1)} &= \theta^{(t)} - \eta_1 v^{(t+1)}, \end{aligned}$$

where  $v$  represents the velocity vector initialized as zero,  $\rho$  is the momentum parameter with  $\rho \in [0, 1)$ , and  $\eta_1$  represents the learning rate.

Following the update of  $\theta$ ,  $\lambda$  is updated with the ADAM optimizer (Kingma and Ba, 2014), with a slightly modified implementation. Specifically,

$$\begin{aligned}\mu^{(t+1)} &= \beta_1 \mu^{(t)} + (1 - \beta_1) \cdot \nabla_{\lambda} \left\| \frac{\partial V_{\hat{\mathbb{P}}_b^{(k)}, \tilde{\mathbb{P}}_b^{(k)}}(\theta^{(t+1)}, \lambda^{(t)})}{\partial \theta^{(t+1)}} \right\|_2^2 \\ \nu^{(t+1)} &= \beta_2 \nu^{(t)} + (1 - \beta_2) \left( \nabla_{\lambda} \left\| \frac{\partial V_{\hat{\mathbb{P}}_b^{(k)}, \tilde{\mathbb{P}}_b^{(k)}}(\theta^{(t+1)}, \lambda^{(t)})}{\partial \theta^{(t+1)}} \right\|_2^2 \right)^2 \\ \lambda^{(t+1)} &= \left( \lambda^{(t)} - \eta_2 \frac{\mu_t^{(t+1)} / (1 + \beta_1)}{\sqrt{\nu_t^{(t+1)} / (1 - \beta_2) + \epsilon}} \right)_+, \end{aligned}$$

where  $\mu$  and  $\nu$  represent the first and second momentum vectors initialized as zero, the two scalars  $\beta_1$  and  $\beta_2$  are the momentum parameters with  $\beta_1 \in [0, 1)$  and  $\beta_2 \in [0, 1)$ , the hyper-parameter  $\eta_2$  represents the learning rate and  $\epsilon$  is a small constant added for numerical stability. Additionally, the learning rates  $\eta_1$  and  $\eta_2$  are controlled by a scheduler and are updated every epoch with  $\eta_1 = \eta_1 \cdot \gamma$  and  $\eta_2 = \eta_2 \cdot \gamma$ , where  $\gamma$  is the pre-specified learning rate-decay rate.

The procedure of estimating one imputation model is considered complete once  $\theta^{(t)}$  or the training loss has converged. The resulting model, characterized by the parameter vector  $\hat{\theta}_b^{(k)}$ , is then applied on the hold-out set  $(\mathbf{x}_b^{(k)}, \mathbf{y}_b^{(k)})$ . Depending on the objective, this can be used for the purpose of imputing future observations using Algorithm 2, or for assessing the efficiency of the imputation model to select the resampling parameter with Algorithm 3.

Performing Algorithm 3 for selecting the resampling parameter  $\tilde{\alpha}$  requires obtaining surrogate CDF values. The details are provided in Section 5.3 and Section S.11.4. After iterating through  $k = 1, \dots, K$ , we obtain  $n$  such surrogate CDF values. This collection of surrogate CDF values is then tested against the standard uniform distribution with the KS-test for the selection of the best  $\tilde{\alpha}$ .

Note that performing Algorithm 3 already yields an imputation model obtained with the selected  $\tilde{\alpha}$ , thus Algorithm 2 only requires  $B - 1$  iterations. When generating imputed future observations, new labels are created by generating

$$\mathbf{y}_{*bi}^{(k)} \sim \text{Multinomial} \left( \hat{\mathbf{y}} \left( x_{bi}^{(k)}; \hat{\theta}_b^{(k)} \right) \right)$$

for  $i = 1, \dots, n - n_k$ . In this expression,  $\hat{\theta}_b^{(k)}$  represents the estimated parameters of the imputation model, and  $\hat{\mathbf{y}}(x_{bi}^{(k)}; \hat{\theta}_b^{(k)})$  denotes the estimated probability vector for the 10 digits, given the image  $x_{bi}^{(k)}$  as the input. By iteratively conducting the imputation model estimation and the imputation process for  $b = 1, \dots, B$  and  $k = 1, \dots, K$ , we construct the imputation distribution  $\mathbb{Q}$ . The imputation distribution  $\mathbb{Q}$  consists of  $60,000 \times B$  images, each with its newly imputed label.

The estimation process with Algorithm 1 follows the same implementation for estimating an imputation model as described above, with a straightforward modification:  $\hat{\mathbb{P}}$  is replaced with  $\mathbb{Q}$  and  $\tilde{\mathbb{P}}_b^{(k)}$  with  $\hat{\mathbb{P}}$ , where the latter represents the full empirical observations.

### S.11.2 Implementation Details of AM

We implemented AM using the PyTorch framework (Paszke et al., 2019), with CUDA being used for faster training. During the data preprocessing phase, the images are normalized to



have a mean of 0 and a standard deviation of 1. Beyond this normalization, no additional techniques, including data augmentation, are used. Before training, the neural network model is initialized using the default setting in Pytorch.

The batch training process introduced in Section S.11.1 is implemented in the following way. An epoch is defined as a complete pass over the current observations through the neural network. That is, within each epoch, there are  $B_{\text{batch}} = \text{floor}(m/n_{\text{batch}})$  batches for the imputation process and  $B_{\text{batch}} = \text{floor}(n/n_{\text{batch}})$  batches for the estimation process. The future observations are similarly shuffled and divided into mini-batches of size  $n_{\text{batch}}$ , indexed as  $1, \dots, B'_{\text{batch}}$ . During the  $b'$ -th iteration, the  $b'$ -th mini-batch from the current observations is used to calculate the current gradient (referred to as  $\tilde{g}(\theta; \tilde{\mathbf{x}}, \tilde{\mathbf{y}})$  in Section S.11.1) and the  $b$ -th mini-batch from the future observations is used for the future gradient (denoted as  $\hat{g}(\theta; \mathbf{x}, \mathbf{y})$  in Section S.11.1). If the number of future observations is smaller than that of the current observations, which occurs when using a resampling parameter  $\alpha > 1$ , the data in the future observations are duplicated before creating mini-batches. For the estimation process, the imputed data from the  $B$  imputation iterations are cyclically used as future observations for each epoch.

For faster convergence, a “warm-up” training phase is conducted before the estimation process, utilizing only the observed data  $\hat{\mathbb{P}}$ . The “warm-up” training phase is carried out as follows. We implement the AM estimation, as detailed in Section S.11.1, by utilizing  $\hat{\mathbb{P}}$  as both the current and future observations. This phase employs the weighted- $L_1$  duality function. Despite  $\hat{\mathbb{P}}$  serving a dual role, the use of the duality function remains meaningful due to the inherent randomness in the mini-batch creation. This warm-up training lasts 50 epochs. The values of neural network parameters obtained at the end of this phase are then used as the initial values for the estimation process.

The training-related hyper-parameters are specified as follows. The imputation process is performed by applying Algorithm 2 with  $B = 5$  and  $K = 2$ . Algorithm 3 is used to select the resampling parameter  $\tilde{\alpha}$ , with the candidate set  $\{0.5, 0.8, 1.0, 1.2\}$ . The optimization related parameters are listed as follows (apply to all experiments):

- Imputation process:  $\eta_1 = 0.01$ ,  $\rho = 0.95$ ,  $\eta_2 = 0.001$ ,  $\beta_1 = 0.99$ ,  $\beta_2 = 0.9999$ ,  $\epsilon = 1e - 8$ , and  $\gamma = 0.98$ . Training stops after 50 epochs;
- “Warm-up” training:  $\eta_1 = 0.01$ ,  $\rho = 0.95$ ,  $\eta_2 = 0.001$ ,  $\beta_1 = 0.99$ ,  $\beta_2 = 0.9999$ ,  $\epsilon = 1e - 8$ , and  $\gamma = 1$ . Training stops after 50 epochs;
- Estimation process:  $\eta_1 = 0.001$ ,  $\rho = 0.95$ ,  $\eta_2 = 0.0001$  (weighted duality functions),  $\eta_2 = 0.00001$  (unweighted duality functions),  $\beta_1 = 0.99$ ,  $\beta_2 = 0.9999$ ,  $\epsilon = 1e - 8$ , and  $\gamma = 0.99$ . Training stops after 50 epochs; and
- Batch size is chosen to be  $n_{\text{batch}} = 64$ .

### S.11.3 Implementation Details of Other Methods

We implemented other methods using the PyTorch framework (Paszke et al., 2019), with CUDA being used for faster training. Before training, the neural network model is initialized using the default setting in Pytorch.

For  $L_1$  and  $L_2$  regularized training, the model was trained using  $\lambda$  values from the set  $\{1e - 1, 1e - 2, 1e - 3, 1e - 4, 1e - 5, 1e - 6\}$ , with the best results reported. For early-stopping, we allocated 10% of the training images as a random validation set. In the case of Dropout, it was implemented after the input layer and before each fully connected

layer, using dropout ratios selected from  $\{0.2, 0.5, 0.8\}$ , reflecting common choices in the literature (Srivastava et al., 2014). All methods employ SGDM for training with a learning rate of 0.01 and a momentum parameter of 0.95. This learning rate was chosen from the set  $\{0.1, 0.01, 0.001, 0.0001\}$  based on optimal performance.

#### S.11.4 Surrogate CDF Values

When applying Algorithm 3 to choose  $m$  for the  $m$ -out-of- $n$  resampling scheme, a continuous CDF value of the data distribution within the range of 0 to 1 is necessary. Here, we adopt and extend the randomization approach proposed by Dunn and Smyth (1996). For an observed pair of  $x$  and  $y$ , let  $p = (p_0, \dots, p_9)'$  represent the vector of predictive probabilities for the digits 0 through 9. If  $y$  is drawn from the multinomial distribution  $\text{Multinomial}_{10}(1, p)$ , the data generation process can be described as follows

$$\text{Sample } U \sim \text{Unif}(0, 1) \quad \text{and find } y \text{ such that: } \sum_{k=0}^{y-1} p_k \leq U < \sum_{k=0}^y p_k.$$

where we define  $\sum_{k=0}^{-1} p_k = 0$ . Reversing this data generation process requires finding  $U$  given the observed  $y$ , resulting the interval  $[\sum_{k=0}^{y-1} p_k, \sum_{k=0}^y p_k]$ . From this interval, We draw a random sample,  $U_{x,y}$ , uniformly distributed over this interval. This  $U_{x,y}$  serves as the surrogate value of the original  $U$ , allowing for the application of one-sample testing methods that maintain desired frequency properties for goodness-of-fit testing with induced noise; see, *i.e.*, Cheng et al. (2021); Gerber and Craig (2023); Liu and Zhang (2018); Yang (2021, 2024) and references therein. Consequently,  $U_{x,y}$  also functions as a surrogate value of  $F(y|x)$ , which can be tested against the standard uniform distribution for selecting an appropriate resampling scheme. The properties outlined in Section S.8 remain valid with similar arguments, given that

$$U_{x,y} \sim \text{Uniform}(0, 1).$$

Notably, reordering the indices for alternative intervals  $[\sum_{k=0}^{y-1} p_k, \sum_{k=0}^y p_k]$ , independent of the observed  $y$ , can be considered elsewhere for improved efficiency of the underlying goodness-of-fit test.

#### S.11.5 Estimation Process of AM

The details of the estimation process and the resultant parameters are visually depicted in Figure S.4. This illustration clearly demonstrates how AM effectively shrinks the parameters toward zero.

#### S.11.6 Questionable Labels Found by AM

All 62 training images detected by AM as having potential questionable labels are shown in Figure S.5.

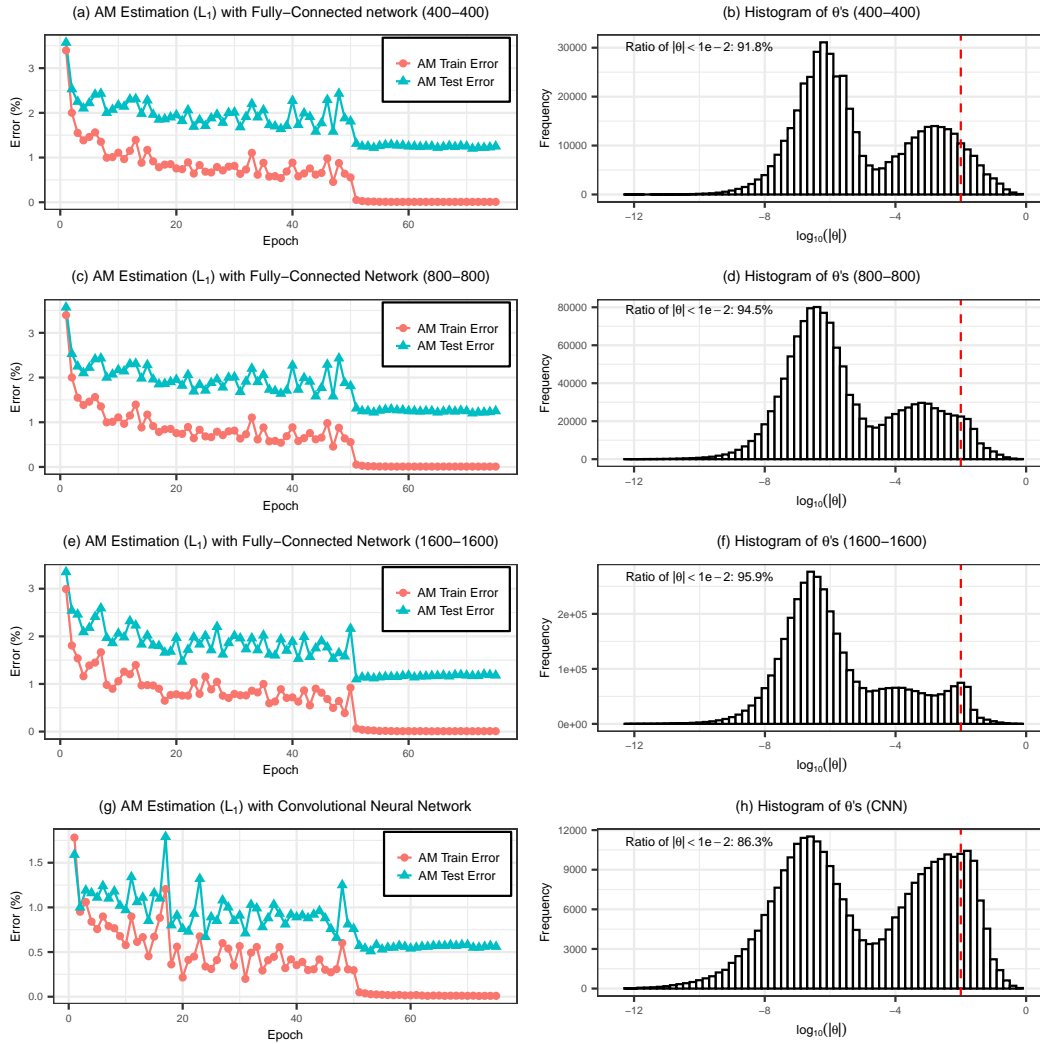


**Figure S.4:** The learning curves in the estimation process and the histograms of the estimated parameters using AM (weighted  $L_1$  duality function) with different model structures.

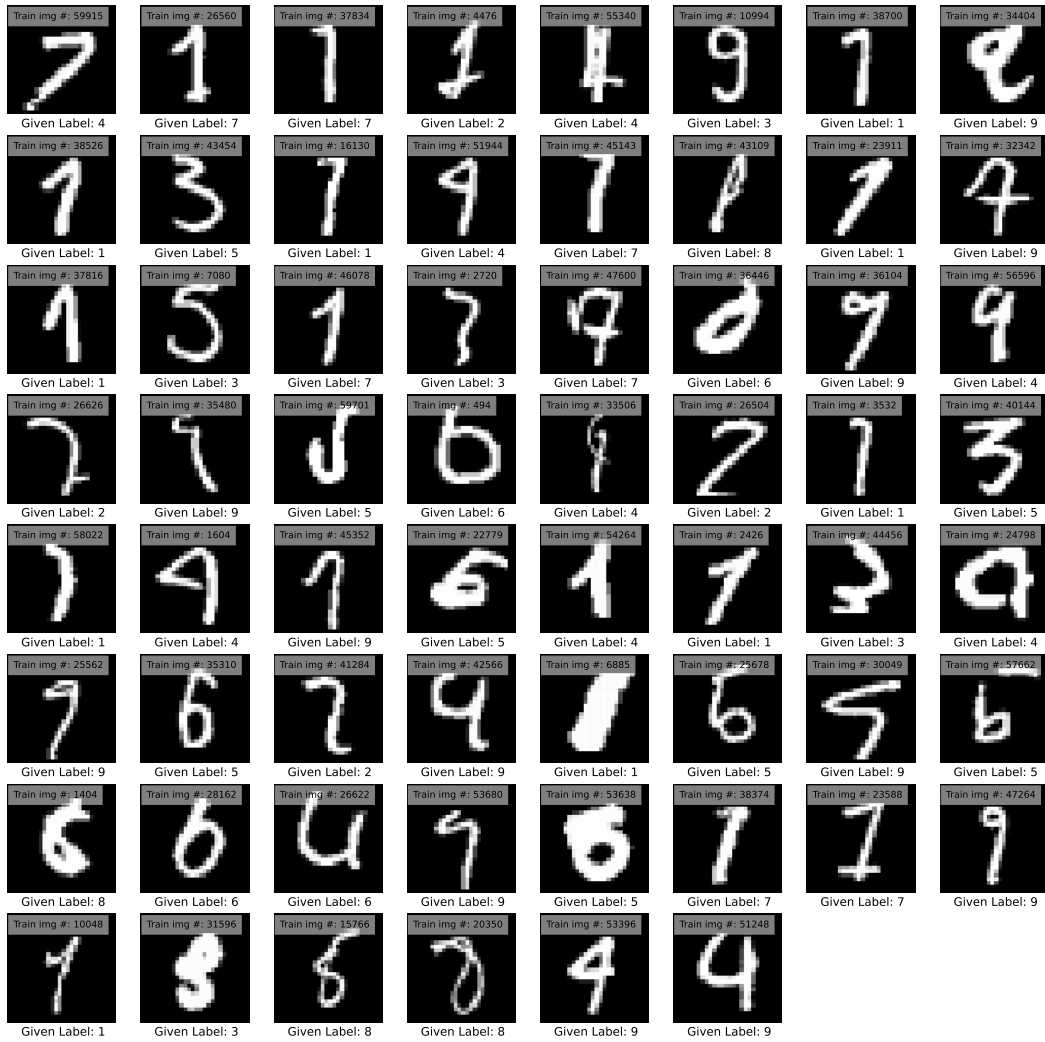


**Figure S.5:** All images detected by AM as having questionable labels, displayed in a left-to-right, top-to-bottom sequence, and sorted by the decreasing frequency of their identification.

## S.12 Imputation Efficiency Evaluation with Q-Q Plots

### S.12.1 The Effect of $m$ on Imputation Efficiency

The imputation efficiency is measured by how good each imputation model fits its holdout sample (12). Besides the KS-test approach used in Algorithm 3, such efficiency can be further visually inspected by Q-Q plots, with the estimated CDF values against the standard uniform distribution. Note that the Q-Q plots here can also be viewed as Probability-Probability (P-P) plots. Alternatively, one can also visualize Q-Q plots with normal quantile transformation.

The Q-Q plots in Figure S.6 demonstrate the effect of  $m$  on the imputation efficiency in a typical linear regression simulation study in Section 5.2. It can be seen that when the standard bootstrap does not work well in estimating the data distribution, the  $m$ -out-of- $n$  bootstrap with the optimal  $m$  can result in a much better approximation to the true data distribution with regard to (12). Furthermore,  $\tilde{\alpha}$  values spanning a wide range, from 0.1 to 0.5, consistently yield satisfactory results. This demonstrates the robustness of Algorithm 3 to the grid density of the candidate set for  $\tilde{\alpha}$ .

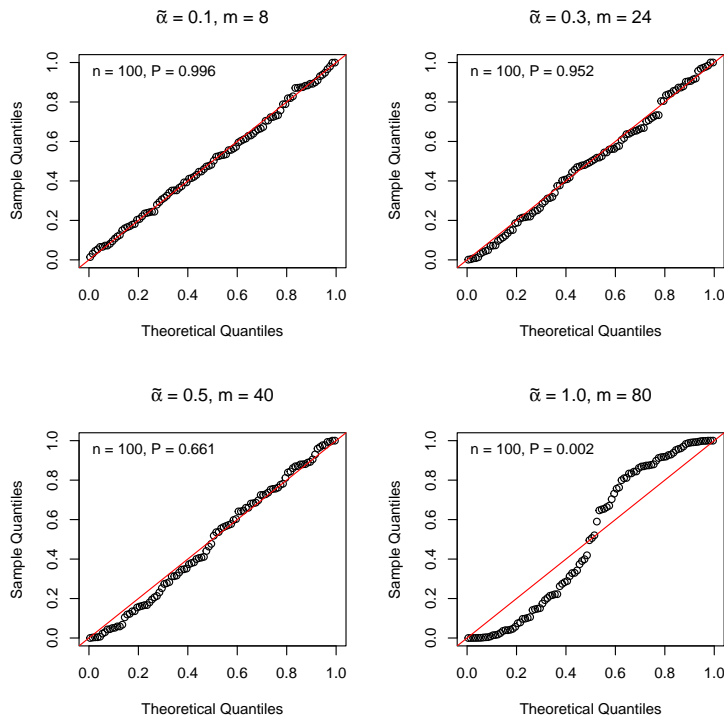


**Figure S.6:** Q-Q plots of the estimated CDF values from the imputation model obtained using the  $m$ -out-of- $n$  bootstrap with varying  $m = \lceil \tilde{\alpha} n_k \rceil$  values, against the standard uniform distribution, in a typical linear regression simulation example in Section 5.2. The CDF values are obtained on the holdout set, following the  $K$ -fold data-splitting method introduced in Algorithm 3. Here  $n_k$  denotes the sample size of the future observations used to fit the  $k$ -th imputation model, and  $n_k = \lceil n(K-1)/K \rceil = 80$  for  $k = 1, \dots, K$ . In this example we have  $K = 5$  and  $n_1 = \dots = n_5$ , resulting in a uniform  $m$  value across  $K$  imputation models for each  $\tilde{\alpha}$ . The observed sample size and the  $p$ -value of the KS-test are indicated as  $n$  and  $P$ , respectively, in the top-left corner of each plot. Notably, the case with  $\tilde{\alpha} = 1$  and  $m = 80$  corresponds to the standard bootstrap and shows that the resulting imputation model is severely underdispersed.

### S.12.2 Imputation Efficiency with the Optimal $m$

The Q-Q plots in Figure S.7 to S.11 demonstrate the imputation efficiency with the optimal  $m$  selected by Algorithm 3. These plots cover all three application examples discussed in Section 5, with observed sample sizes ranging from  $n = 10$  to  $n = 60,000$ . It can be seen that Algorithm 3 effectively approximates the target specified in (12) across all scenarios.

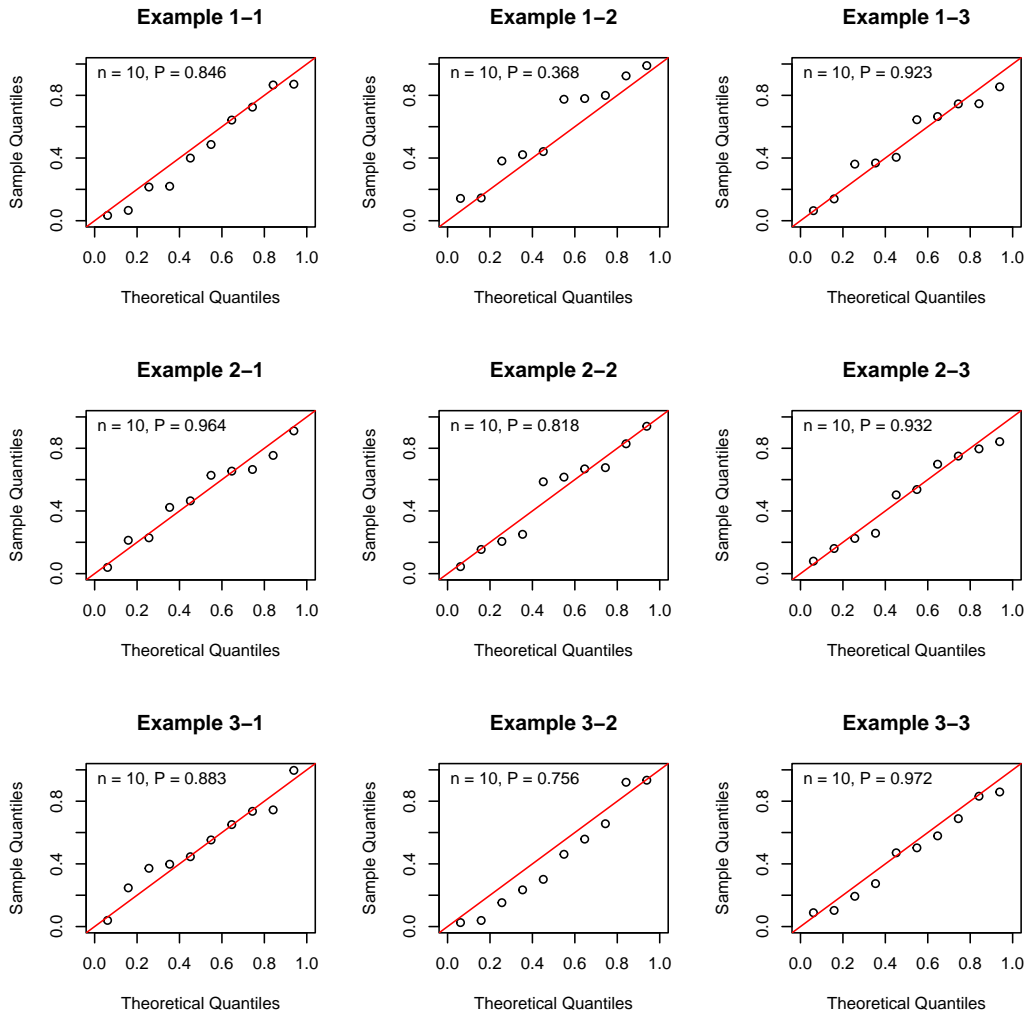


**Figure S.7:** Q-Q plots of the estimated CDF values from the imputation model obtained using Algorithm 3, against the standard uniform distribution, in the many-normal-means simulation study (Section 5.1) with sample size  $n = 10$ . The  $p$ -value of the KS-test is indicated as  $P$  in the top-left corner of each plot. Presented here are the results from the first three repetitions across the three settings.

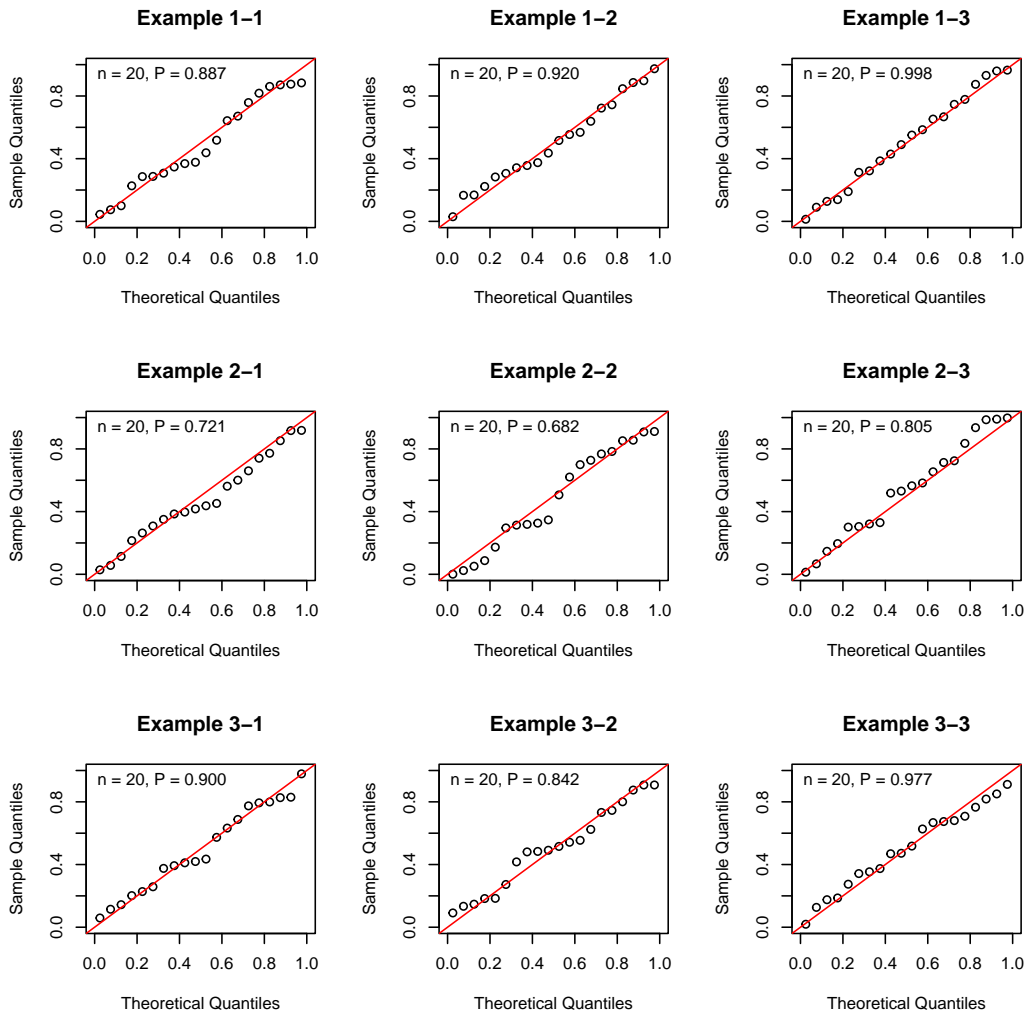


**Figure S.8:** The same legend as Figure S.7, but for  $n = 20$ .

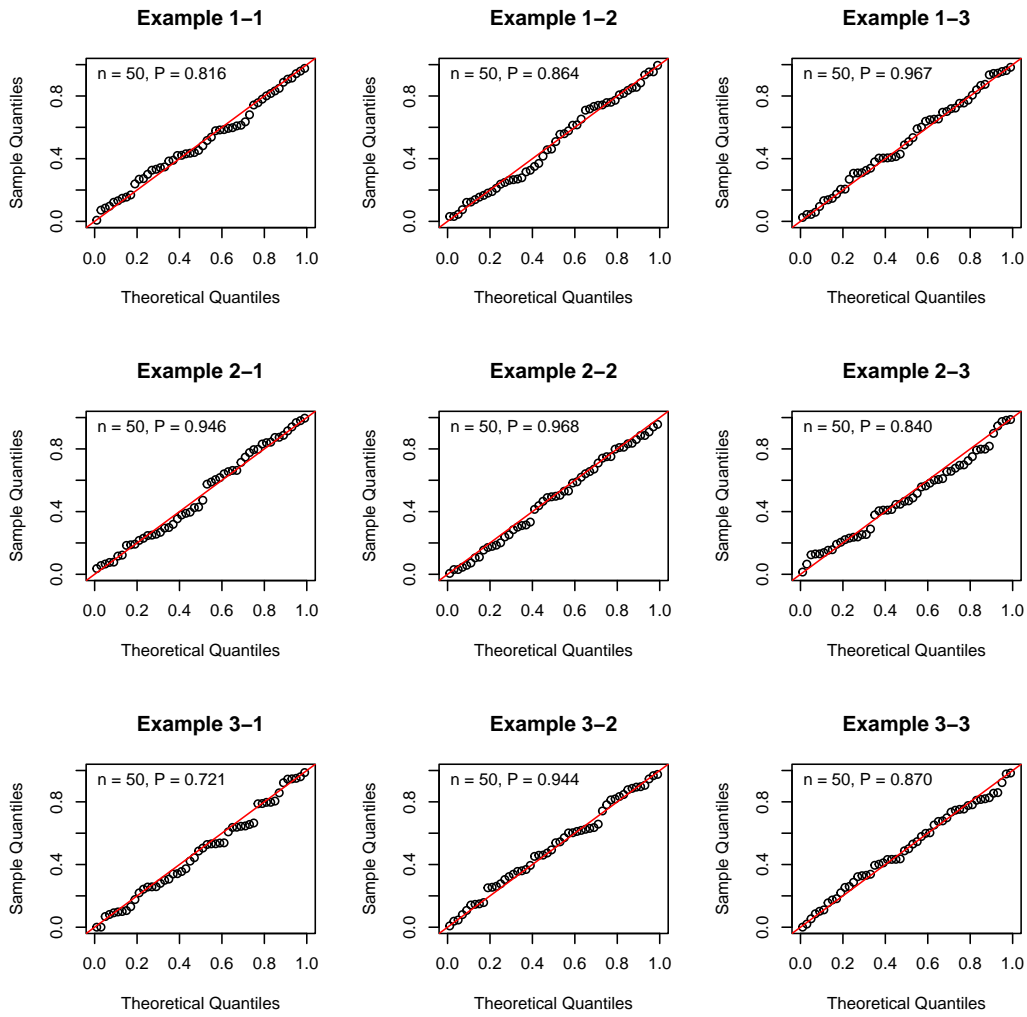


**Figure S.9:** The same legend as Figure S.7, but for  $n = 50$ .



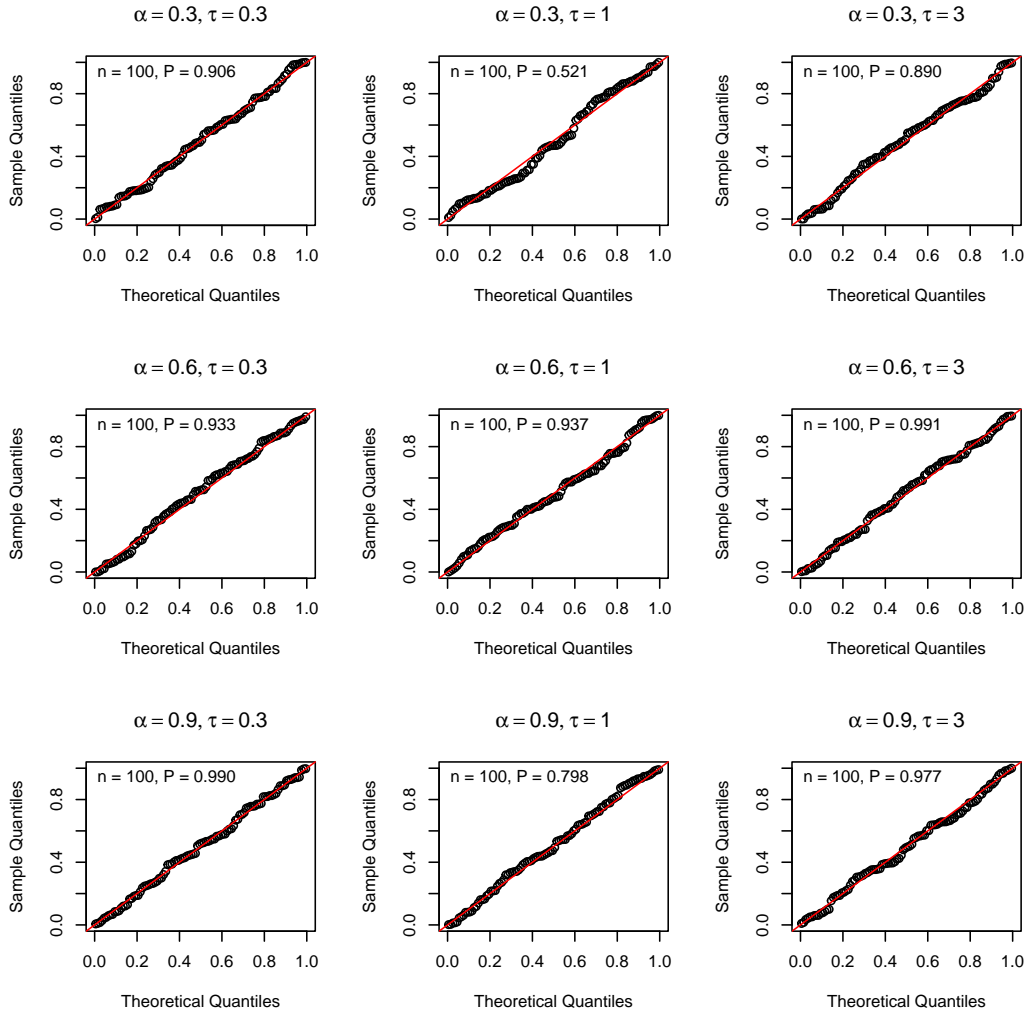


**Figure S.10:** Q-Q plots of the estimated CDF values from the imputation model obtained using Algorithm 3, against the standard uniform distribution, in the linear regression example (Section 5.2). The  $p$ -value of the KS-test is indicated as  $P$  in the top-left corner of each plot. Presented here are the results from the first repetition across various settings, using the (unweighted)  $L_1$  duality function.

Q-Q Plot of Surrogate CDF Estimates with FC-800-800 ( $L_1$ )

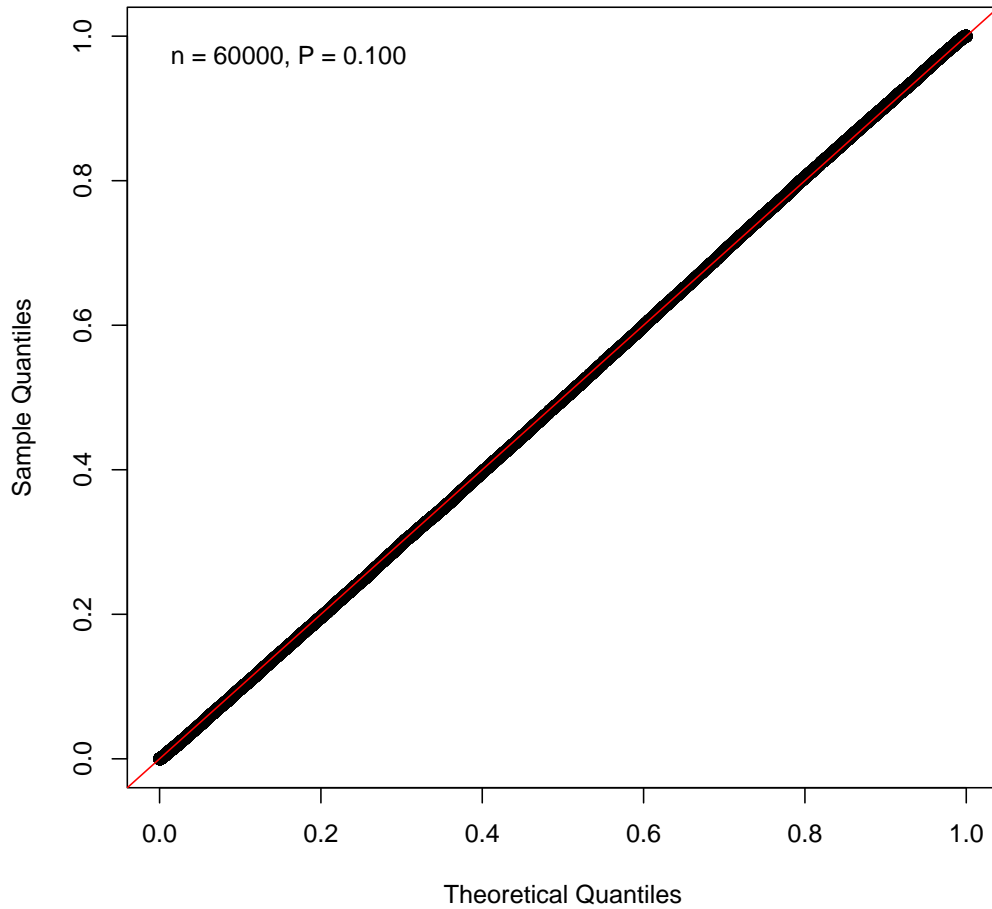


**Figure S.11:** Q-Q plots of the estimated (surrogate) CDF values from the imputation model obtained using Algorithm 3, against the standard uniform distribution, in the neural network example (Section 5.3). The observed sample size and the  $p$ -value of the KS-test are indicated as  $n$  and  $P$ , respectively, in the top-left corner of each plot. Presented here are the results obtained using the (weighted)  $L_1$  duality function in fully connected networks featuring 800 hidden nodes.

## S.13 Computational Efficiency of AM

### S.13.1 Computational Time Analysis

The imputation and estimation scheme is computationally efficient and does not exceed the computational cost typically associated with widely used cross-validation frameworks, when using the same model for imputation and estimation. This efficiency stems primarily from the development of effective numerical optimization methods, detailed in Section 3 for solving the AM objective (8). These methods ensure that the computational complexity of fitting a single AM model is comparable to that of standard model estimation procedures with fixed hyper-parameters, commonly employed in cross-validation. Given this efficiency, the entire AM imputation-estimation process, including Algorithms 1, 2, and 3, aligns computationally with performing  $K$ -fold cross-validation across  $(B - 1) + |\tilde{\alpha}|$  different hyper-parameter combinations. Here,  $|\tilde{\alpha}|$  denotes the number of candidate  $\tilde{\alpha}$  values used in Algorithm 3. Notably, we typically use  $B + |\tilde{\alpha}| \leq 10$  in practice. The term  $B - 1$  arises because selecting  $\tilde{\alpha}$  via Algorithm 3 inherently produces an imputation model for generating future observations. Furthermore, similar to cross-validation, AM can be easily parallelizable.

Another notable computational advantage of the AM framework over cross-validation is its applicability for estimating extremely large models, where even a single model can be computationally demanding. In such cases, the AM framework allows the use of less resource-intensive yet effective models for imputation, substantially reducing the overall computational cost compared to cross-validation.

### S.13.2 Computational Time of the Application Examples

In this study, we present the computational times of AM recorded for the application examples discussed in the paper. These times are based on the first repetition of each application example. The evaluations were performed on a personal computer equipped with an Intel Core i7-12700KF CPU and an NVIDIA GeForce RTX 3070 Ti GPU. We conducted the computations without employing any parallel processing techniques. The detailed computational results are summarized in Table S.2. Notably, the application of AM in both the many-normal-means and linear regression scenarios was implemented with R. It is important to note that a further acceleration in performance is achievable through implementation in C. The result presented in Table S.2 effectively demonstrates the scalability of AM when applied to large-scale problems.

**Table S.2:** Computation times required for AM to estimate a single imputation model and complete the entire imputation-estimation scheme. The results are obtained with the first repetition under the first setting across various application examples, and are measured in seconds. It is observed that both weighted and unweighted duality functions exhibit similar computation times. Furthermore, the execution times for neural networks, employing various duality functions and structures as described in the paper, are approximately equivalent, due to the use of CUDA.

	Time Per Imputation Model (s)	Total Time (s)
Many-Normal-Means ( $n = 10$ )	0.02	0.87
Many-Normal-Means ( $n = 20$ )	0.06	2.63
Many-Normal-Means ( $n = 50$ )	0.29	15.71
Linear Regression- $L_1$ ( $n = 100$ )	2.25	118.74
Linear Regression- $L_2$ ( $n = 100$ )	0.23	34.88
Neural Network ( $n = 60,000$ )	53.78	1127.56

## References

- Blondel, M., Fujino, A., and Ueda, N. (2014). Large-scale multiclass support vector machine training via euclidean projection onto the simplex. In *2014 22nd International Conference on Pattern Recognition*, pages 1289–1294.
- Boyd, S., Xiao, L., and Mutapcic, A. (2003). Subgradient methods. *lecture notes of EE392o, Stanford University, Autumn Quarter, 2004*(01).
- Cheng, C., Wang, R., and Zhang, H. (2021). Surrogate residuals for discrete choice models. *Journal of Computational and Graphical Statistics*, 30(1):67–77.
- Dunn, P. K. and Smyth, G. K. (1996). Randomized quantile residuals. *Journal of Computational and graphical statistics*, 5(3):236–244.
- Friedman, J., Hastie, T., and Tibshirani, R. (2010). Regularization paths for generalized linear models via coordinate descent. *Journal of statistical software*, 33(1):1–22.
- Gerber, E. A. E. and Craig, B. A. (2023). Residuals and diagnostics for multinomial regression models. *The ASA Data Science Journal*. <https://doi.org/10.1002/sam.1164530>.
- Kingma, D. P. and Ba, J. (2014). Adam: A method for stochastic optimization. *arXiv preprint arXiv:1412.6980*.
- Liu, D. and Zhang, H. (2018). Residuals and diagnostics for ordinal regression models: a surrogate approach. *Journal of the American Statistical Association*, 113(522):845–854.
- Narasimhan, B. and Efron, B. (2020). deconvolveR : A  $g$ -modeling program for deconvolution and empirical bayes estimation. *Journal of Statistical Software*, 94(11).
- Newey, W. K. and McFadden, D. (1994). Chapter 36 large sample estimation and hypothesis testing. volume 4 of *Handbook of Econometrics*, pages 2111–2245. Elsevier.
- Parikh, N. and Boyd, S. (2014). Proximal algorithms. *Found. Trends Optim.*, 1(3):127–239.
- Paszke, A., Gross, S., Massa, F., Lerer, A., Bradbury, J., Chanan, G., Killeen, T., Lin, Z., Gimelshein, N., Antiga, L., Desmaison, A., Köpf, A., Yang, E., DeVito, Z., Raison, M., Tejani, A., Chilamkurthy, S., Steiner, B., Lu, F., Bai, J., and Chintala, S. (2019). Pytorch: An imperative style, high-performance deep learning library. Technical report, Cornell University Library, arXiv.org.
- Reid, S., Tibshirani, R., and Friedman, J. (2016). A study of error variance estimation in lasso regression. *Statistica Sinica*, 26(1):35–67.
- Shalev-Shwartz, S., Shamir, O., Srebro, N., and Sridharan, K. (2010). Learnability, stability and uniform convergence. *Journal of Machine Learning Research*, 11(90):2635–2670.
- Shor, N. Z., Kiwiel, K. C., and Ruszcayński, A. (1985). *Minimization methods for non-differentiable functions*. Springer-Verlag New York, Inc., New York, NY, USA.
- Spencer, N. A. and Miller, J. W. (2023). Strong uniform laws of large numbers for bootstrap means and other randomly weighted sums.

- Srivastava, N., Hinton, G., Krizhevsky, A., Sutskever, I., and Salakhutdinov, R. (2014). Dropout: A simple way to prevent neural networks from overfitting. *Journal of machine learning research*, 15:1929–1958.
- Tsybakov, A. B. (2009). *Introduction to Nonparametric Estimation*. Springer series in statistics. Springer, Dordrecht.
- Yang, L. (2021). Assessment of regression models with discrete outcomes using quasi-empirical residual distribution functions. *Journal of Computational and Graphical Statistics*, 30(4):1019–1035.
- Yang, L. (2024). Double probability integral transform residuals for regression models with discrete outcomes. *Journal of Computational and Graphical Statistics*, (just-accepted):1–21.
- Yu, G. and Bien, J. (2019). Estimating the error variance in a high-dimensional linear model. *Biometrika*, 106(3):533–546.